DESIGN, SYNTHESIS AND CHARACTERIZATION OF NOVEL RHENIUM(V) AND TECHNETIUM(V) COMPLEXES AS POTENTIAL RADIOPHARMACEUTICALS

A thesis submitted in fulfilment of the
requirements for the

MASTER'S DEGREE

of

RHODES UNIVERSITY
GRAHAMSTOWN

by

PATRICK SIMON HLABELA

September 2000

ABSTRACT

A number of bidentate *N,N*-diethyl-*N'*-(R')benzoylthiourea ligands (where R' = H, CH_3, Cl, OCH_3 and NO_2) have been synthesized, as well as the three Re(V) precursor complexes, $ReOCl_3(PPh_3)_2$, $[ReO_2(py)_4]Cl$ and [*n*-Bu_4N][$ReOCl_4$]. The reaction of *N,N*-diethyl-*N'*-benzoylthiourea (LH) with these three metal precursor complexes in methanol in the presence of a base gave a novel mixed-ligand complex *bis*(*N,N*-diethyl-*N'*-benzoylthioureato)methoxyoxorhenium(V), $[ReO(L)_2(OMe)]$ **(1)**. In the absence of a base and under an inert atmosphere, the reaction between [*n*-Bu_4N][$ReOCl_4$] and LH yielded *bis*(*N,N*-diethyl-*N'*-benzoylthioureato)chlorooxorhenium(V), $[ReO(L)_2Cl]$ **(1b)**. The reaction of LH with $[ReO_2(py)_4]Cl$ in ethanol and *iso*-propanol in the presence of sodium acetate gave the novel mixed ligand complexes *bis*(*N,N*-diethyl-*N'*-benzoylthioureato)ethoxyoxorhenium(V), $[ReO(L)_2(OEt)]$ **(6)** and *bis*(*N,N*-diethyl-*N'*-benzoylthioureato)(*iso*-propoxy)oxorhenium(V), $[ReO(L)_2(OiPr)]$ **(7)**, respectively. An oxygen bridged dirhenium complex, $[(L)_2ORe\text{-}O\text{-}ReO(L)_2]$ **(15)** was obtained when the reaction was carried out in acetonitrile.

A series of mixed ligand Re(V)-oxo complexes using *N, N*-diethyl-*N'*-(R')benzoylthiourea (LR'), *N,N*-morpholino-*N'*-(R')benzoylthiourea (morph-LR') and 8-(*N*-(R')benzoylthiocarbamoyl)-1,4-dioxa-8-azaspiro[4.5]decane ligands (spiro-LR') (where R' = H, CH_3, Cl, OCH_3 and NO_2) (**(1)-(14)** have been prepared by the reaction of $[ReO_2(py)_4]Cl$ and the ligand in the presence of sodium acetate in methanol. The solution state chemistry of these complexes has shown that complexes **(1)-(14)** (with the exception of **(1b)**) undergo dimerization in solution to give complex **(15)** in the presence of water. Preliminary ^1H NMR kinetics studies of the dimerization of **(1)**, **(6)** and **(7)** to **(15)** have shown that the rate of dimerization decreases in the order **(7)** > **(6)** > **(1)**. The rate of dimerization has also been compared for complexes **(1)**, $[ReO(morph\text{-}L)_2(OMe)]$ **(8)** and $[ReO(spiro\text{-}L)_2(OMe)]$ **(13)** and the rate of dimerization was found to be fastest for **(13)**.

The crystal structures of **(1)**, $[ReO(LNO_2)_2(OMe)]$ **(4)**, **(6)** and **(15)** have been determined. The Re(V)-oxo complexes **(1)**, **(4)** and **(6)** have a slightly distorted octahedral geometry with the two acylthiourea ligands binding in a *cis* arrangement in the equatorial plane of the octahedron. The alkoxy and oxo ligands occupy the axial positions and are situated *trans* to each other. The

crystal and molecular structure of complex **(15)**, consist of two slightly distorted octahedral $[ReO(L)_2]$ moieties bridged by an oxygen atom with a Re-O-Re bond angle of 175.2(2)°.

The preliminary studies done in the present study have indicated that the complexation chemistry of technetium(V) with the *N,N*-diethyl-*N'*-benzoylthiourea is different to that of rhenium(V). The reaction between $[n\text{-}Bu_4N][TcOCl_4]$ and *N,N*-diethyl-*N'*-benzoylthiourea yielded the square pyramidal cationic complex $[TcO(L)_2]Cl$. By contrast the octahedral methoxy complex $[ReO(L)_2(OMe)]$ was obtained when the analogous Re(V)-oxo precursor, $[n\text{-}Bu_4N][ReOCl_4]$, was reacted with *N,N*-diethyl-*N'*-benzoylthiourea under the same reaction conditions.

CONTENTS

ACKNOWLEDGEMENTS.

There are indeed many people who have given much assistance from the beginning until the end of this work and I would like to extend my sincere gratitude to all of them.

Dr Cheryl Sacht, my supervisor, for her exquisite supervision, understanding, motivation and moral support, a special thank you to her. Dr Neil Jarvis and Mr Otto Knoesen at AEC are being thanked for their input of ideas. Ms Leanne Cook at the University of Witwatersrand for doing the crystal structures for me, thanks. Mr Piero Benincasa at the University of Cape Town is being acknowledged for doing the elemental analysis for all of my compounds. Mr Moses Rotich is being thanked for proof-reading my thesis. Thank you to Mr Michael Datt and Mr Brian Corneny for generously offering some of the ligands. The technical staff at Rhodes Chemistry Department stores is thanked for their cooperation and patience every time I needed chemicals and special glass-ware.

Thanks to the Chemistry Department secretary Mrs Benita Tarr for all her kind assistance. A special thanks to all my brothers and sisters for their continued support. A handful of thanks to my beloved mother, Meiggy Tlhabela, for her unending moral support and for believing in me. I would like to thank DAAD, AEC and Rhodes University for their generous financial support. Finally, praise be to God Almighty for helping me stand against all odds of life.

"Dedicated to my late brother, William Tlhabela (RIP)"

List of figures.

List of schemes.

List of tables.

List of abbreviations and acronyms,

ACS	American Cancer Society.
AIDS	Acquired Immuno Deficiency Syndrome.
BAM	Biologically Active Moiety.
$CDCl_3$	Deuterated chloroform.
^{13}C NMR	Carbon 13 nuclear magnetic resonance.
DEBTH	*N,N*-diethyl-*N'*- benzoylthiourea (as abbreviated by Dilworth *et al.*).
DHFR	Dihydrofolate reductase.
DMSO	Dimethylsulfoxide.
DNA	Deoxyribonucleic acid.
dUMP	2'-Deoxyuridylic acid.
HASB	Hard-acid and soft-base theory.
HEDP	Hydroxyethylidenephosphonate.
H_3pen	Penicillamine.
HPLC	High pressure liquid chromatography.
IR	Infrared spectroscopy.
keV	kiloelectron volts.
LCH_3	*N,N*-diethyl-*N'*-(*p*-methyl)benzoylthiourea.
LCl	*N,N*-diethyl-*N'*-(*m*-chloro)benzoylthiourea.
LET	Linear Energy Transfer.
LH	*N,N*-diethyl-*N'*-benzoylthiourea (as abbreviated in the present study).
LH_2	*N*-alkyl-*N'*-benzoylthiourea.
LNO_2	*N,N*-diethyl-*N'*-(*m*-nitro)benzoylthiourea.
$LOCH_3$	*N,N*-diethyl-*N'*-(*m*-methoxy)benzoylthiourea.
MDP	Methyldiphosphonate.
MoAb	Monoclonal antibodies.
morph-LH	*N*-morpholino-*N'*-benzoylthiourea.
morph-LCH_3	*N*-morpholino-*N'*-(*m*-methyl)benzoylthiourea.
morph-LCl	*N*-morpholino-*N'*-(*m*-chloro)benzoylthiourea.
morph-LNO_2	*N*-morpholino-*N'*-(*m*-nitro)benzoylthiourea.

morph-$LOCH_3$	*N*-morpholino-*N'*-(*m*-methoxy)benzoylthiourea.
NMR	Nuclear magnetic resonance spectroscopy.
PET	Positron Emission Tomography.
PGM	Platinum group metals.
py	Pyridine.
RNA	Ribonucleic acid.
salpd	*N,N'*-propane-1,3-diylbis(salicyledeneiminate).
spiro-LH	8-(*N*-benzoylcarbamoyl)-1,4-dioxa-8-azaspiro[4.5]decane.
spiro-LNO_2	8-(*N*-(*m*-nitrobenzoylcarbamoyl))-1,4-dioxa-8-azaspiro[4.5]decane.
TATU	Thiol-amide-thiourea.
TLC	Thin layer chromatography.
TMP	Thymidylic acid.
TS	Thymidylate synthase.
tu	Thiourea.

CHAPTER 1

INTRODUCTION: CANCER AND ITS TREATMENT.

1.1. Cancer.

Cancer is one of the most feared diseases, with America being the leading victim of this disease.[1] The American Cancer Society (ACS) tracks cancer occurrence and it has been found that since 1990, approximately 13 million new cases of cancer have been diagnosed. This year (2000) about 552,200 Americans are expected to die of cancer, more than 1,500 people a day.[1] Perhaps no other disease known to modern civilization, apart from AIDS, is viewed with so much general fear as cancer. This fear of the indiscriminative nature of cancer, is unquestionably heightened by common knowledge about other aspects of the disease. Considerable efforts are continually directed at improving the treatment and diagnosis of cancer.[2] However, the development of completely successful treatment regimes will not be feasible until we have a deeper understanding of the biology of cancer.

What is cancer? What do we know for sure about this disease, and what is still in the realm of hypothesis and speculation? Let us begin by defining some terms, since popular usage, particularly in the lay community, has led to their frequent misuse. First, the term tumor refers to any localized swelling, regardless of its pathogenesis.[2] Thus, for example, inflammatory swellings or haematomas are approximately defined as tumors. Tumors are either benign or malignant.[1] Many tumors are of course neoplasms, that is, localized swelling consisting of neoplastic tissue and the terms neoplasm and tumor are commonly used interchangeably.[2]

The term cancer refers to the full spectrum of neoplasms, of which well over 100 are known to affect humans. All cancers involve out-of-control growth and spread of abnormal cells by a process called metastasis and they are divided into three broad groups. The carcinomas arise in the epithelia, the sheets of cells covering the surface of the body and lining of the various glands. The much rarer

sarcomas arise in supporting structures such as fibrous tissue and blood vessels. The leukemias and lymphomas arise in blood forming cells of the bone marrow and lymph nodes.[2]

Cancers are classified mainly by the organ in which they originate and the kind of cell involved. When they are considered this way, there are 100 distinct varieties of the disease.[2] Such an elaborate classification would be of no general interest were it not that the different varieties have different causes, since the incidence of each one changes independently when the environment is altered. Most of the 100 varieties are rare, and so we can account for most cancer mortalities by considering a fairly short list of diseases. Roughly half of all cancer deaths are caused by cancers of three organs: the lung, the large intestine and the breast (see figure 1.1.).[2]

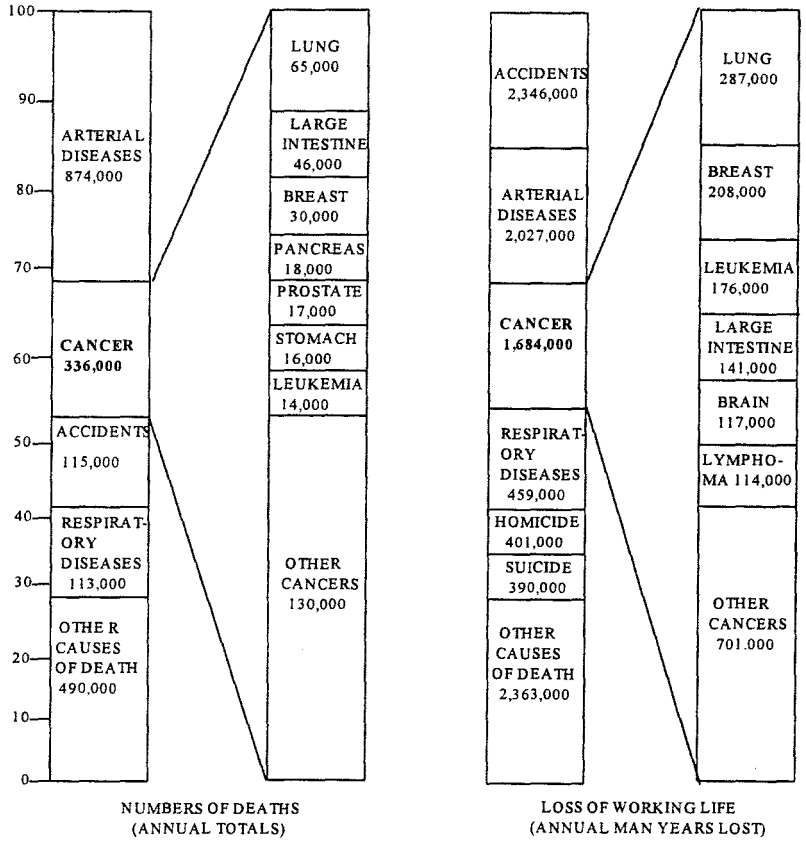

Figure 1.1. A chart of death causes accounting for cancer mortality.[2]

There can therefore be no major inroad on overall cancer mortality until some means are found for curing or preventing these three kinds of cancer. Each of them can be considered a discrete entity because the frequency of each varies independently when factors in the environment are changed.

1.1.1. Cancer at the cellular and molecular level.

The center of the problem of curing/treating cancer is an understanding of the differences between normal and cancer cells. At the cellular level, cancer can be defined with just five words: displaced, disorderly, destructive cell proliferation.[3] It is nothing more or less than the proliferation of cells which should have taken place, in an orderly manner and in accordance with perfectly definite and fixed laws, back in the uterus. A deeper knowledge at the molecular level of the cell, can give a better understanding of how this disordered proliferation of cells originates, and thus ways of antagonizing it.

The cell contains within its cytoplasm a body called a nucleus, which controls the process of cell division. Within the nucleus is a chemical compound which contains the genetic information. This compound is known as DNA.[4] DNA consists of two strands of which each is made up of small units called nucleotides. The nucleotides constitute a ribose sugar unit, nitrogenous base and a phosphate group. There are four different kinds of nucleotides, namely, guanine (G), cytosine (C), thymidine (T) and adenine (A) all differing according to the nitrogenous base component.[4] As an example, the structural formula of guanine is given in figure 1.2.

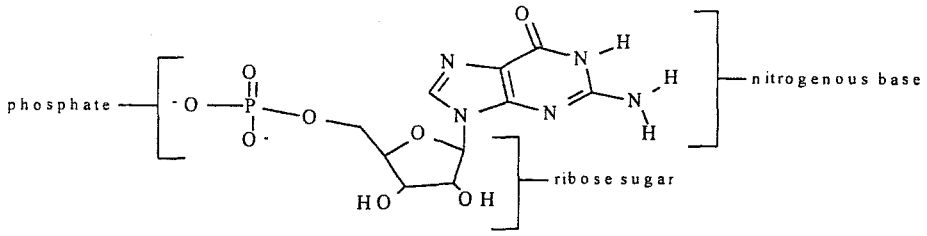

Figure1.2. Structural formula of guanine, as an example of a nucleotide.[4]

The nucleotides are linked together by a phospho-diester bond to form a DNA strand. Two DNA strands are then held together by hydrogen bonding between nucleotides from opposite strands as shown by the example in figure 1.3.

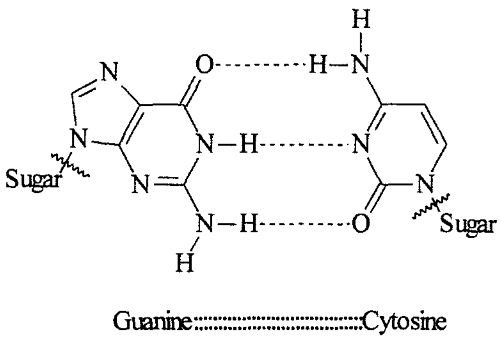

Figure 1.3. Shows the hydrogen bond between guanine and cytosine in DNA.

This double strand of DNA then intertwines to form a double helix.[4] During cell division (proliferation), this double helix unwinds and the DNA undergoes a process called replication.[5] DNA replication is the synthesis of new daughter DNA molecules which are identical to the existing ones. The purpose of DNA replication is to ensure that the same genetic information is carried down from a parent cell to a daughter cell during cell division. Each parental single strand of DNA serves as a template for the synthesis of one new daughter strand. As each new strand is formed, it is hydrogen-bonded to its parental template. Thus, as replication proceeds, the DNA double helices each contain one original parent strand and one newly formed strand.[5]

1.1.2. Carcinogenesis and carcinogens.

Carcinogenesis can be simply defined as cancer origination. Carcinogenesis is the result of gene mutations which occur during the DNA replication. Mutation refers to any change in the base sequence of DNA which gives rise to a gene that is different from the normal gene.[5] Agents which cause the changes in the base sequence of DNA are named carcinogens. Known carcinogens are

chemicals and ultraviolet radiation. These carcinogens cause cancer by interacting with DNA. For example, chemicals such as polycyclic aromatic hydrocarbons intercalate between the base pairs in DNA causing DNA damage and exposure to ultraviolet radiation can cause some deleterious changes to the base pairing of the DNA strands.[2]

In consideration of cancer biology, it is important to determine the cellular response to DNA damage induced by carcinogens. It is important to understand the mechanism involved in the repair of this damage or tolerance of such in DNA. Living cells are endowed with multiple mechanisms for the repair and tolerance of DNA damage. If not properly repaired, the damage becomes fixed in replicated DNA as mutations.[2] Mutations affecting one or more genes involved in growth regulation can result in neoplastic transformation. One of the singular features of neoplasia is that the transformed phenotype is faithfully inherited through the lineage of most affected cells. Hence it is not surprising that the notation of altered structure and/or function of DNA is central to most theories of carcinogenesis.[2]

1.2. Cancer treatment.

If a tumor is discovered in its early stages, it can be removed surgically (surgery), treated with radiation (radiation therapy), treated with hormones (hormone therapy), treated biologically (immunotherapy) or a combination of the above mentioned chemothrerapy treatments.[1, 6] If metastasis has occurred, however, the secondary tumors must also be eliminated and chemotherapy is necessary. Chemotherapy is the treatment of cancer using drugs. This drug treatment aims to control the abnormal cellular reproduction often by interfering with the synthesis and replication of DNA of the cancer cell or by destruction of the cancer cell.[6] The development of anticancer drugs is one of steady progress rather than sudden dramatic developments, as there are many factors which need to be taken into consideration when such drugs are being designed.

The drugs used for cancer therapy can be divided into three categories:

(i) Chemical class.

(ii) Mode of action.

(iii) Origin, *i.e.* whether derived synthetically or from natural sources.

These categories include alkylating agents, platinum derivatives, radioisotopic drugs, antimetabolites and antihormonal agents as well as numerous others such as the plant products, vincristine, vinblastine and podophylotoxins and the antibiotics, bleomycin and adriamycin.[6] Whilst these drugs are sometimes used as single agents, it is more usual to administer them either in combination or sequentially, to avoid the onset of resistance.[6]

1.2.1. DNA targeting drugs.

This group of drugs targets DNA and interferes with DNA replication thus reducing the cell division of the cancer cells. This group of drugs covers a wide spectrum of cancers as they are non-specific to the kinds of cancers they can treat.[2] A number of DNA targeting drugs have entered clinical trials. Among these drugs, the following have received a lot of attention and some of them are currently in clinical use.

1.2.1.1. Alkylating agents.

Alkylating agents were the earliest successful anticancer drugs.[6] Although the largest category is the so-called 'nitrogen mustards', the mode of action of all members of this class is the same. They all have the ability to cross-link opposing strands in the DNA double helix by bifunctional alkylation.[7] The two alkylating functions react typically with guanine bases in DNA, binding opposing strands and preventing the separation needed for cell division to occur.

The simple aliphatic nitrogen mustards, such as the parent member mechlorethamine (see figure 1.4), are reactive and corrosive, hence modification and reduction of the reactivity of these compounds to

get a more acceptable drug was needed.

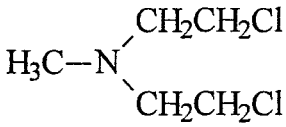

Figure 1.4. Structural formula of mechlorethamine.[6]

It was thought that two refinements of the parent structure mechlorethamine would improve its anticancer viability. The attachment of the nitrogen mustard function to an aromatic ring, thus making the lone pair of electrons on the nitrogen delocalize into the ring, could reduce the reactivity of this structure. The attachment of this alkylating residue to a naturally occurring molecule could encourage selective transport into cells. The drug melphalan, in which the nitrogen mustard is attached to the naturally occurring amino acid L-phenylalanine is an early example of these two concepts and is still in use as an anticancer drug today.[1, 8]

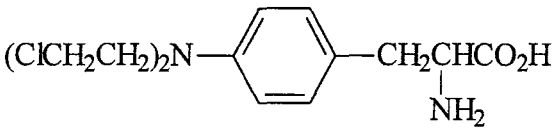

Figure 1.5. Structural formula of Melphalan.[6]

The most widely used alkylating agent is cyclophosphamide, the parent member of the oxazaphosphorine group. Cyclophosphamide and the more recently introduced analogue, isophosphamide, are converted by a multi step pathway (see Scheme 1.1) involving both enzymatic and spontaneous chemical transformations, respectively into phosphoramide mustard and isophosphoramide mustard which are the reactive alkylating agents responsible for these drugs'

anticancer activities.[9] During this process another metabolite called acrolein is also produced (see Scheme1.1).[9,10] Unfortunately, acrolein is toxic to the bladder and has no anticancer activity, but by exploiting its reactivity towards thiols, this toxicity can now be prevented by giving the antidote, mesnum to patients treated with these drugs (see Scheme1.1).[11] Mesnum reacts only with acrolein and not with the active metabolite, to form a non-toxic product and this was shown recently when isophosphamide was used to treat patients with advanced lung cancer.[12]

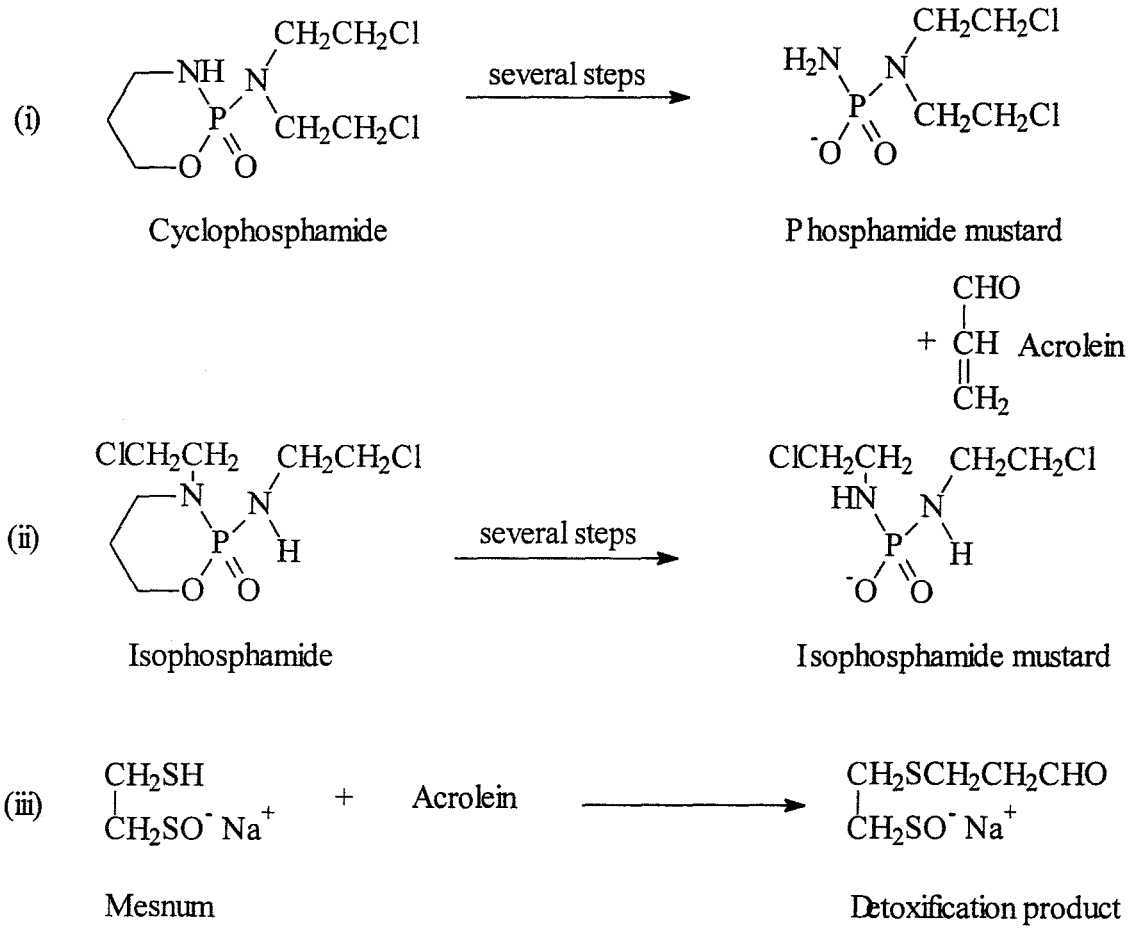

Scheme 1.1. Formation of acrolein during metabolism of oxazaphosphorine drugs and its detoxification.[6]

Although this group of drugs shows some interesting anticancer activities, there are drawbacks

associated with it. Alkylating agents also cross-link the DNA of normal cells. While repair enzymes can reverse this process, given time, rapidly dividing normal cells such as those of the bone marrow, are vulnerable and toxicity to these cells limits both the dose which can be given and the drug's ability to kill cancer cells.[9, 10] However in recent years a new clinical technique called marrow autotransplantation has been used to reduce toxicity to the bone marrow which is usually the most vulnerable organ to alkylating agents.[9]

1.2.1.2. Platinum drugs.

A relatively new important group of DNA targeting drugs are those containing platinum metal.[2] These drugs are similar to alkylating agents in that they act by binding to DNA in a bifunctional manner. *cis*-Diamminedichloroplatinum(II) (commonly known as cisplatin) is the first platinum antitumor drug to enter clinical trials.[13] The first clinical trials in 1971 confirmed that cisplatin was active against several human tumors.[14] It was after this discovery that considerable interest in the pharmacology of metal-based drugs was generated.

The action of cisplatin against cancers has been interpreted in terms of a mechanism whereby the drug is introduced into the bloodstream and is transported to the tumor cell where it undergoes hydrolysis because of the low chloride concentration, and the hydrolyzed species then reacts with pyrimidine or purine bases on the DNA chain.[15-17]

Cisplatin is the most widely used oncolytic agent for the treatment of testicular, ovarian, bladder, and head and neck cancers. It is also an important adjunct for cancers of the cervix, lung, and breast. Its most spectacular success has been in the treatment of testicular cancer, a form of cancer previously resistant to any therapy but now considered to be curable in most cases.[18, 19]

However, cisplatin has three major drawbacks:

(i) It causes toxic side effects, such as nephrotoxicity, nausea/vomiting, myelosuppression,

ototoxicity and neurological complications.

(ii) It only affects a narrow range of tumors.

(iii) Tumor cells develop resistance towards cisplatin.[18]

Attempts to overcome these drawbacks has led to the development of other platinum drugs which could satisfy the following basic criteria.

(i) Development of selectivity as well as a broader spectrum of activity than cisplatin, especially activity in cisplatin resistant tumor lines.

(ii) Modification of the pharmacological properties such as solubility which would allow for other modes of adminstration.

These studies have led to the development of "second generation" platinum complexes. *cis*-Diammine(1,1-cyclobutanedicarboxylato)platinum(II) (commonly known as carboplatin), is the only clinically successful second-generation platinum complex.[20] Unlike cisplatin, carboplatin does not result in significant nephrotoxicity and emesis. Its relatively lower toxicities as compared to cisplatin have been related to the greater pharmacokinetics stability of the 1,1-cyclobutanedicarboxylate ligand in solution.[20] Although carboplatin shows some relative improvements as compared to cisplatin, it still has some drawbacks in that it only affects a narrow range of tumors and tumor cells develop resistance towards this drug.

The major drawback still associated with all DNA-interacting drugs is their interference with the production of normal cells. This is more pronounced in those cells which are rapidly dividing, for instance marrow cells and intestinal mucosa cells. This results in poor selective toxicity towards normal as well as cancerous tissue.[6]

1.2.2. Non-DNA targeting drugs.

1.2.2.1. Antimetabolites.

Antimetabolites are drugs with structures similar to those of naturally occurring molecules that they are designed to antagonize. The most common antimetabolite is methotrexate [21] and it is used in the treatment of acute leukemia in children and also against other cancers, particularly in combination with other drugs. Methotrexate inhibits the enzyme dihydrofolate reductase (DHFR) in folate metabolism by virtue of its close structural resemblance to natural folates, e.g. folic acid. Unfortunately folate reduction takes place in other biochemical pathways besides DNA synthesis, such as the synthesis of RNA, (see Scheme 1.2).[6]

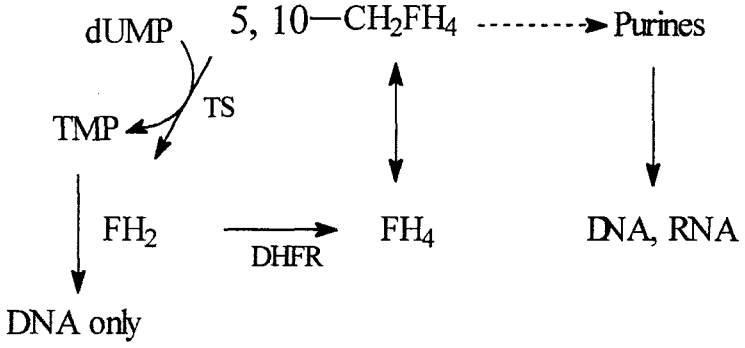

F - Folic acid; TS-Thymidylate synthase; DHFR- Dihydrofolate reductase; TMP-Thymidylic acid; dUMP-2'-Deoxyuridylic acid.

Scheme 1.2. Pathways of folate metabolism.[6]

Methotrexate therefore interferes with processes needed for the normal functioning of cells and hence may contribute to the toxic, as opposed to the tumor-inhibitory, effects of the drug.

Another example of this class of drugs is CB3717 (see figure 1.6). This drug inhibits the enzyme, thymidylate synthase (TS), which catalyzes the formation of the only nucleotide specific to DNA, namely thymidylic acid.[22] This drug's activity against some ovarian, breast and lung cancers resistant to previous treatment coupled with low haematological toxicity, shows the promise of this approach.[23]

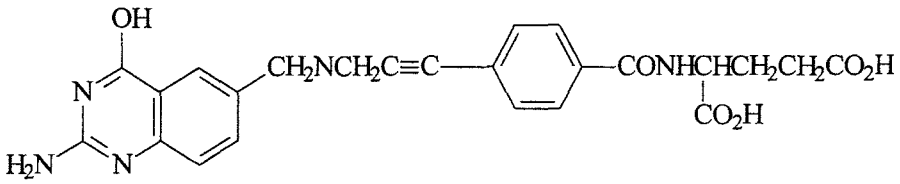

Figure 1.6. Structural formula of CB 3717.[6]

1.2.2.2. Antihormonal agents.

Certain cancers depend on circulating steroid hormones for their growth specifically the female sex hormones estrone and oestradiol in breast cancer and the male hormones testorone and dihydrosterone in prostatic cancer.[24] Formerly these cancers were usually treated by surgery in that affected organs or those responsible for hormone production were removed. The 1970's saw the introduction of a new class of drugs which promised to achieve the same effect by non-surgical means.[24] Such drugs have proved most effective against post-menopausal breast cancer in women, where natural production of steroid hormones is low and most easily counteracted. In particular the drug tamoxifen, acts by competing with the binding of natural oestrogen to an intracellular protein receptor responsible for stimulating cell growth and division.[24] Because these drugs are toxic only to hormone producing cells they are therefore highly selective for the target cancer. However, though prolonging life, these drugs are not curative and therefore further research into their mechanisms of action, and to the causes of relapse, is needed.

1.2.2.3. Immunotherapy.

The advances made in the development of anticancer monoclonal antibodies (MoAbs), and their successful use in diverse laboratory and clinical procedures, have spurred considerable interest in their potential role in the treatment of cancer.[25] Monoclonal antibodies can be administered as

unconjugated antibodies for direct killing of the cells, vaccines, or as carriers of drugs, toxins or isotopes. The use of antibodies as carriers of isotopes plays a role in another form of cancer therapy which is gradually advancing, namely radiopharmaceutical therapy.

1.2.3. Radiopharmaceutical approach.

Radiopharmacy is the field of research in which radioisotopes are used in nuclear medicine. The utilization of radioisotopes in nuclear medicine has been promoted for diagnostic and therapeutic purposes.[26] This field of research clearly shows the relationship between chemistry, pharmacy and medicine aimed at the final goal of overcoming one of the great enemies of human kind, namely cancer.

Technetium and rhenium have shown some interesting properties for use in radiopharmaceuticals and hence studies have recently concentrated on the coordination chemistry of these two elements. Technetium has been thoroughly exploited mainly for its suitable properties for diagnostic purposes. Rhenium is widely used as a non-radioactive model for technetium. However, rhenium itself also has a potential to serve as a nuclide in radiotherapy since its isotopes Re-186 and Re-188 emit β radiation.[27, 28]

1.2.3.1. Technetium radiopharmaceuticals.

Studies indicate that of the millions of diagnostic imaging procedures conducted each year over 80% involve the use of technetium-99m. Even with the advent of more sophisticated procedures such as Positron Emission Tomography (PET) and Magnetic Resonance Imaging (MRI) imaging, technetium radiopharmaceuticals remain the workhorse of nuclear medicine.[29]

The discovery of element 43 (known today as technetium) was reported by Nodack *et al.* in1925 and was named masurium. This element could not be extracted from naturally occurring minerals.

However, in 1937 Perrier and Segre found radioactivity ascribed to this element and on the basis of its chemical properties which were expected from the position between manganese and rhenium in the periodic table, this element (element 43) was firmly established and named technetium. Perrier and Segre are universally credited with the discovery of this element because they were the first to produce this element in weighable quantities from transmutation reactions of deuterons and protons with molybdenum.[31] Technetium then became available because of nuclear fission leading to production of technetium-99 in nuclear reactors.

Technetium is the element of choice in diagnostic nuclear medicine because of the following advantages over other radionuclides: cost, availability and low radiation-absorbed dose. These advantages are in part manifested by the nuclear properties of technetium-99m ($t_{1/2}$ = 6.02 h; γ = 140.6 keV) which also enable imaging results to be applied to clinical evaluation quite rapidly.[32] This radionuclide has relatively little nonpenetrating radiation and decays to a long-lived ground state that is a low-energy beta emitter. The six hour half-life of this radioisotope allows ample time for synthesis and quality control procedures. The emission of γ-rays with a linear energy transfer (LET) of 140.6 keV in a long range, meshes well with the efficiency of sodium iodide detectors in modern gamma cameras thus making external imaging possible.[33] These properties ensure that the absorbed radiation dose to the patient is kept at acceptable levels, as is proper for a diagnostic test and imaging studies.[34]

Technetium-99m radiopharmaceuticals are used in nuclear medicine as diagnostic agents to visualize anatomical structures, metabolic disorders and tumor tissue.[31] A wide variety of tissues can be visualized with technetium-99m radiopharmaceuticals, including the kidneys, bones, lungs, heart, liver, brain and thyroid.

Biodistribution of technetium radiopharmaceuticals.

The modes of biodistribution of technetium radiopharmaceuticals are generally divided into two

distinct classes.[35] The first class, referred to as the technetium-tagged radiopharmaceuticals, consists of technetium-labeled molecules whose biodistribution is entirely determined by the species to which the technetium is attached. This means that the native molecules, if not labeled with the technetium, would exhibit an *in vivo* distribution identical to the technetium-labeled substance. Among many technetium-tagged radiopharmaceuticals are technetium-tagged antibodies, which have been developed in an attempt to image various soft tissue tumors.[35]

The second group of technetium radiopharmaceuticals is the technetium-essential class, which consists of small technetium ligand coordination complexes. In this class of technetium radiopharmaceuticals, the biodistributions are controlled by the physical properties of the technetium complexes themselves. The *in vivo* biodistribution of these radiopharmaceuticals can vary with the structure of the technetium complexes as governed by the technetium oxidation state, functional groups on the ligand and the technetium core configuration.[36]

The technetium-essential class includes technetium complexes used to image tissues such as the kidney, liver, heart and bone. Isolation of pure technetium complexes after HPLC has enabled investigators correlate the physical properties of single technetium complexes to tissue uptake. These structure-activity relationships shed light on the physiological uptake mechanisms of the technetium complexes and provide a better understanding of their biodistribution. This fundamental information aids in the design of new, more effective technetium-99m imaging agents. The applicability of the imaging agents is evidenced by the steady flow of new radiopharmaceuticals into the clinic and by the numerous new compounds being investigated in the research laboratory.[34]

Development of new technetium imaging agents.

The first incentive behind the research into new technetium-99m agents is a direct result of the ever increasing amount of fission products being generated by power reactors, and hence the long-lived nuclide technetium-99. The availability of this isotope in weighable quantities makes it possible for

conventional studies of technetium chemistry to be carried out, applying the usual spectroscopic and analytical methodologies of the inorganic chemist. This work began in the 1970's and is still continuing today. In these studies the new classes of technetium-99 complexes are generated, fully characterized and cellular or tissue preparations are used to study the biodistribution of these complexes.[34]

A classic example of the successful use of technetium-99m for diagnostic purposes, is the use of technetium-99m agents as bone seekers. In these studies diphosphonic acid derivatives labeled with technetium-99m were used as imaging agents for bone diseases.[29] Initially it was thought that because the primary constituent of the mature mineralized matrix of the bone is a crystallized hydroxyapatite ($Ca_{10}(PO_4)_6(OH)_2$), the source of phosphate in the form of pyrophosphate and phosphate esters can be labeled with technetium-99m and be used as diagnostic/imaging agents for bone.[29] The pyrophosphates in these agents direct the technetium-99m to the bone tissue (bone-seeking effect) due to its affinity for ($Ca_{10}(PO_4)_6(OH)_2$). These studies have shown that though the technetium-99m pyrophosphate is localized in bone, the hydrolysis of the pyrophosphate produced complications in blood clearance and soft tissue uptake. However, technetium-99m bone imaging agents could be produced with hydroxyethylidene diphosphonate (HEDP) and polyphosphonates (see figure1.7).[31] HEDP was known to inhibit bone growth, thus its interaction with the ($Ca_{10}(PO_4)_6(OH)_2$) mineralization process had been established.[29]

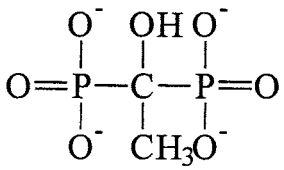

Figure 1.7. Structural formular of Hydroxyethylidene diphosphonate (HEDP).[29]

Since then technetium-99m with diphosphonate derivatives have proved to be the agents of choice because they are not metabolized, thus giving suitable blood and soft tissue clearances. Because technetium-99m diphosphonates accumulate in regions of new bone formation (where phosphate is needed), these agents are used to image skeletal conditions including accelerated bone turnover, such as remodelling of a bone break or in the compensatory new bone response that accompanies a cancerous osteolytic lesion. Technetium-99m(MDP), (MDP = methyldiphosphonate), has proved to be the most popular bone scanning agent because of its rapid blood clearance.[29]

Technetium chemistry in development for radiopharmaceuticals.

The original effort in these studies was directed towards new complexes that could be synthesized in high yield in aqueous media, because the starting material in practice is the pertechnetate $[^{99}TcO]^{3+}$ ion in isotonic saline.[34] Among the various oxidation states of technetium explored in imaging/diagnostic agents design, technetium(V) has proven to be the most suitable for synthesis of well-defined monomeric complexes that are sufficiently stable in aqueous solution and permit great variability in molecular structure and properties.[33]

As far as radiopharmaceutically relevant chemistry in aqueous solution is concerned, technetium(V) chemistry is governed by the oxotechnetium species. The reason for this is the need for neutralization of the high formal charge on technetium(V).[35] Oxotechnetium species are most conveniently categorized on the basis of their cores (see figure 1.8). One dominant structural element is the monooxotechnetium core, $[TcO]^{3+}$.

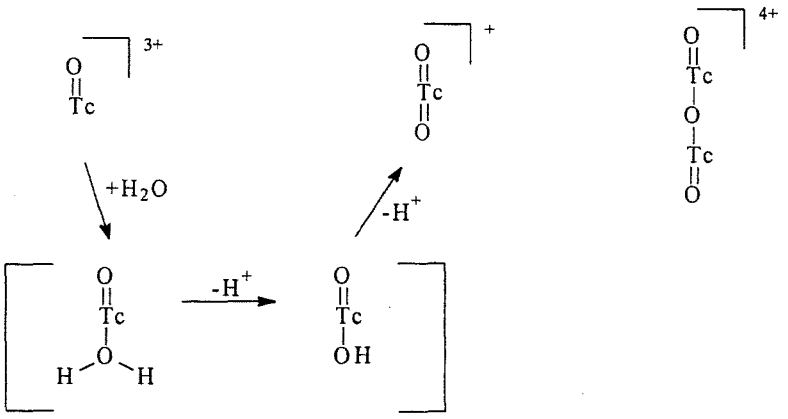

Figure 1.8. Oxotechnetium cores.[33]

The oxo ligand has a significant affect on the structure and reactivity of the derived complex. For instance the TcO group induces a large *trans* effect which labilizes the group *trans* to it and as a result 5-coordinate complexes are generally formed. The large steric requirement related to the short Tc=O distance also plays a role in that it causes the technetium to be displaced significantly above the plane of the four ancillary ligand donor atoms. This results in a square-pyramidal arrangement of the donor atoms with the oxo group at the apex (see figure 1.9). This has been observed from X- ray crystal data, which are available for a variety of complexes, ranging from the most simple one such as the five coordinate $[TcOCl_4]^-$ complex containing four monodentate ligands, to those containing more complicated ligands having two or more donor groups. The presence of Tc=O in the complex is indicated by its stretching vibration in the infrared (IR) spectra as a sharp, intense band in the region of 890 to 1020 cm^{-1}. The position of the band can be related to the electronegativities of the ligands in the equatorial plane.[33]

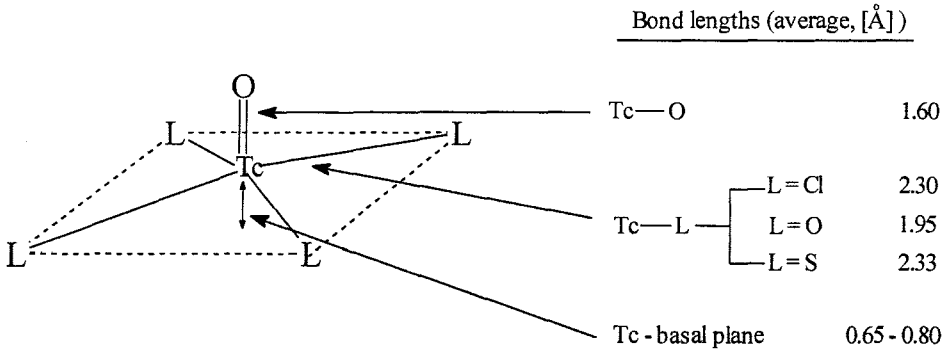

Figure 1.9. Schematic representation of the square-pyramidal $TcOL_4$ unit.[33]

In the complex, $[TcOCl_4]^-$, the ligands have different labilities. The oxo position is very inert to substitution, but the chloride ligands may be replaced by other ligands to give a variety of complexes. The position *trans* to the oxo group is very labile and is free in the $[TcOCl_4]^-$ complex. Occasionally, the coordination of the sixth position may occur. This happens when $[TcO]^{3+}$ complexes with ligands which occupy equatorial positions and force an additional donor group of the ligand in a position *trans* to the oxo group, for example complexes of $[TcO]^{3+}$ with the penicillamine (see figure 1.10).

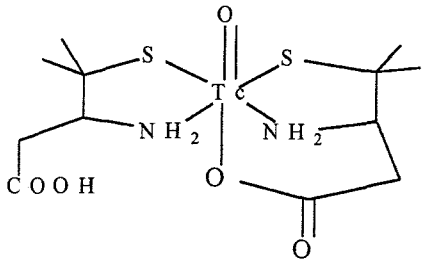

Figure 1.10. Structural formula of [TcO(Hpen) (pen)], Hpen = penicillamine.[33]

The second technetium(V) core, $[TcO_2]^+$ (bisoxotechnetium(V)), is favored by neutral ligands such

as amines or those with efficient π-back-bonding properties. This core forms complexes which adopt an octahedral geometry. An example of this type of technetium(V) complexes is $[TcO_2(py)_4]^+$ (see figure 1.11).[37, 38, 39]

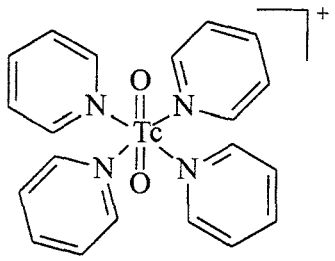

Figure 1.11. Structural formula of $[TcO_2(py)_4]^+$.[39]

The one oxo group of the bis-oxo core can function as a ligand to a second technetium center, thus generating a nearly linear oxygen bridged structure which leads to a third group of oxotechnetium complexes containing a $[Tc_2O_3]^{4+}$ core. Examples of complexes derived from this structural element are tetradentate N_2O_2 Schiff base ligands and bidentate neutral thioethers (see figure 1.12). Because the bridge-formation converts a double-bonded oxo ligand into a bis-monodentate ligand, the Tc-O bond lengthens considerably.[33]

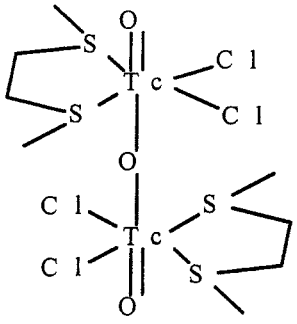

Figure 1.12. Structural formula of μ-O[TcO($C_2H_4S_2R_2$)Cl_2]$_2$.[33]

The complexes discussed above are examples of the occurrence of technetium(V)-oxo cores shown in figure 1.8. The formation of each one of these cores depends on the type of ligands around the technetium nucleus and the pH conditions of the reaction mixture.

The coordination chemistry of technetium(V) has been studied extensively and a variety of complexes with O, S, P and N donor ligands have been reported.[26, 29, 32, 33] The incentive behind the design and synthesis of all these complexes was a search for new improved imaging/diagnostic agents.

1.2.3.2. Rhenium radiopharmaceuticals.

While technetium has proved to be the best radionuclide for imaging and diagnosis of abnormal tissue, its properties do not meet the requirements for therapeutic purposes. The reason is that γ-rays are long ranged and have a low LET and also the short half life (6 h) of technetium-99m does not provide ample time for therapeutic purposes.[33] Long range radiation is not good because normal cells around the tumor area can also be destroyed during a therapy session. The low energy (140.6 keV) associated with γ-emission by technetium, does not provide enough LET to kill tumor cells.[33] However, the success in the study of technetium chemistry and its utilization in nuclear medicine has provoked an interest in the search for suitable therapeutic radiopharmaceuticals.[26] More recently, radiopharmaceuticals using rhenium, the group 7 congener of technetium, in the form of rhenium-186 and rhenium-188 have been developed and further research in this area is still underway.[32, 33]

The physical properties of rhenium-186 are particularly attractive because of its half-life (90 h) and strong β-emission (β_{max} = 1070 keV) which enable this isotope to deliver high-radiation doses to tissues. β-particles have penetration ranges in tissue in the order of few millimeters to a few centimeters and are useful for the irradiation of small- to medium-size tumors. The range of β-particles provides uniform irradiation to a tumor despite a nonuniform distribution of labeled compound within the tumor.[26] The longer half life of this radioisotope compared to that of technetium provides enough time for accumulation of the compound in tumors before it decays. Also

rhenium-186 has a photon emission at approximately the same energy as technetium-99m (γ = 137 keV) in low abundance, allowing the radioisotope to be imaged by γ-cameras utilized in conventional technetium-99m imaging.[29, 33]

Rhenium was first detected in the X-ray spectra of certain mineral concentrates by Nodack, Tacke, and Berg in 1925 and it was the last of the stable elements to be discovered.[40] Rhenium is among the least abundant elements, both in the crust of the earth and in the solar system. There are no sufficiently elevated concentrations anywhere in nature to permit economic extraction as the primary commodity, and the only source is as a by-product of the molybdenum industry. Rhenium is obtained as a volatile dirhenium heptoxide which passes into the effluent gases when molybdenite is roasted to molybdenum trioxide.[40] It is then recovered by wet scrubbing or leaching with water and isolated from aqueous extracts either by selective adsorption as $[ReO_4]^-$ on an anion exchanger or extraction. Rhenium is finally precipitated as the commercial products, $[NH_4ReO_4]$ or $[Re_2S_7]$.

Rhenium-186 is usually produced by the thermal neutron capture reaction of rhenium-185 (rhenium-185(n,γ)) in a nuclear reactor. However, the specificity of rhenium-186 produced in this manner is limited by the neutron flux in the reactor. Because of the lack of high flux neutron reactors worldwide, which can produce rhenium-186 in high specific activity, rhenium obtained from neutron capture reactions is of low specific activity. Use of a radionuclide in labelling of monoclonal antibodies requires higher specific activity of the radioisotope so that a higher therapeutic effect is achieved, hence there is a need for enhancement of the specific activity of rhenium-186.[26] Rhenium-186 with very high specific activity is produced by the tungsten-186(p,n)-rhenium-186 reaction using a cyclotron. The chemical separation of rhenium-186 from tungsten by an anion exchange method gives no carrier added rhenium-186 and a product solution with radiochemical purity above 99% is obtained.[26]

The biodistribution of rhenium-186 radiopharmaceuticals.

The periodic relationship between technetium and rhenium suggests that the therapeutic rhenium radiopharmaceuticals can be designed by analogy to existing technetium-99m diagnostic agents. It is therefore anticipated that rhenium-186 therapeutic agents will be distributed in a similar way to technetium-99m diagnostic agents in a biological environment.[32]

Developments in therapeutic radiopharmaceutical agents.

The radiopharmaceutical chemistry of rhenium for cancer therapy is a new and developing field. The rapid increase in the number of papers concerned with rhenium-186 and rhenium-188 complexes for nuclear medicine clearly shows the importance of the chemistry of rhenium complexes. The need for effective cancer therapy with radiopharmaceuticals is the incentive for the development of new and more effective radiopharmaceuticals for the treatment of cancer. Even if complete recovery from the disease has not yet been achieved, positive changes in the quality of life (in about 80% of all patients) were reported by rhenium treatment of bone metastases.[26]

Studies have shown that rhenium-186 labeled diphosphonate compounds are as good as the technetium-99m diphosphonate bone seeker agents. The rhenium-186(HEDP) complex has been investigated clinically because of its specifically high labelling yields in a neutral pH range and it has demonstrated effective palliation of bone pain due to primary metastases of primary carcinomas.[26]

The use of bifunctional ligands in labeling of monoclonal antibodies with metallic radiosisotopes in cancer therapy is one area which has gained great popularity in nuclear medicine. More recently the labeling of antibodies has been investigated using a diamide dimercaptide (N_2S_2) ligand and a triamide mercaptide (N_3S) ligand.[26] The attachment between the monoclonal antibody (MoAb) and the rhenium complex was carried out by coupling of the active ester groups of the rhenium-complex (Re-N_2S_2 or Re-N_3S) with the lysine amino groups (MoAb-NH_2) of the proteins (see Scheme 1.3).[26]

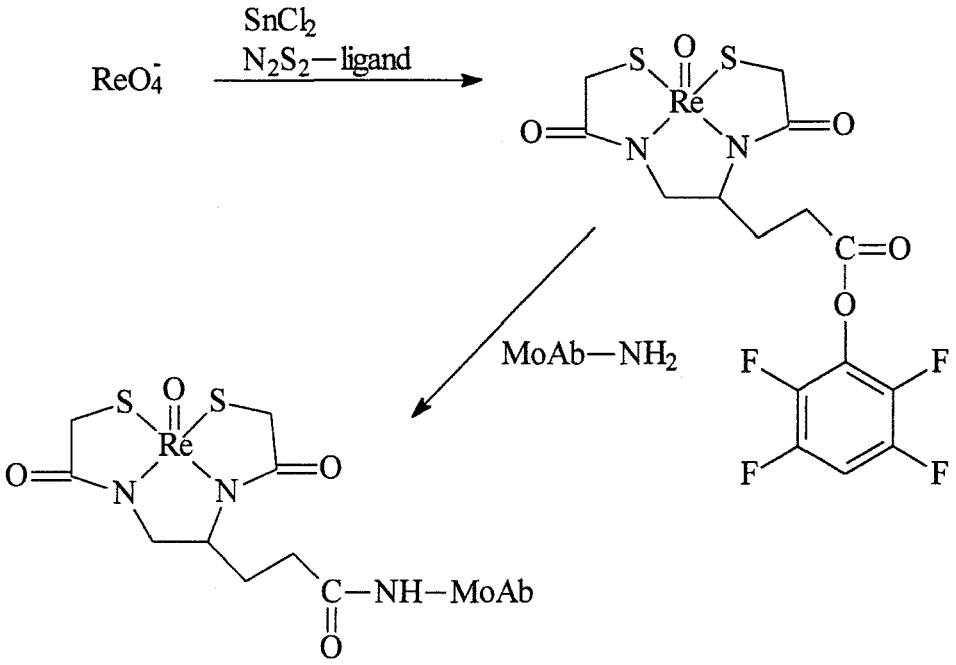

Scheme 1.3. General scheme for MoAb radiolabeling with rhenium using an N_2S_2-ligand.[26]

When effective site-specific therapeutic or diagnostic radiopharmaceuticals are developed many important factors must be considered. It is essential that the metallic radionuclide upon interaction with a bifunctional chelating agent should form an *in vivo* stable complex in high specific activities with 1:1 metal to ligand stoichiometry.[41] These stringent requirements restrict the choice to only a few ligand backbones and, therefore, necessitates the design and development of new bifunctional chelating agents. Most importantly, an understanding of the coordination chemistry of new ligand systems with non-radioactive rhenium is important for the subsequent extension of these reactions at the tracer levels to label bifunctional chelating agents using the radioactive rhenium.

Rhenium chemistry in the development of radiopharmaceuticals.

Entry into the chemistry of rhenium is usually afforded by access to the commercially available perrhenate salts [NH_4ReO_4] and [$KReO_4$], although rhenium itself is sometimes used as the starting material.[42] Rhenium has oxidation numbers ranging from 0 to 7. Of these, Re(VI), Re(I) and Re(0) are rare while Re(II) is encountered mainly in triply bonded dirhenium complexes, that is those possessing a Re_2^{4+} core.[42]

For the present study, Re(V)-oxo complexes were considered. With few exceptions, complexes of rhenium(V) have been found to be essentially diamagnetic and of all these cores, $[Re=O]^{3+}$, $[O=Re=O]^{+}$ and $[O=Re-O-Re=O]^{4+}$, have been found to be the dominant ones. Rhenium in this oxidation state generally has a coordination number of 6 and it is nearly always found in a pseudo-octahedral geometry (see examples in figure 1.13).[40, 42]

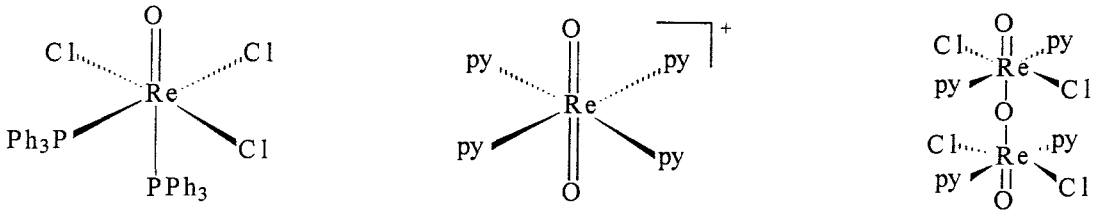

Figure 1.13. Examples of $[Re=O]^{3+}$, $[O=Re=O]^{+}$and $[O=Re-O-Re=O]^{4+}$ cores, respectively.[42]

Tetrachlorooxorhenate(V), $[ReOCl_4]^-$, is an example of a rhenium(V) complex with a $[ReO]^{3+}$ core (see figure 1.14). As in the case of technetium, the chloride ligands form a square basal plane with the oxo ligand at the apex of the square pyramid. The oxo ligand is very inert to substitution and it exerts a *trans* effect to the position *trans* to it.[40, 42] The 5 coordinate complexes are unsaturated and readily increase their coordination number to 6.[40]

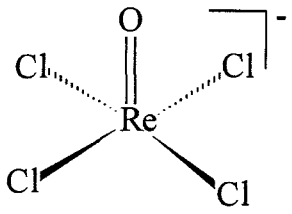

Figure 1.14. Structural formula of $[ReOCl_4]^-$ as an example of the $[Re=O]^{3+}$ core.[40]

The $[O=Re-O-Re=O]^{4+}$ core results from the dimerization of $[ReO]^{3+}$ containing complexes in the presence of water. In this process the ligand *trans* to the oxo ligand exchanges with water from air, after which two molecules of the monooxo species dimerize through the formation of an μ-oxo bond.[27,43] For example, during the synthesis of $[ReO(py)_4]Cl$ from $ReOCl_3(PPh_3)_2$ and in the presence of water, the intermediate, $ReO(OH)Cl_2(py)_2$, loses the OH^- ligand in the form of H_2O and undergoes dimerization, as shown in Scheme 1.4.[43]

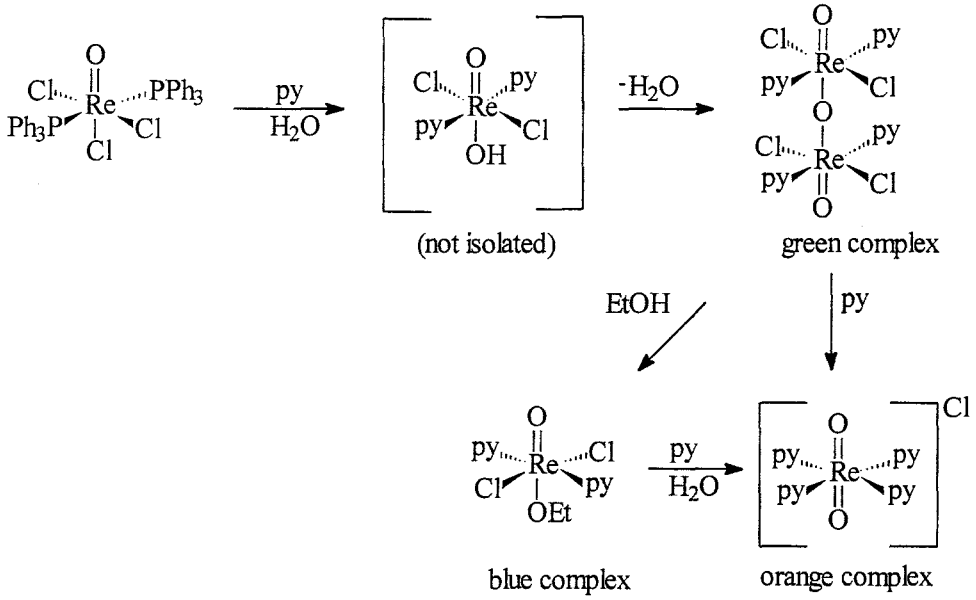

Scheme 1.4. Shows an example of the inter-conversion between the $[ReO_n]^{n+}$ cores.[43]

The oxo-bridge of the green $[Re_2O_3Cl_4(py_4)]$ complex can be cleaved by heating the complex in ethanol to give the blue $[ReOCl_2(OEt)py_2]$ complex. In a further reaction with excess moist pyridine, this blue complex gives the dioxo complex, *trans*-$[ReO_2(py_4)]Cl$.[43] This example shows that the three cores, $[Re=O]^{3+}$, $[O=Re=O]^{+}$ and $[O=Re-O-Re=O]^{4+}$, are interchangeable under suitable conditions. The type of core present in the complex is indicated by the IR stretch of the Re=O bond. Depending on the type of ligands around the rhenium nucleus, the stretching frequencies of the Re-O bonds in these cores are normally found in the following regions: ν(Re=O) in $[Re=O]^{3+}$ and $[O=Re-O-Re=O]^{4+}$ is observed between 912 and 995 cm^{-1}, ν(Re=O) in $[O=Re=O]^{+}$ is observed between 775 and 835 cm^{-1}, and ν(Re-O) for the μ-oxo species has additional bands between 660 and 670 cm^{-1} assigned to (Re-O-Re).[40, 43, 44]

The coordination chemistry of rhenium(V), like that of technetium(V), has been studied extensively with ligands containing O, N, S and P donor atoms for radiopharmaceutical purposes. Rhenium complexes with the monodentate thiourea and various substituted thiourea ligands are also known.[45-49] However, to the best of our knowledge, only one example of a rhenium(V) complex with an acylthiourea ligand has been reported. Dilworth *et al.* have shown that the reaction between the rhenium(V) precursor $[ReOCl_4]^-$ and *N, N*-diethyl-*N'*-benzoylthiourea (DEBTH) in methanol at room temperature under an inert atmosphere resulted in the formation of $[ReO(DEBT)_2Cl]$, shown in figure 1.15.[50]

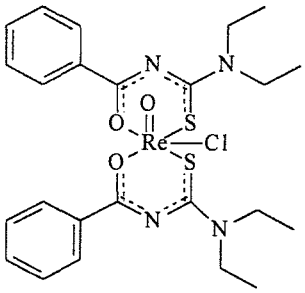

Figure 1.15. Structural formula of $[ReO(DEBT)_2Cl]$.[50]

The crystallographic study of this complex showed that the geometry about the rhenium atom is essentially octahedral, with the chloride and oxo ligand *cis* to each other and the sulphur and oxygen donor atoms of the two acylthiourea ligands in a *cis* arrangement. The *cis* arrangement of the chelated ligands results in one of the oxygen atoms occupying an axial site *trans* to the oxo ligand and hence the non-symmetrical coordination of the two bidentate ligands.[50]

Despite the large number of technetium and rhenium complexes discovered thus far, there is still a demand for fundamental knowledge about the structural and spectroscopic properties of these complexes and mechanism of ligand substitution reactions to develop new and improved rhenium and technetium radiopharmaceuticals.[28]

1.3. Research objective of the present study.

The objective of the present study is the preparation and characterization of Re(V)-oxo and Tc(V)-oxo complexes with *O,S* chelating ligands, namely *N,N*-dialkyl-*N'*-(substituted)benzoylthioureas (see figure 1.16), for potential use as radiopharmaceutical agents.

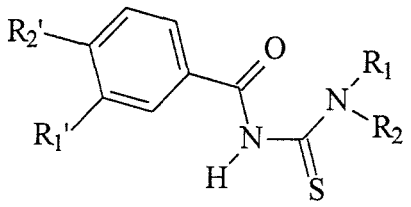

Figure 1.16. The general structure of *N,N*-dialkyl-*N'*-(substituted)benzoylthiourea ligands.

The *N,N*-dialkyl-*N'*-(substituted)benzoylthiourea ligand systems were chosen for the following reasons:

1. The ease of preparation of these ligand systems. The synthesis of these ligand systems is simple and straightforward, being completed in one reaction vessel and generally results in high yields of the product.
2. The versatility of the acylthiourea as a synthon makes it possible to synthesize a range of ligands with different chemical and physical properties by simply varying the R and the R' groups and this could lead to different biological activities of the resultant rhenium(V) and technetium(V) complexes.
3. The possibility of varying the R and the R' groups could also allow for the incorporation of suitable functional groups for the attachment of a biological molecule.
4. Two acylthiourea ligands could be linked to form tetradentate ligands, which could lead to more stable rhenium(V) and technetium(V) complexes.

1.4. Research Approach.

Since the coordination chemistry of rhenium(V) and technetium(V) with these ligand systems have not been studied in any great detail, the main focus of the present study is to examine the coordination chemistry of rhenium(V) with a series of *N,N*-dialkyl-*N'*-(substituted)benzoylthiourea ligand systems and to prepare analogous technetium(V) complexes.

In order to achieve this, the following studies were carried out:

1. Synthesis of a series of acylthiourea ligands (Chapter 2).
2. Synthesis of different Re(V)-oxo precursors (Chapter 3).
3. Preparation of Re(V)-oxo complexes of the acylthiourea ligands using different Re(V)-oxo precursor complexes and optimization of reaction conditions, as well as full characterization of the resultant complexes using various techniques (Chapter 4).
4. Preparation and characterization of an analogous Tc(V)-oxo complex (Chapter 5).

REFERENCES.

1. American Cancer Society, http://www.cancer.org/statistics/index.html.
2. E. C. Friedberg, *Cancer Biology,* W. H. Freeman and Company, New York, (1986).
3. C. W. G. Rohrer, *Research in Cancer: Part one*, Brentwood, Baltimore, (1934).
4. A. Kornberg, *DNA Replication*, W. H. Freeman and Company, San Francisco, (1980).
5. D. Freidfelder, G. M. Malacinski, *Essentials of Molecular Biology, 2nd ed.,* 112, Jones & Bartlet publishers, Boston, (1992).
6. M. Jarman, *Chemistry in Britain*, **25**, 51, (1989).
7. R. J. Goldacre, A. Loveless, W. C. J. Ross, *Nature (London)*, **163,** 667, (1949).
8. F. Bergel, J. A. Stock, *J. Chem. Soc.*, 2409, (1954).
9. M. Colvin, C. A. Padgett, C Fenselau, *Cancer Res.*, **33**, 915, (1973).
10. T. A. Connors, *Biochem. Pharmacol.*, **23**, 115, (1974).
11. J. R. Jones, *Eur. J. Cancer,* **17**, 11, (1981).
12. B. M. Bryant, *Lancet*, **2**, 657, (1980).
13. B. Rosenberg, L. van Camp, T. Krigas, *Nature (London)*, **205**, 698, (1965).
14. C. F. J. Barnard, M. J. Cleare, P. C. Hydes, *Chemistry in Britain*, **22**,1001, (1986).
15. M. J. Cleare, *Coord. Chem. Rev.*, **12**, 349, (1974).
16. A. J. Thomson, *"Platinum Coordination Complexes in Cancer Chemotherapy"*, Connor & Roberts publishers, New York, (1956).
17. M. J. Cleare, *J. Clinical Hemat. Oncol.,* 7, 1, (1965).
18. B. Rosenberg, L. van Camp, J. F. Trosko, V. H. Masour, *Nature (London)*, **222**, 385, (1969).
19. P. J. Loehrer, Sr. S. D. Williams, L. H. Einhorn, *J. Natl. Cancer Inst.*, **80**, 1373, (1988).
20. S. J. Harlad, D. R. Newell, L. M. Atkins, A. H. Smith, K. R. Harrap, *Cancer Res.*, **44**, 693, (1984).
21. J. R. Bertino, *Cancer Treat. Rep.*, **17,** 11, (1981).
22. B. M. Bryant, *Lancet*, **2**, 657, (1980).

23. A. H. Calvert, *J. Clin. Oncol.*, **4**, 1245, (1986).

24. R. I. Nicholson, *Nonsteroidal antioestrogens: molecular pharmacology and antitumour activity*, Sutherland & Jordan, New York Academic, (1982).

25. D. M. Goldberg, G. L. Griffiths, *J. Nucl. Med.*, **33**, 1110, 1992).

26. K. Hashimoto, K. Yoshihara, *Top. Curr. Chem.*, **176**, 276, (1996).

27. K. J. C. Van Bommel, W. Verboom, H. Kooijman, A. L. Spek, D. N. Reinhoudt., *Inorg. Chem.*, **37**, 4197, (1998).

28. J. M. Botha, K. Umakhoshi, Y. Sasaki, G. J. Lamprecht, *Inorg. Chem.*, **37**, 1609, (1998).

29. T. C. Pinkerton, C. P. Desilets, D J. Hoch, M. V. Mikelson, G. M. Wilson, *J. Chem. Ed.*, **62**, 965, (1985).

30. W. Nodack, I. Tacke., *Naturwiss.*, **13**, 567, (1925).

31. C. Perrier, E. Segre., *J. Chem. Phys.*, **7**, 155, (1939).

32. D. J. Rose, K. P. Maresca, P. B. Kettler, Y. Da Chang, V. Soghomomian, Q. Chen, M. J. Abrams, S. K. Larsen, J. Zobieta, *Inorg. Chem.*, **35**, 3548, (1996).

33. B. Johannsen, H. Spies, *Top. Curr. Chem.*, **175**, 79, (1995).

34 A. G. Jones, *Radiochimica Acta*, **70/71**. 289, (1995).

35. L. G. Marzilli, A. V. Kramer, H. D. Burns, L. A. Epps, *"Technetium in Chemistry and Nuclear Medicine"*, E. Deutsch, M. Nicolini, H. N. Wagner, Verona, Italy, (1983).

36. C. Srivastava, P. Richard, *"Radiotracers for Medical Application"*, CRC Press, Raton,(1983).

37. A. F. Kuzina, A.A Oblova, V. I. Spitsyn, *Inorg. Chem.*, **17**, 1377, (1972).

38. P. H. Fackler, M. E. Kastner, M. J. Clarke, *Inorg. Chem.*, **23**, 3968, (1984).

39. M. Melnik, J. E. Van Lier, *Coord. Chem. Rev.*, **77**, 275, (1987).

40. G. Rouschias, *Chem. Rev.*, **74**, 531, (1974).

41. C. J. Smith, K. V. Katti, W. A. Volkert, L. J. Barbour, *Inorg. Chem*, **36**, 3928, (1997).

42. G. Wilkinson (editor-in chief), *Comprehensive Coordination Chemistry,* **4**, 125, Pergamon Press, Great Britain, (1987).

43. N. P. Johnson, C. J. L. Lock, G. Wilkinson, *J. Chem. Soc.*, 1054, (1964).

44. N. P. Johnson, F. I. M. Taha, G. Wilkinson, *Inorg. Synth.*, 2614, (1964).

45. T. Lis, *Acta Cryst.*, **B 32**, 2707, (1976).

46. T. Lis, *Acta Cryst.*, **B 33**, 944, (1977).

47. M. Lipowska, B. L. Hayes, L. Hansen, A. Taylor, Jr., L. G. Marzilli, *Inorg. Chem.*, **35** 4227, (1996).

48 R. D. Adams, J. H. Yamamoto, L. Zhang, M. Huang, *Chem. Ber.*, **129**, 137, (1996).

49. U. Abram, S. Abram, R. Alberto, R. Schibli, *Inorg. Chim. Acta*, **248**, 193, (1996).

50. J. R. Dilworth, J. S. Lewis, J. R. Miller, Y. Zheng, *Polyhedron*, **12**, 221, (1993).

CHAPTER 2

SYNTHESIS AND CHARACTERIZATION OF ACYLTHIOUREA LIGANDS.

Introduction.

2.1. Thiourea.

The monodentate thiourea ligand ($S=C(NH_2)_2$) has played a considerable role in the development of the coordination chemistry of the transition metals. In metal complexes the thiourea coordinates effectively through the sulfur atom.[1] The coordination of the thiourea through the sulfur atom, like all other S-donor ligands, exerts a high *trans* effect on the ligand coordinated *trans* to it.[2] This can be exemplified by the stepwise substitution of NH_3 and Cl by the thiourea ligand (tu) in the formation of *cis*-$[Pt(CS(H_2N)_2)_4]^{2+}$ (see Scheme 2.1).

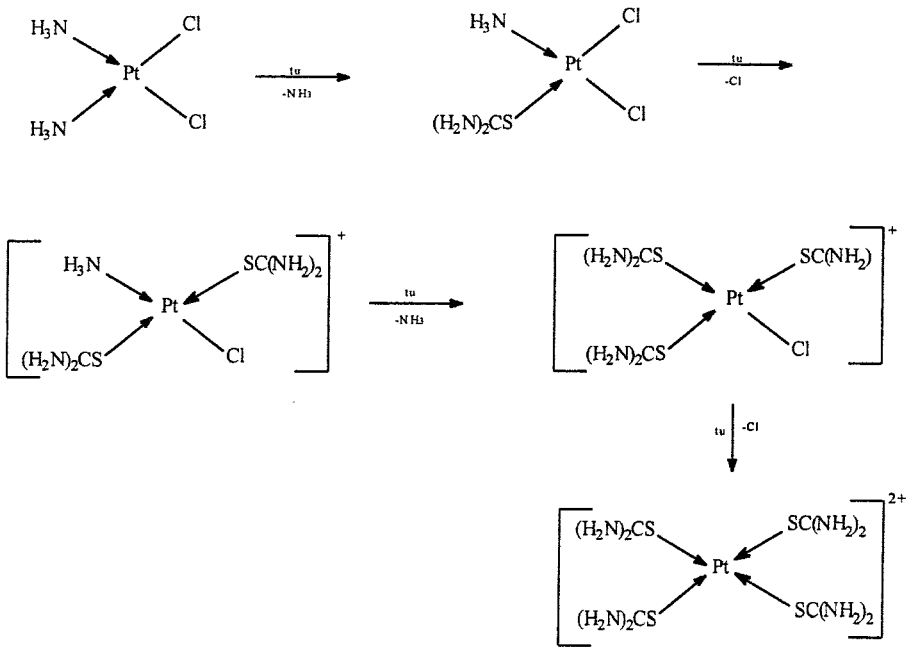

Scheme 2.1. The formation of $[Pt(SC(H_2N)_2)_4]^{2+}$ from $[Pt(NH_3)_2Cl_2]$, showing the high *trans* effect exerted by the thiourea on the ligand coordinated *trans* to it.[2]

2.2. The acyl derivatives of thiourea.

The thiourea derivatives in which a hydrogen on one of the nitrogens has been substituted for an acyl group (RC=O) are called acylthiourea ligands. The other nitrogen atom can either be disubstituted or monosubstituted to give *N, N*-dialkyl-*N'*-acylthiourea (LH) and *N*-alkyl-*N'*-acylthiourea (LH_2) ligands, respectively (see figure 2.1). This class of ligands has the potential of coordinating to a metal bidentately through the sulfur and oxygen atoms.

The selective binding of *N, N*-dialkyl-*N'*-benzoylthiourea and *N*-alkyl-*N'*-benzoylthiourea (i.e R' = phenyl ring and R = alkyl) to the platinum group metals (PGM) has stimulated interest in this class of ligands.[3-5] Due to their selective binding property, these ligands have found extensive use in selective extraction, separation and the trace enrichment of the platinum group metals.[3-8] Since then a range of different acylthiourea ligands have been synthesized and used in the preparation of metal complexes for various purposes including chemotherapy.[3-14]

Figure 2.1. General structures of *N*-alkyl-*N'*-acylthiourea (LH_2) and *N, N*-dialkyl-*N'*-acylthiourea (LH), respectively.

Crystallographic studies have shown that the structures of the monoalkyl- and dialkyl-substituted acylthioureas are significantly different. The difference between these two ligand structures is the presence of an intramolecular N-H---O hydrogen bond (see figure 2.2) in LH_2 which locks the carbonyl oxygen atom into a virtually planar six-membered ring.[13, 14]

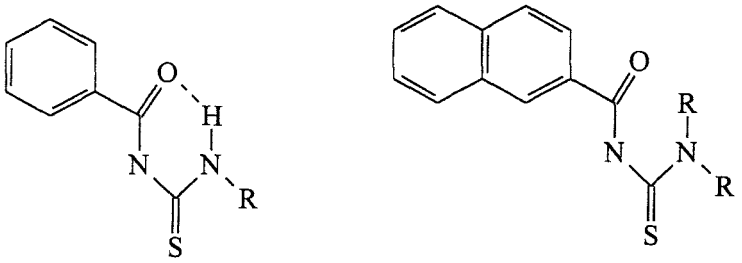

Figure 2.2. *N*-(*n*-butyl)-*N'*-benzoylthiourea and *N,N*-di(n-butyl)-*N'*-naphthoylthiourea exemplifying the structural difference in LH_2 and LH ligands.[14]

Consequently, it has been found that the coordination chemistry of platinum group metals with LH_2 differs considerably from the LH analogues.[14,15] For example, studies with platinum(II) have shown that LH coordinates to platinum(II) in a bidentate manner, through the S and O donor atoms to give predominantly *cis*-$[PtL_2]$ complexes. On the other hand, the LH_2 tends to bind monodentately to the platinum ion, thorough the S donor atom, to yield a mixture of *cis*- and *trans*-$[Pt(LH_2)Cl_2]$ complexes.[15]

The coordination chemistry of *N,N*-dialkyl-*N'*-(substituted)benzoylthiourea ligands, shown by the general structural formula in figure 1.16 (Chapter 1), with copper, nickel and cobalt has been examined to study the effect of different R groups on the nature, geometry and the redox properties of the resultant complexes. In these studies ligands with $R_1 = R_2$ = ethyl and R_1, R_2 = morpholine and R_1', and R_2'= H, NO_2, Cl, OCH_3 and CH_3 were used. It has been shown that while R_1 and R_2 have very little effect on the nature, the geometry, and the redox properties of the resultant compounds, R_1', and R_2' can induce a large alteration of the electronic effects of the ligand and therefore a change in the properties of the complex.[9,10]

Considering the properties discussed above, the present studies concentrated on the synthesis of *N,N*-dialkyl-*N'*-(substituted)benzoylthiourea ligands with different R and R' in order to synthesize a range of these type of ligands with various chemical properties. The structural formulae and the corresponding full names of the ligands used for these studies are given in figures 2.3 (a) - (c).

The names of these ligands are cumbersome for repeated use hence abbreviated names have been introduced for their ready identification. These abbreviated names are given in parentheses in figures 2.3 (a) - (c). In addition to the synthesized ligands, a number of ligands used for this project were readily available in the laboratory and were therefore not resynthesized. These ligands are identified by an asterix (*) after their full names in figures 2.3 (a) - (c).

In light of the fact that the R groups on the thioamide do not appear to have a significant affect on the nature, geometry, and the redox properties of the resultant compounds as discussed above, these groups were only varied to increase the water solubility of these ligands and the corresponding rhenium(V) and technetium(V) complexes. These variations have the potential to maintain the balance between hydrophilicity and hydrophobicity of these ligands and the corresponding rhenium(V) and technetium(V) complexes, which is crucial for biological studies.

The R' groups on the phenyl ring (see figure 2.3(a)-(c)) were varied to include electron releasing groups (R' = CH_3, OCH_3) and electron withdrawing (R' = NO_2, Cl) groups from the aromatic ring. The altered electron density in the aromatic ring could affect the binding of the these ligands to rhenium(V) and technetium(V) metals and this could also have an affect on the biological activity of the resultant complexes.

In addition to the expected balance between the hydrophilicity and hydrophobicity properties and the altered electronic effect introduced by the R and R' groups, these groups might also serve as sites for the attachment of a biologically active moiety (BAM). For an example, reduction of the NO_2 group in LNO_2 to NH_2 could serve as the attachment site for peptides. The ability to attach a BAM to the ligand is very important in cases where the biological molecules are used as vehicles to selectively deliver the radiopharmaceutical to the desired site.

2.3. Ligand synthesis.

The bidentate *N,N*-dialkyl-*N'*-(substituted)benzoylthiourea ligands can be readily synthesized using the method of Douglass and Dains as shown in Scheme 2.2.[16] The first step in this procedure is the reaction of potassium thiocyanate (KSCN) with the desired acid chloride in dry acetone under an inert atmosphere at room temperature. The products of this step are the two isomers, the acylthiocyanate and acyl-*iso*-thiocyanate, which are in equilibrium with each other. The acyl-*iso*-thiocyanate is the thermodynamically favoured isomer and therefore on heating the reaction mixture the acyl-*iso*-thiocyanate is formed predominantly. A secondary amine is then added and this reacts with the acyl-*iso*-thiocyanate to form the bidentate acylthiourea ligand. The full details of the synthesis of these ligands are given in the experimental section (Chapter 6).

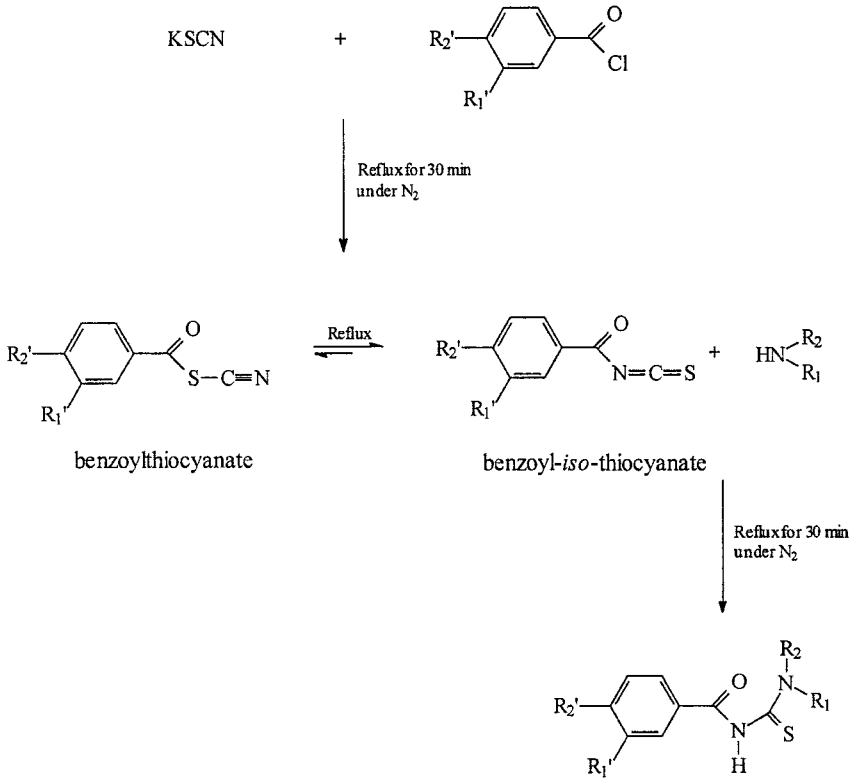

Scheme 2.2. The synthetic scheme for the synthesis of *N,N*-dialkyl-*N'*-(substituted)benzoylthiourea ligands.

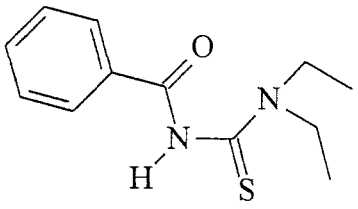

N,N-diethyl-*N'*-benzoylthiourea
(LH)

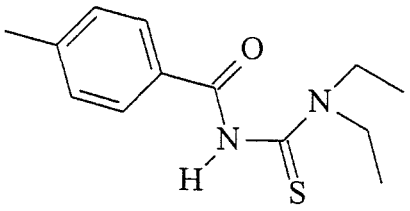

N,N-diethyl-*N'*-(*p*-methylbenzoyl)thiourea
(LCH_3)

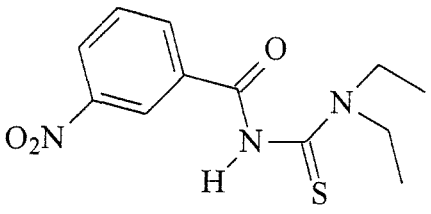

N,N-diethyl-*N'*-(*m*-nitrobenzoyl)thiourea*
(LNO_2)

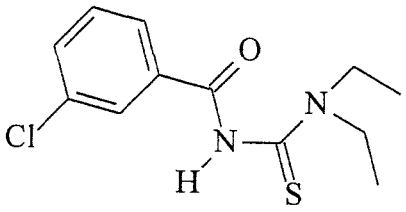

N,N-diethyl-*N'*-(*m*-chlorobenzoyl)thiourea
(LCl)

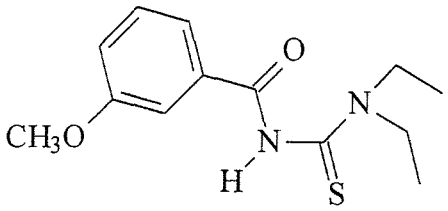

N,N-diethyl-*N'*-(*m*-methoxybenzoyl)thiourea
($LOCH_3$)

Figure 2.3 (a). Structural formulae and IUPAC names of *N, N*-diethyl-*N'*-(substituted)benzoylthiourea ligands with abbreviated names given in parentheses.

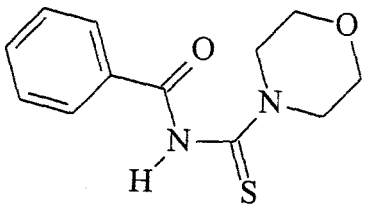

N-morpholino-*N'*-benzoylthiourea*
(morph-LH)

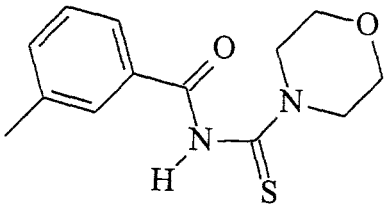

N-morpholino-*N'*-(*m*-methylbenzoyl)thiourea*
(morph-LCH_3)

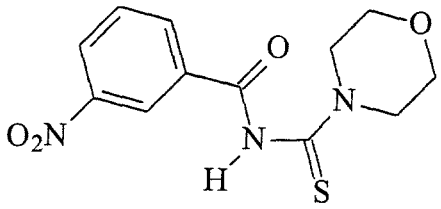

N-morpholino-*N'*-(*m*-nitrobenzoyl)thiourea*
(morph-LNO_2)

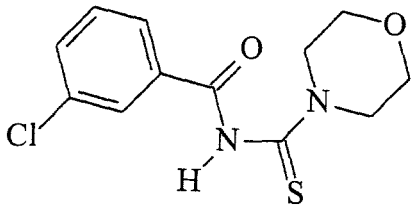

N-morpholino-*N'*-
(*m*-chlorobenzoyl)thiourea*
(morph-LCl

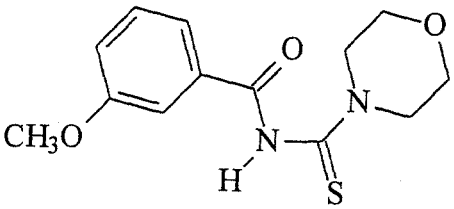

N-morpholino-*N'*-(*m*-nitrobenzoyl)thiourea*
(morph-$LOCH_3$)

Figure 2.3 (b). Structural formulae and IUPAC names of the *N*-morpholino-*N'*-(substituted)benzoylthiourea ligands with abbreviated names given in parentheses.

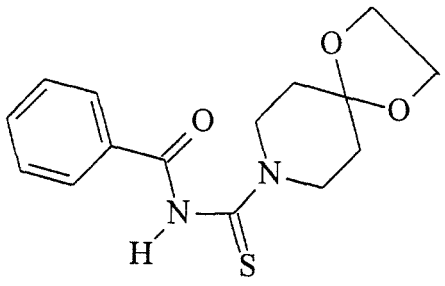

8-(*N*-benzoylthiocarbamoyl)-1,4-dioxa-8-azaspiro[4.5]decane*

(spiro-LH)

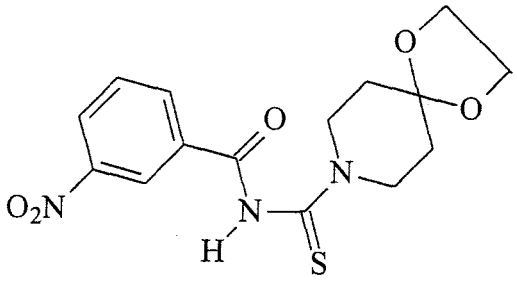

8-[*N*-(*m*-nitrobenzoyl)thiocarbamoyl]-1,4-dioxa-8-azaspiro[4.5]decane*

(spiro-LNO_2)

Figure 2.3 (c). Structural formulae and IUPAC names of the 8-(*N*-(substituted)benzoylcarbamoyl)-1,4-dioxa-8-azaspiro[4.5]decane ligands with abbreviated names given in parentheses.

2.4. Results and discussion.

The R_f values, yields, melting points and the analytical data for the synthesized *N,N*-dialkyl-*N'*-(substituted)benzoylthiourea ligands are given in Table 2.1. Selected IR stretching frequencies for all the ligands are given in Table 2.2. The ^{1}H NMR chemical shift data for all the ligands are given in Table 2.3. The assignments of the resonance peaks are according to the numbering schemes given in figure 2.4. The IR and ^{1}H NMR data are consistent with the bidentate acylthiourea ligand structures given in figures 2.3 (a)-(c) and the data are also in agreement with that reported in the literature.[11, 12]

Table 2.1. Properties and the elemental analysis for the synthesized *N,N*-dialkyl-*N'*-(substituted)benzoylthiourea ligands.

Compound	R_f. value	% Yield	Mp (°C)	Elemental analysis (% C/H/N/S)[a]
LH	0.77	76	95	60.80; 6.91; 11.58; 13.64 (60.98; 6.82; 11.86; 13.57)
LCl	0.77	65	94-95	53.20; 5.64; 9.57; 11.64 (53.22; 5.58; 10.35; 11.82)
LCH_3	0.88	81	134-135	62.64; 7.50; 11.33; 12.21 (62.36; 7.25; 11.19; 12.81)
$LOCH_3$	0.73	61	90-91	59.25; 7.23; 9.80; 11.70 (58.62; 6.81; 10.52; 12.06)

[a] Calculated values are given in parentheses

Table 2.2. Selected IR stretches for the *N,N*-dialkyl-*N'*-(susbtituted)benzoylthiourea ligands.

Compound	ν(N-H) (cm^{-1})	ν(C=O) (cm^{-1})
LH	3206 (s, br)	1682 (vs, sh)
LCl	3153 (s, sh)	1697 (vs, sh)
LCH_3	3293 (s, br)	1639 (v, sh)
$LOCH_3$	3183 (s, sh)	1691 (vs, sh)
LNO_2	3285 (s, sh)	1663 (vs,sh)
morph-LH	3250 (s, shld)	1667 (vs, sh)
morph-LCl	3256 (s, sh)	1657 (vs, sh)
morph-LCH_3	3150 (s, br)	1652 (vs, sh)
morph-$LOCH_3$	3136 (s, sh)	1698 (vs, sh)
morph-LNO_2	3188 (vs, br)	1699 (vs, sh)
spiro-LH	3198 (w, sh)	1651 (vs, sh)
spiro-LNO_2	3239 (w, sh)	1671 (vs, sh)

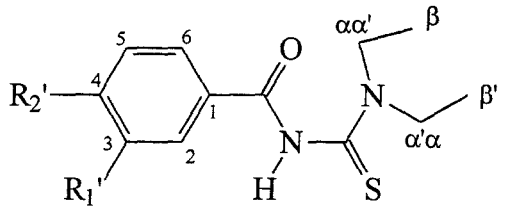

N,N-diethyl-*N'*-(substituted)benzoylthiourea

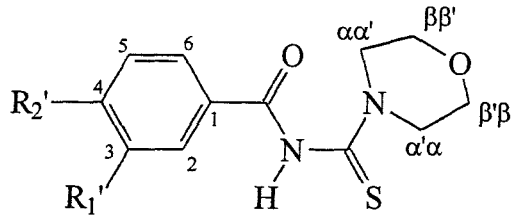

N,N-morpholino-*N'*-(substituted)benzoylthiourea

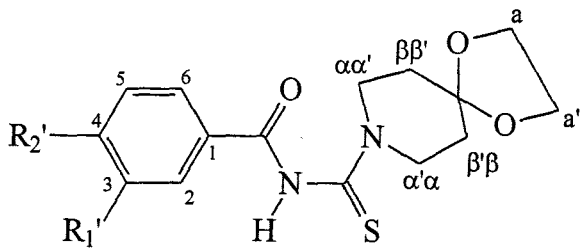

8-(*N*-(substituted)benzoylthiocarbamoyl)-1,4-dioxa-8-azaspiro[4.5]decane

Figure 2.4. Numbering scheme for the *N,N*-dialkyl-*N'*-(substituted)benzoylthiourea ligands.

Table 2.3. ^{1}H NMR chemical shift data for the *N,N*-dialkyl-*N'*-(substituted)benzoylthiourea ligands in $CDCl_3$ at 300 K.

Compound	$H_{(\beta)}$	$H_{(\beta')}$	$H_{(\alpha)}$	$H_{(\alpha')}$	$H_{(a)}$	$H_{(a')}$	$H_{(2)}$	$H_{(3)}$	$H_{(4)}$	$H_{(5)}$	$H_{(6)}$	$H_{(R')}$	$H_{(NH)}$
LH	1.30	1.34	3.60	4.02			7.82	7.46	7.56	7.46	7.82		8.24
LCH_3	1.31	1.34	3.60	3.86			7.73	7.27		7.27	7.73	2.41	8.14
LCl	1.31	1.34	3.58	4.01			7.81		7.53	7.40	7.69		8.23
$LOCH_3$	1.29	1.34	2.42	3.61			7.34		7.09	7.34	7.34	3.85	8.45
LNO_2	1.32	1.34	3.61	3.99			8.66		8.18	7.68	8.42		8.76
morph-LH	3.84	3.87	3.66	4.24			7.83	7.49	7.59	7.49	7.83		8.39
morph-LCH_3	3.82	3.84	3.66	4.23			7.64		7.39	7.36	7.62	2.41	8.40
morph-LCl	3.82	3.84	3.64	4.23			7.83		7.57	7.43	7.70		8.36
morph-$LOCH_3$	3.84	3.85	3.67	4.23			7.37		7.12	7.37	7.37	3.86	8.39
morph-LNO_2	3.82	3.84	3.66	4.23			8.68		8.18	7.71	8.44		8.58
spiro-LH	1.89	1.91	3.72	4.31	3.99	3.99	7.83	7.57	7.48	7.48	7.83		8.38
spiro-LNO_2	1.90	1.92	3.72	4.31	4.00	4.00	8.69		8.19	7.72	8.44		8.48

Examination of the ^{1}H NMR chemical shift data in Table 2.3 shows an interesting trend in the chemical shift position of the aromatic protons of the ligands. This trend agrees with the overall inductive and mesomeric effect of the substituents on the phenyl ring in the ligands shown in figures 2.5-2.7. On increasing the electron withdrawing properties of the R' group on the phenyl ring, there is a downfield shift in the proton resonances. The most pronounced shifts are observed for the ligands containing the nitro substituent.

The aliphatic portion of the ^{1}H NMR spectra for the bidentate acylthiourea ligands also shows some interesting features. Separate resonances are observed for the methylene protons ($H_{\alpha\alpha'}$) attached to the nitrogen of the thioamide functionality. This effect extends to the $H_{\beta\beta'}$ protons of

the two alkyl chains although separation between these two peaks is not so pronounced. The magnetic inequivalence of the $H_{\alpha\alpha'}$ and $H_{\beta\beta'}$ protons can be ascribed to the restricted rotation around the C-N bond between the thiocarbonyl and the amine nitrogen due to the partial double bond character of this bond.

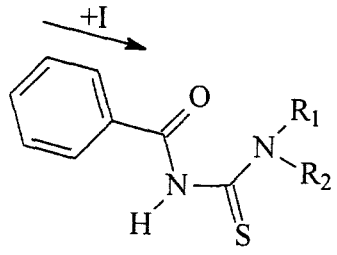

N, N-dialkyl-*N'*-benzoylthiourea

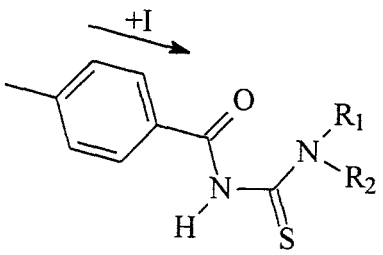

N, N-dialkyl-*N'*-(*p*-methylbenzoyl)thiourea

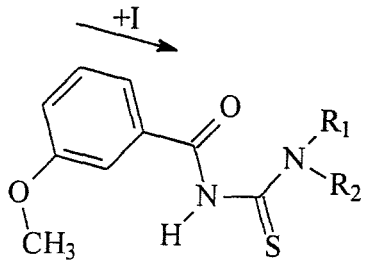

N, N-dialkyl-*N'*-(*m*-methoxybenzoyl)thiourea

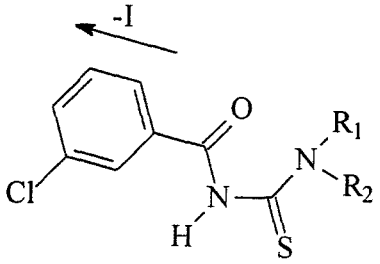

N, N-dialkyl-*N'*-(*m*-chlorobenzoyl)thiourea

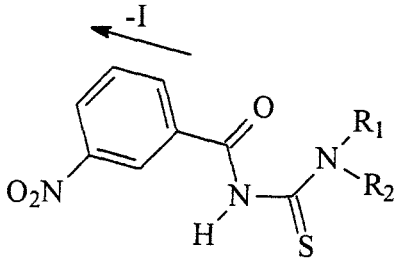

N, N-dialkyl-*N'*-(*m*-nitrobenzoyl)thiourea

Figure 2.5. Inductive effect in *N, N*-dialkyl-*N'*-(substituted) benzoylthiourea ligands.

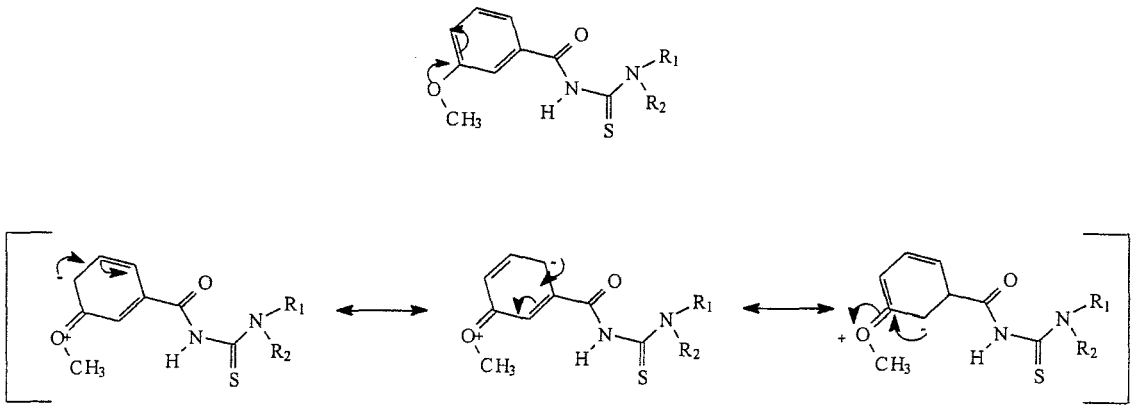

N,N-dialkyl-*N'*-(*m*-methoxybenzoyl)thiourea

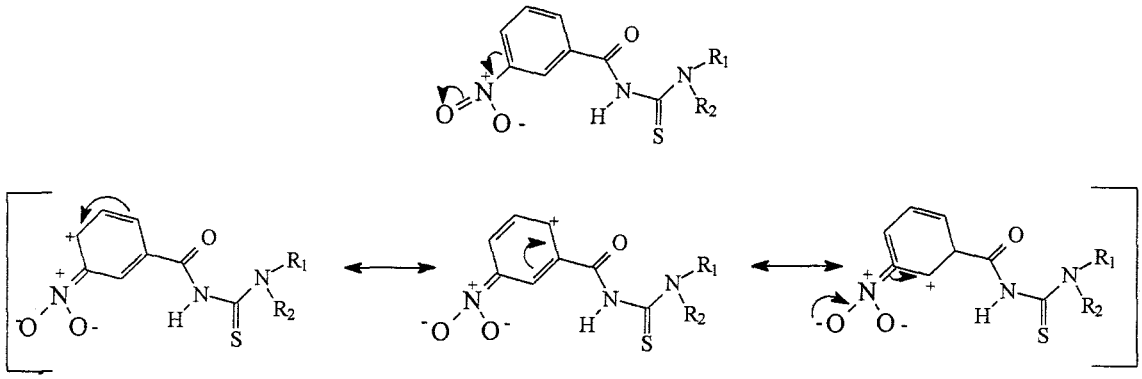

N,N-dialkyl-*N'*-(*m*-nitrobenzoyl)thiourea

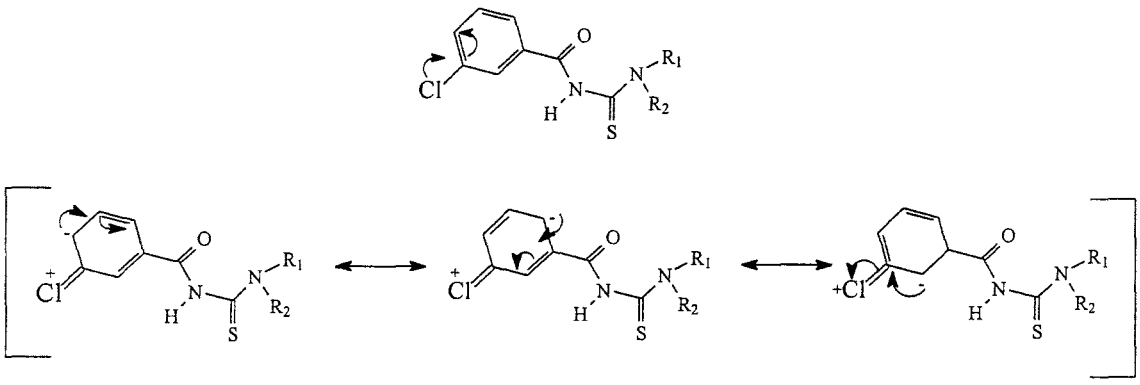

N,N-dialkyl-*N'*-(*m*-chlorobenzoyl)thiourea

Figure 2.6. Mesomeric effect in *N,N*-dialkyl-*N'*-(substituted)benzoylthiourea ligands.

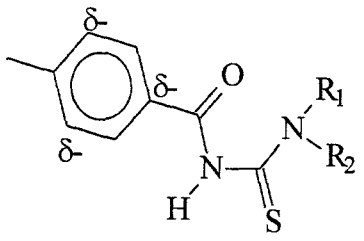

N, N-dialkyl-*N'*-(*p*-methylbenzoyl)thiourea

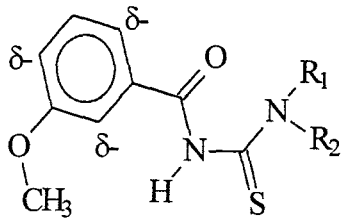

N, N-dialkyl-*N'*-(*m*-methoxybenzoyl)thiourea

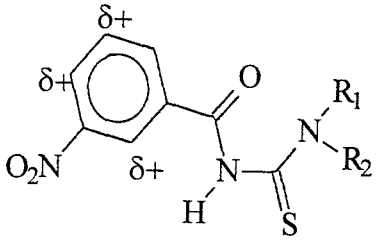

N, N-dialkyl-*N'*-(*m*-nitrobenzoyl)thiourea

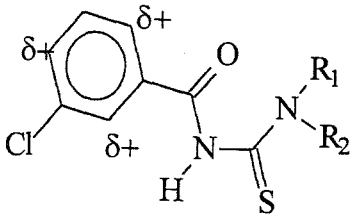

N, N-dialkyl-*N'*-(*m*-chlorobenzoyl)thiourea

Figure 2.7. The overall mesomeric effect in *N,N*-dialkyl-*N'*-(substituted)benzoylthiourea ligands.

REFERENCES.

1. R. D. Adams, M. Huang, J. H. Yamamoto, and L. Zhang, *Chem. Ber,* **129**, 137 (1996).
2. G. Wilkinson (editor-in chief), *Comprehensive Coordination Chemistry*, **2**, 639, Pergamon Press, Great Britain (1987).
3. P. Mühl, K. Gloe, F. Dietze, E. Hoyer, L. Beyer, *Z. Chem.,* **26**, 81, (1986).
4. R. A. Bailey, K. L. Rothaupt, K. Kullning, *Inorg. Chim. Acta,* **147**, 233, (1988).
5. K. R. Koch, A. Irving, M. Matoetoe, *Inorg. Chim. Acta,* **206**, 193, (1993).
6. K. -H. Köning, M. Schuster, G. Scheewis, B. Stichnbrecht, *Fresenius' Z. Anal. Chem.,* **325**, 621, (1984).
7. P. Vest, M. Schuster, K. -H. Köning, *Fresenius' Z. Anal. Chem.,* **335**, 759, (1989).
8. M. Schuster, *Fresenius' Z. Anal. Chem.,* **342**, 791, (1992).
9. A. Mohamadou, I. De'champs-Olivier and J. P Barbier, *Polyhedron*, **13**, 3277,(1994).
10. I. De'champs-Olivier, E. Guillon, A. Mohamadou and J. P. Barbier, *Polyhedron*, **15**, 3617, (1996).
11. C. Sacht, M. Datt, *Polyhedron*, **19**, 1347, (2000).
12. C. Sacht, M. Datt, S. Otto, A. Roodt, *J. Chem.* Soc. *Dalton Trans.,* 727, (2000).
13. S. Bourne, K. R. Koch, *J. Chem. Soc. Dalton Trans.,* 2071, (1993).
14. K. R. Koch, C. Sacht, T. Grimmbacher and S. Bourne, *S. Afr. J. Chem.*, **48**, 71, (1995).
15. K. R. Koch, J. du Toit, M. R. Caira, C. Sacht, *J. Chem. Soc. Dalton Trans.*, 785, (1994).
16. I. B. Douglass and F. B. Dains, *J. Am. Chem. Soc.*, **56**, 719, (1934).

CHAPTER 3

Re(V)-oxo AND Tc(V)-oxo PRECURSOR COMPLEXES.

Introduction.

Reactions involving ligand exchange require a good metal precursor complex. The following important factors need to be taken into consideration when searching for a good metal precursor: the ease and convenience of preparing such a material, the lability and the type of ligands to be exchanged (leaving groups) for the desired ligand (incoming groups), and the stability of this material under the reaction conditions required for the synthesis of the desired complex.

A number of Re(V)-oxo and Tc(V)-oxo complexes which serve as precursors have been reported in the literature and are used in the preparation of radiopharmaceuticals.[1-20] Entry into these starting materials is afforded by access into commercially available but relatively expensive perrhenate and pertechnetate salts, ammonium-perrhenate and -pertechnetate (NH_4ReO_4 and NH_4TcO_4) or potassium-perrhenate and -pertechnetate ($KReO_4$ and $KTcO_4$). In some instances the desired complexes have been prepared directly from the rhenium and technetium pure metals. These complexes are then used either as radiopharmaceuticals or as metal precursors from which other complexes can be synthesized.[1]

In the present study, the three Re(V)-oxo metal precursors, $ReOCl_3(PPh_3)_2$, $[ReO_2(py)_4]Cl$, and $[n\text{-}Bu_4N][ReOCl_4]$, were prepared and used to synthesize the Re(V)-oxo complexes with the acylthiourea ligands. These metal precursor complexes were prepared according to literature methods[1-17] and characterized by IR, as discussed in the following section. In cases where more than one method of synthesis for the same compound exists in the literature, the best method in terms of good yield, availability of reagents and ease of preparation was considered and applied.

$[n\text{-}Bu_4N][TcOCl_4]$, the only Tc(V)-oxo precursor complex that was used in the present study, was readily available in the laboratory at AEC, hence it was not resynthesized.

3.1. Synthesis of metal precursors.

3.1.1. Trichlorooxobis(triphenylphosphine)rhenium(V): $ReOCl_3(PPh_3)_2$.

Monodentate tertiary phosphines, stibines and arsines form a very large number of six-coordinate complexes of the types $ReOX_3(L)_2$, $ReOX_3(L)(L')$ and $ReO(OR)X_2(L)_2$, where X = halide or NCS, L = tertiary phosphine, arsine or stibine ligand, L' = DMSO, Ph_3PO or a phosphite ligand and R = alkyl group. Complexes of the type $ReOX_3(L)_2$ have been prepared for X = Cl, Br, I or NCS and L = PPh_3, PEt_2Ph, PEt_3, $AsMe_2Ph$ and Ph_3Sb.[1-3] Of these complexes, $ReOCl_3(PPh_3)_2$ is by far the most important since it is commonly used as a starting material for the synthesis of many other rhenium complexes.

3.1.1.1. Synthesis of $ReOCl_3(PPh_3)_2$.

The original procedure for the preparation of this compound involves the interaction of triphenylphosphine, perrhenic acid and mineral acid in ethanol (see equation 3.1).[4]
The perrhenic acid ($HReO_4$) may be prepared by any of the following methods: (1) Oxidation of

$$HReO_4 + 3\,HCl + 3\,(PPh_3)\,(excess) \longrightarrow ReOCl_3(PPh_3)_2 + (OPPh_3) + 2\,H_2O \quad \textbf{(3.1)}$$

the rhenium metal by dropwise addition of 30% hydrogen peroxide followed by cooling of the solution. The solution is then evaporated to dryness to give the crystals of perrhenic acid which can be dissolved in HCl. (2) Rhenium (VII) oxide is dissolved in concentrated HCl.[2]

In the present study the reaction was carried out according to equation 3.1 but potassium perrhenate ($KReO_4$) instead of $HReO_4$ was used. The details of this reaction procedure are given in the experimental section (Chapter 6).

3.1.2. Dioxotetrapyridinerhenium(V) chloride: $[ReO_2(py_4)]Cl$.

This is one of the few cationic rhenium complexes that have been thoroughly studied. As mentioned in Chapter 1, this complex belongs to the group of dioxorhenium complexes with a ReO_2^+ core. These complexes have attracted considerable attention on account of their redox, catalytic,[5, 6] persistent photophysical activity[7 - 12] and multielectrochemical behaviour.[6, 13] $[ReO_2(py_4)]^+$ has also been found to be an effective probe of hydrophobicity of binding regions in micelles.[14] However, most usefully, $[ReO_2(py_4)]Cl$ (commonly referred to as the pyridine complex) has found a role as a rhenium(V) precursor for the preparation of rhenium(V) complexes with a diverse range of ligands. This is because the pyridine ligands are good leaving groups and this material tends to yield pure products.[15, 16]

3 .1.2.1. Synthesis of $[ReO_2(py)_4]Cl$.

Numerous methods for preparing the pyridine complex exist in the literature.[17] These include (a) the reaction of $K_2[ReOCl_5]$[17] or $K_2[ReCl_6]$[17, 18] with aqueous pyridine, and (b) the reaction of $ReOCl_3(PPh_3)_2$ with aqueous pyridine in acetone.

For the current studies, method (b) was used for the preparation of $[ReO_2(py_4)]Cl$ because of the availability of the starting material, $ReOCl_3(PPh_3)_2$, from the preparation discussed above and because a higher yield (90 %) could be obtained using this method.[13, 19] The full details of this reaction, which was carried out according to equation 3.2, are given in the experimental section (Chapter 6).

$$ReOCl_3(PPh_3)_2 + \text{excess (py)} \xrightarrow[\text{acetone}]{H_2O} [ReO_2(py_4)]Cl \quad \textbf{(3.2)}$$

3.1.3. Tetrabutylammonium tetrachlorooxorhenate(V): $[n\text{-}Bu_4N][ReOCl_4]$.

The $[ReOCl_4]^-$ anion is a very useful precursor for the preparation of a variety of complexes containing the ReO^{3+} core because the chloride ligands are easily replaced by other ligands. The

tetrabutylammonium or tetraphenylphosphonium salts of this complex can be prepared and these counter ions provide a material with superior solubility in organic solvents.[20]

3.1.3.1. Synthesis of [n-Bu$_4$N][ReOCl$_4$].

The synthesis of $[ReOCl_4]^-$ was previously done through the reduction of ReO_4^- with zinc in acid. This method has been proven unreliable and hence a convenient alternative synthetic route, which proceeds in a good yield, was developed.[20] This is a two step reaction:

Step1: The preparation of [*n*-Bu$_4$N][ReO$_4$] from the reaction of K[ReO$_4$] and [*n*-Bu$_4$N]Cl in deionized water as shown by equation 3.3.

$$[n\text{-}Bu_4N]Cl + K[ReO_4] \rightarrow [n\text{-}Bu_4N][ReO_4] + NaCl \quad \textbf{(3.3)}$$

Step 2: This step of the reaction is done under inert conditions. The [*n*-Bu$_4$N][ReO$_4$] prepared in step1 is reacted with Me_3SiCl and methanol to give the final product [*n*-Bu$_4$N][ReOCl$_4$] as shown by equation 3.4.

$$[n\text{-}Bu_4N][ReO_4] + 6Me_3SiCl + 6MeOH \rightarrow$$
$$[n\text{-}Bu_4N][ReOCl_4] + 6Me_3SiOMe + 3H_2O + Cl_2 \quad \textbf{(3.4)}$$

In the present study the [*n*-Bu$_4$N][ReOCl$_4$] was prepared according to reaction equations 3.3 and 3.4 and the full details of these reactions can be found in the experimental section (Chapter 6).

3.2. Results and discussion.

The complexes were characterized using IR spectroscopy. The IR data are consistent with that reported in the literature[4, 14, 20] and are given in the experimental section. The percentage yields, melting points and ν(Re=O) are given in Table 3.1.

Table 3.1. Properties, % yields, melting points and ν(Re=O) of the synthesized Re(V)-oxo precursors.

Compound	Colour	%Yield	Mp(°C)	ν(Re=O)/(cm^{-1})
$ReOCl_3(PPh_3)_2$	yellow-green	98	186-190	969
$[ReO_2(py_4)]Cl$	orange	92	188-191	821
$[n\text{-}Bu_4N][ReOCl_4]$	yellow-green	72	118-121	1030

The $ReOCl_3(PPh_3)_2$ and $[ReO_2(py_4)]Cl$ complexes are stable in air and can be stored under normal atmospheric conditions. On the other hand, $[n\text{-}Bu_4N][ReOCl_4]$ is very hygroscopic and moisture sensitive and this compound decomposes to give a black material under normal atmospheric conditions. Storage of this compound under inert conditions is therefore necessary.

As can be seen in Table 3.1, there is an increase in the stretching frequency of the Re=O bond in the order: $[ReO_2(py)_4]Cl$, $ReOCl_3(PPh_3)_2$, $[n\text{-}Bu_4N][ReOCl_4]$. The stretching frequency of the Re=O bond is determined, to a large extent, by the type of ligand coordinated *trans* to the oxo ligand in the complex. The more electron donating the ligand *trans* to the oxo ligand, the weaker the Re=O bond and hence the ν(Re=O) shifts to lower frequencies.[4]

In the complex $[ReO_2(py_4)]Cl$, two equally strong electron donating oxo ligands are situated *trans* to each other. The linear O=Re=O system in this complex leads to a competition between the two oxo ligands for the d_{xz} and d_{yz} orbitals of the metal to form multiple bonds, the effect of which is the lowering of the stretching frequencies of both Re=O bonds.[4] In $ReOCl_3(PPh_3)_2$, the chloro ligand is coordinated *trans* to the oxo ligand. The chloro ligand in the complex exerts a smaller

trans effect on the Re=O bond compared to the oxo ligand in $[ReO_2(py)_4]Cl$. It is therefore expected that the stretching frequency of the Re=O bond in $ReOCl_3(PPh_3)_2$ will shift to a higher frequency relative to the stretching frequency of the Re=O bond in $[ReO_2(py)_4]Cl$ which is consistent with the data obtained.

For the $[ReOCl_4]^-$ complex, the coordinating site *trans* to the oxo ligand is left vacant. Since there is no competition for the metal centre, the Re=O bond in this complex will be much stronger than the Re=O bond in $ReOCl_3(PPh_3)_2$ and therefore the stretching frequency of the Re=O bond in the $[n\text{-}Bu_4N][ReOCl_4]$ complex is expected be at a higher frequency compared to the stretching frequency of the Re=O bond in $ReOCl_3(PPh_3)_2$, which is in agreement with the results obtained.

REFERENCES

1. G. Wilkinson (editor-in chief), *Comprehensive Coordination Chemistry,* **4**, 125, Pergamon Press, Great Britain, (1987).
2. G. Rouchias, *Chem. Rev.,* **74**. 531, (1984).
3. J. E. Fergusson, *Coord. Chem. Rev.*, **1**, 459, (1966).
4. N. P. Johnson, C. J. L. Lock, G. Wilkinson, *J. Chem. Soc.,* 105, (1964).
5. J. C. Dobson, K. J. Takeuchi, D. W. Pipes, T. J. Meyer, D. A. Gaselowitz, *Inorg. Chem.,* **25**, 2357, (1986).
6. H. H. Thorp, J. Van Houten, H. B. Gray, *Inorg.Chem.,* **28**, 889, (1989).
7. J. R. Winkler, H. B. Gray, *J. Am. Chem. Soc.*, **105**, 1373, (1983).
8. J. R. Winkler, H. B. Gray, *Inorg. Chem.*, **24**, 346, (1985).
9. M. D. Newsham, E. P. Giannelis, T. J. Pinnavaia, D. G. Nocera, *J. Am. Chem. Soc.,* **110**, 3885, (1988).
10. H. H. Thorp, C. V. Kumar, N. J. Turro, H. B. Gray, *J. Am. Chem. Soc.,* **111**, 4364, (1989).
11. J. G. Goll, W. Liu, H. H. Thorp, *J. Am. Chem. Soc.,* **115**, 11048, (1993).
12. W. Liu, H. H. Thorp, *J. Am. Chem. Soc.*, **117**, 9822, (1995).
13. M. S. Ram, J. T. Hupp, *Inorg. Chem.*, **30**, 130, (1991).
14. J. C. Brewer, H. B. Gray, *Inorg. Chem.*, **28**, 3334, (1989).
15. B. Chen, M. J. Heeg, E. Deutsh, *Inorg. Chem.,* **31**, 4683, (1992).
16. D. E. Berning, K. V. Katti, L. J. Barbour, W. A. Volkert, *Inorg. Chem.*, **37**, 334, (1998).
17. M. C. Chakravorti, *Inorg. Synth.*, **21**, 116, (1982).
18 J. H. Beard, J. Casey, R. K. Murmann, *Inorg. Chem.,* **4**, 747, (1965).
19. G. Parkin, *Chem. Rev.*, **93**, 887, (1993).
20. J. R. Dilworth, W. Hussain, A. J. Hutson, C. J. Jones, F.S. McQuillan, *Inorg. Synth.*, **31**, 257, (1997).

CHAPTER 4

Re(V)-oxo COMPLEXES WITH BENZOYLTHIOUREA LIGANDS.

Introduction.

As mentioned in Chapter 1, there is to the best of our knowledge only one report in the literature on the complexation formation of a Re(V)-oxo complex with *N,N*-dialkyl-*N'*-benzoylthiourea ligands. Dilworth *et al.* reported that the reaction of [*n*-Bu_4N][$ReOCl_4$] with *N,N*-diethyl-*N'*-benzoylthiourea ligand (DEBTH as abbreviated by Dilworth *et al.*) in methanol at room temperature under an inert atmosphere gives the emerald green neutral Re(V)-oxo complex, [$ReO(DEBT)_2Cl$], in high yield (see Scheme 4.1).[1]

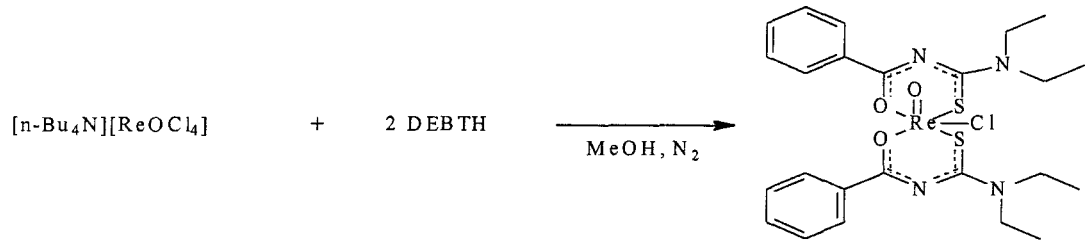

Scheme 4.1. Synthesis of [$ReO(DEBT)_2Cl$].[1]

By contrast, our preliminary studies revealed that the coordination chemistry of rhenium(V) with *N,N*-diethyl-*N'*-benzoylthiourea ligand (LH as denoted in the present studies) is not straight-forward and that the final product(s) depends on the starting material and the reaction conditions used. Hence the coordination chemistry of Re(V)-oxo precursor complexes with LH was examined in more detail by varying the following parameters:

(a) Re(V)-oxo precursor.

(b) Reaction solvent.

(c) Basicity of the reaction and the type of base used for the reaction.

Once optimum reaction conditions were established, a series of Re(V)-oxo complexes of the type shown by the general structural formula given in figure 4.1 were also prepared using the ligands described in Chapter 2.

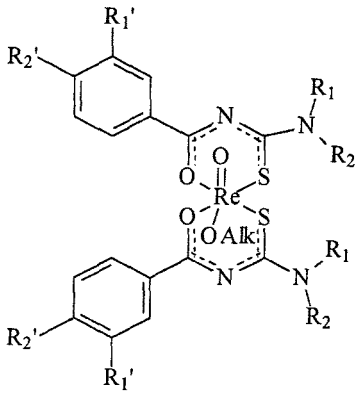

Figure 4.1. The general structural formula of the prepared Re(V)-oxo complexes.

The resultant complexes were characterized using ^{1}H NMR and IR spectroscopy and elemental analysis. X-ray crystallographic studies of a few of these complexes have also been carried out.

4.1. Synthetic studies: Results.

4.1.1. Complexation reaction with LH.

The complexation reaction of LH with Re(V)-oxo precursor complexes, according to equation 4.1, yielded the mixed ligand Re(V)-oxo complex $[ReO(L)_2(OMe)]$.

$$\text{Re(V)-oxo precursor} + 2\,LH \xrightarrow[MeOH]{NaOAc} [ReO(L)_2(OMe)] \quad \textbf{(4.1)}$$

This reaction was investigated in more detail by varying:

(a) Re(V)-oxo precursor

(b) Reaction solvent

(c) The basicity of the reaction and the type of the base used for the reaction.

Full details of all the reactions are given in (Chapter 6).

4.1.1.1. Variation of the Re(V)-oxo precursor.

In these studies the bidentate acylthiourea ligand, LH, was reacted with different Re(V)-oxo precursor complexes under the same reaction conditions.

Reaction of $ReOCl_3(PPh_3)_2$ with LH.

$ReOCl_3(PPh_3)_2$ was reacted with LH in the presence of sodium acetate in methanol and the solution was refluxed for 30 min. (equation 4.2).

$$ReOCl_3(PPh_3)_2 \quad + \quad 2\,HL \xrightarrow[MeOH]{2\,NaOAc} [ReO(L)_2(OMe)] \quad \textbf{(4.2)}$$

The colour of the reaction mixture changed from green to dark brown. This reaction yielded a mixture of products as was indicated by four spots on the TLC plate. The isolation of the desired product by flash chromatography and recrystallization from methanol/chloroform yielded $[ReO(L)_2(OMe)]$ as purple coloured crystals. This reaction takes place very slowly at room temperature as indicated by the slow change in the colour of the reaction mixture.

Reaction of $[ReO_2(py)_4]Cl$ with LH.

This reaction, according to equation 4.3, was carried out under the same reaction conditions as those described above.

$$[ReO_2(py)_4]Cl \quad + \quad 2\,HL \xrightarrow[MeOH]{2\,NaOAc} [ReO(L)_2(OMe)] \quad \textbf{(4.3)}$$

The colour of the reaction mixture changed from orange to red-brown and the product started to precipitate out of solution as fine purple coloured crystals. Recrystallization of this compound from methanol/chloroform yielded $[ReO(L)_2(OMe)]$ as purple coloured crystals. This reaction also takes place slowly at room temperature.

Reaction of [n-Bu$_4$N][ReOCl$_4$] with LH.

$$[n\text{-}Bu_4N][ReOCl_4] + 2\,LH \xrightarrow[MeOH]{2\,NaOAc} [ReO(L)_2(OMe)] \qquad \textbf{(4.4)}$$

This reaction, according to equation 4.4, gave a black coloured solution when heated to reflux, presumably due to the decomposition of [*n*-Bu$_4$N][ReOCl$_4$] at elevated temperature. The reaction was then carried out at room temperature and fine brown coloured crystals started to precipitate out of the solution after 5 min. of stirring. Recrystallization of this brown coloured crystalline product from methanol/chloroform yielded [ReO(L)$_2$(OMe)] as fine purple coloured crystals. It is important to mention that the reaction according to equation 4.4 gives the same product with a slightly higher yield (3% more) when carried out under N_2.

Characterization of the complexes isolated from the above-mentioned reactions was done by ^{1}H NMR and IR spectroscopy. The ^{1}H NMR and IR spectra of the three products were virtually identical indicating that the same complex was isolated irrespective of the Re(V)-oxo precursor used. The melting points and percentage yields of [ReO(L)$_2$(OMe)] obtained from these three reactions are given in Table 4.1. The percentage yields were calculated directly from the commercial starting material $KReO_4$.

Table 4.1. The percentage yields and melting points of [ReO (L)$_2$(O Me)] prepared from different Re(V)-oxo precursors.

Re(V)-oxo precursor	% Yield of [ReO (L)$_2$(O Me)]	Mp/°C
$ReOCl_3(PPh_3)_2$	11	167-171
$[ReO_2(py)_4]Cl$	62	166-169
[*n*-Bu$_4$N][ReOCl$_4$]	51, (54)[a]	165-168

[a] % yield for the reaction carried out under N_2 is given in parenthesis.

In light of the results obtained, it was decided that the Re(V)-oxo precursor, $[ReO_2(py)_4]Cl$, be used in the preparation of the Re(V)-oxo complexes with the other bidentate acylthiourea ligands

and in the further preliminary studies described below. Thus the results given in section 4.2 are for complexes synthesized using $[ReO_2(py)_4]Cl$.

4.1.1.2. The effect of base on the reaction of $[ReO_2(py)_4]Cl$ with LH.

The purpose of these studies was to examine whether (1) the complex, $[ReO(L)_2(OMe)]$, can be obtained in the absence of a base, (2) the type of a base used for the reaction determines the type of product obtained and (3) the type of base has an affect on the yield of the reaction. The reaction described by equation 4.3 was therefore carried out with the following variations:

(a) the absence of sodium acetate.

(b) the use of triethylamine instead of sodium acetate.

When the reaction of $[ReO_2(py)_4]Cl$ with LH was carried out in the absence of sodium acetate the colour of the reaction mixture turned dark brown and no precipitate was formed. TLC of the solution showed the presence of five compounds in the mixture. These compounds were separated by flash chromatography, however the amounts obtained for each of these compounds were too small for characterization. On the other hand when this reaction was carried out in the presence of the same stoichiometric amount of triethylamine as that of sodium acetate in equation 4.3, the reaction yielded $[ReO(L)_2(OMe)]$ as fine purple coloured crystals. The composition of this compound was verified using ^1H NMR and IR spectroscopy.

The results of this study are summarized in Table 4.2. In addition to the base studies done with the reaction according to equation 4.3, the reaction described by equation 4.4 was also carried out in the absence of a base under an inert atmosphere and this reaction yielded the chloro complex, $[ReO(L)_2Cl]$. The melting point and percentage yield of this complex are also given in Table 4.2.

Table 4.2. The types, percentage yields and melting points of the products obtained from the effect of the base.

Base	Product	% Yield	Mp/°C
NaOAc	$[ReO(L)_2(OMe)]$	62	166-167
Et_3NH	$[ReO(L)_2(OMe)]$	61	167-170
No base	mixture of products	-------	------
(No base)[a]	$[ReO(L)_2Cl]$	60	169-170

[a] The reaction was carried out using $[n\text{-}Bu_4N][ReOCl_4]$ under N_2.(equation 4.4).

4.1.1.3. Variation of the reaction solvent.

Due to the formation of the mixed ligand complex $[ReO(L)_2(OMe]$ in methanol, studies were undertaken to examine the effect of using different solvents. Two alcohols, ethanol and *iso*-propanol were used for these studies. The reason for using solvents with increasing bulkiness was to see if steric effects, introduced by the bulkiness of the resulting alkoxy ligand, will have an affect on the type and geometry of the resultant complex. In addition to these two alcohols acetonitrile was used in order to examine the effect of a non-alcoholic solvent on the nature of the resultant complex.

Reaction according to equation 4.3 carried out using ethanol.

When the reaction according to equation 4.3 was carried out using ethanol, the colour of the reaction mixture turned maroon and the product started to precipitate out of the solution as fine maroon crystals. Recrystallization of this product from ethanol/chloroform yielded the $[ReO(L)_2(OEt)]$ complex as maroon coloured crystals in a 63 % yield.

Reaction according to equation 4.3 carried out using iso-propanol.

When the same reaction was carried out using *iso*-propanol the colour of the reaction mixture turned dark brown and no solid material was observed after refluxing the reaction mixture for 30 min. The volume of the reaction mixture was reduced by a third using a rotary evaporator and the solution was placed in a fridge for 24 h during which time a dark brown solid separated out of solution. Recrystallization of this precipitate from *iso*-propanol/chloroform yielded $[ReO(L)_2(OiPr)]$ as fine brick-red coloured crystals in a 43 % yield.

Reaction according to equation 4.3 carried out using acetonitrile.

In this reaction the colour of the reaction mixture changed from orange to brown and then to dark green after refluxing for 28 min. The reaction mixture was refluxed for a further 7 min. and then the volume of the mixture was reduced to about a third using a rotary evaporator. The concentrated solution was placed in a fridge for 24 h during which time fine green crystals started to form. Recrystallization of these green crystals from acetonitrile/chloroform yielded the dirhenium complex, $[ReO(L)_2\text{-}O\text{-}ReO(L)_2]$, as fine green coloured crystals in a 32% yield.

All the products of the above mentioned reactions were analysed by ^1H NMR and IR spectroscopy and elemental analysis. The structures of the $[ReO(L)_2(OMe)]$, $[ReO(L)_2(OEt)]$ and $[ReO(L)_2\text{-}O\text{-}ReO(L)_2]$ complexes have also been confirmed by X-ray crystallography. A summary of the type of complexes obtained using different solvents is given in Table 4.3 and the full details of the characterization of these complexes are given in section 4.2 and Chapter 6.

Table 4.3. The type and the colour of complexes obtained from using different solvents.

Solvent used	Product obtained	Product colour
Methanol	$[ReO(L)_2(OMe)]$	purple
Ethanol	$[ReO(L)_2(OEt)]$	maroon
iso-Propanol	$[ReO(L)_2(iPrO)]$	brick-red
Acetonitrile	$[(L)_2ORe\text{-}O\text{-}ReO(L)_2]$	green

It is noteworthy to mention that recrystallization of $[ReO(L)_2(OMe)]$ from ethylacetate or acetone yielded the dirhenium complex $[(L)_2ORe\text{-}O\text{-}ReO(L)_2]$ in a purer form and higher percentage yield (51 - 53%) than when synthesized directly using the reaction according to equation 4.3 in acetonitrile. The characteristics of this compound, given in section 4.2 is of $[(L)_2ORe\text{-}O\text{-}ReO(L)_2]$ obtained from the recrystallization of $[ReO(L)_2(OMe)]$ from acetone. Details of the characterization of this complex obtained from the reaction using acetonitrile and the recrystallization of $[ReO(L)_2(OMe)]$ from ethylacetate are given in Chapter 6.

4.1.2. Synthesized Re(V)-oxo complexes.

As mentioned in sub-section 4.1.1.1, $[ReO_2(py)_4]Cl$ was used to synthesize the Re(V)-oxo complexes of the remaining acylthiourea ligands which were described in Chapter 2. The structural formulae of the synthesized mononuclear Re(V)-oxo complexes of *N,N*-diethyl-*N'*-(substituted)benzoylthiourea, *N*-morpholino-*N'*-(substituted)benzoylthiourea and 8-(*N*-(substituted)benzoylcarbamoyl)-1,4-dioxa-8-azaspiro[4.5]decane ligands are shown in Scheme 4.2. These complexes have been assigned numbers for their ready identification and these are also given in Scheme 4.2.

The structural formula of the dinuclear Re(V)-oxo complex, $[(L)_2ORe\text{-}O\text{-}ReO(L)_2]$ **(15)**, is shown in figure 4.2.

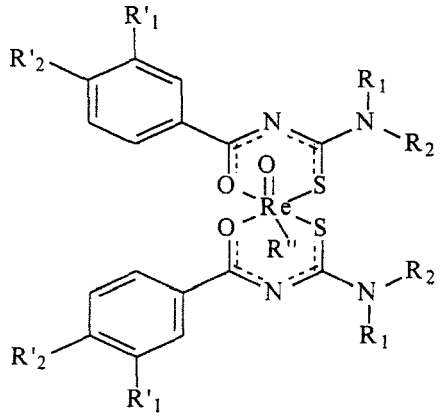

Complex	R_1,R_2	R'_1	R'_2	R"
(1)	diethyl-	H	H	OCH_3
(1b)	diethyl-	H	H	Cl
(2)	diethyl-	H	CH_3	OCH_3
(3)	diethyl-	OCH_3	H	OCH_3
(4)	diethyl-	NO_2	H	OCH_3
(5)	diethyl-	Cl	H	OCH_3
(6)	diethyl-	H	H	OCH_2CH_3
(7)	diethyl-	H	H	$OCH(CH_3)_2$
(8)	morpholino-	H	H	OCH_3
(9)	morpholino-	CH_3	H	OCH_3
(10)	morpholino-	OCH_3	H	OCH_3
(11)	morpholino-	NO_2	H	OCH_3

Scheme 4.2. Structural formulae of the synthesized mononuclear Re(V)-oxo complexes.

Complex	R_1,R_2	R'_1	R'_2	R"
(12)	morpholino-	Cl	H	OCH_3
(13)	spiroamino-[a]	H	H	OCH_3
(14)	spiroamino-[a]	NO_2	H	OCH_3

[a] Spiroamino is the trivial name for 1,4-dioxa-8-oxaspiro-[4,5]decane.

Scheme 4.2. Continued

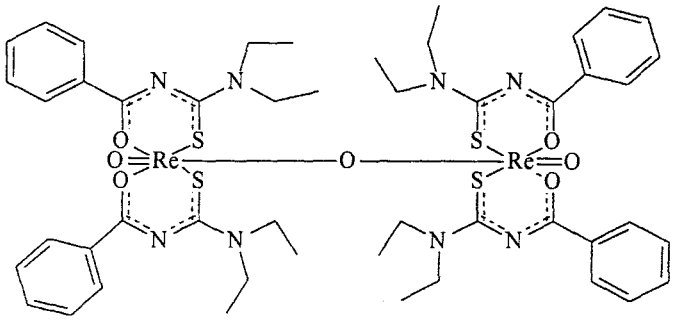

Figure 4.2. The structural formula of the dinuclear Re(V)-oxo **(15)**.

4.2. Characterization: Results.

4.2.1. Solid State Chemistry.

The percentage yields, melting points and elemental analysis for all the complexes are presented in Table 4.4.

Table 4.4. Percentage yields, melting points and elemental analysis for the Re(V)-oxo complexes of *N,N*-dialkyl-*N'*-(substituted)benzoylthiourea ligands.

Complex	R_1,R_2	R'_1	R'_2	R"	%Yield	Mp/°C	Elemental analysis / % [a, d]			
							C	H	N	S
(1)	diethyl-	H	H	$-OCH_3$	62	166 - 169	42.63	4.65	7.97	9.11
							(42.65)	(4.72)	(7.76)	(9.11)
(1b)	diethyl-	H	H	-Cl	60	168 - 170	40.82	4.53	8.01	9.23
							(40.74)	(4.32)	(7.91)	(9.12)
(2)	diethyl-	H	CH_3	$-OCH_3$	60	157 - 159	47.02	4.98	8.15	9.33
							(44.14)	(5.14)	(7.71)	(8.76)
(3)	diethyl-	OCH_3	H	$-OCH_3$	73	122 - 125	42.58	5.02	6.55	8.37
							(42.44)	(4.88)	(7.33)	(8.39)
(4)	diethyl-	NO_2	H	$-OCH_3$	72	170 - 172	38.02	3.91	10.63	8.28
							(37.82)	(3.93)	(10.59)	(8.08)
(5)	diethyl-	Cl	H	$-OCH_3$	59	92 - 94	38.89	3.94	6.25	8.08
							(38.85)	(4.04)	(7.25)	(8.29)
(6)	diethyl-	H	H	$-OCH_2CH_3$	63	196 - 198	41.41	4.60	7.32	8.37
							(42.02)	(4.94)	(7.81)	(8.93)
(7)	diethyl-	H	H	$-OCH(CH_3)_2$	43	194 - 195	44.00	5.01	7.63	8.63
							(44.30)	(5.10)	(7.66)	(8.76)
(8)	morpholino-	H	H	$-OCH_3$	52	180 - 182	38.33	3.62	6.38	8.92
							(39.03)	(3.99)	(7.65)	(8.76)

Table 4.4 continued.

Complex	R_1,R_2	R'_1	R'_2	R"	%Yield	Mp/°C	Elemental analysis/ % [a, b]			
							C	H	N	S
(9)	morpholino-	CH_3	H	$-OCH_3$	70	168 - 171	42.09	4.37	6.41	8.22
							(42.44)	(4.88)	(7.33)	(8.39)
(10)	morpholino-	OCH_3	H	$-OCH_3$	79	154 - 156	40.90	4.20	6.94	7.87
							(41.05)	(4.21)	(7.10)	(8.12)
(11)	morpholino-	NO_2	H	$-OCH_3$	90	>270	36.31	3.25	9.46	7.61
							(36.40)	(3.80)	(10.20)	(7.82)
(12)	morpholino-	Cl	H	$-OCH_3$	83	169 - 172	37.71	3.66	6.87	7.87
							(37.59)	(3.41)	(7.02)	(8.03)
(13)	spiroamino-[c]	H	H	$-OCH_3$	61	188 - 190	42.61	4.60	6.34	7.65
							(42.69)	(4.42)	(6.64)	(7.60)
(14)	spiroamino-[c]	NO_2	H	$-OCH_3$	67	174 - 176	39.73	3.61	8.84	6.56
							(39.75)	(4.20)	(9.02)	(6.85)
(15)[b]	diethyl-	H	H	μO	53	203	42.90	4.46	8.34	9.57
							(42.50)	(5.12)	(8.14)	(9.43)

[a] Calculated values are given in parentheses.

[b] is the dirhenium complex obtained from the recrystallization of $[ReO(L)_2(OMe)]$ from acetone.

[c] Spiroamino is the trivial name for 1.4-dioxa-8-oxaspiro-[4.5]decane.

[d] In some cases, good agreement between the calculated and found values for N% was not obtained. The reason for this is not clear, nevertheless all the other spectroscopic data agree with the proposed structures for these complexes.

IR spectroscopy

The IR spectra of all the complexes show a strong band between 890 and 950 cm^{-1}. The frequency of this band is characteristic of a metal-oxo stretch[2]and is similar to those observed for the ν(Re=O) bands in several well characterized $[ReO]^{3+}$ complexes.[3,4,5] Strong bands are found in the 400 - 600 cm^{-1} range for complexes **(1) - (14),** with the exception of **(1b),** and these bands are attributable to the Re-O bond stretch of the Re-OAlk coordination.[2, 6]

Two very strong bands at 650 and 665 cm^{-1} are observed for compound **(15)** and these bands are characteristic of ν(Re-O-Re) and are similar to those observed for ν(Re-O-Re) bands in well characterized complexes [7,8] The stretching frequencies for the ν(Re=O), ν(Re-OAlk) and ν(Re-O-Re) bands are given in Table 4.6 and all the other IR stretching frequencies are given in the experimental section (Chapter 6).

Table 4.5. Selected bond stretches for the synthesized Re(V)-oxo complexes.

Complex	R_1,R_2	R'$_1$	R'$_2$	R"	ν(Re-OAlk)	ν(Re=O)	ν(Re-O-Re)
(1)	diethyl-	H	H	$-OCH_3$	496	942	------
(1b)	diethyl-	H	H	-Cl	------	938	------
(2)	diethyl-	H	CH_3	$-OCH_3$	500	946	------
(3)	diethyl-	OCH_3	H	OCH_3	504	941	------
(4)	diethyl-	NO_2	H	$-OCH_3$	509	937	------
(5)	diethyl-	Cl	H	$-OCH_3$	496	945	------
(6)	diethyl-	H	H	$-OCH_2CH_3$	584	948	------
(7)	diethyl-	H	H	$-OCH(CH_3)_2$	592	933	------
(8)	morpholino-	H	H	$-OCH_3$	495	941	------
(9)	morpholino-	CH_3	H	$-OCH_3$	495	941	------
(10)	morpholino-	OCH_3	H	$-OCH_3$	491	940	------
(11)	morpholino-	NO_2	H	$-OCH_3$	491	938	------
(12)	morpholino-	Cl	H	$-OCH_3$	491	940	------
(13)	spiroamino-[c]	H	H	$-OCH_3$	496	946	------
(14)	spiroamino-[c]	NO_2	H	$-OCH_3$	499	935	------
(15)	diethyl	H	H	μO	------	891	651, 665

[c] Spiroamino is the trivial name for 1,4-dioxa-8-oxaspiro-[4.5]decane.

X-ray Crystallography.

The crystal structures of complexes **(1)**, **(4)**, **(6)** and **(15)** were solved by Ms. L. Cook at the University of the Witwatersrand. Full details of the data collection and experimental data are given in Chapter 6. The crystallographic data, structure determination and refinement parameters for each complex are given in Table 4.6. The crystal and molecular structures of these complexes confirm the proposed structures given in Scheme 4.2 and figure 4.2.

Perspective drawings of the structures of complexes **(1)**, **(4)**, **(6)** and **(15)**, showing the atom numbering scheme, are given in figures 4.3 - 4.6. Selected bond lengths and angles for these complexes are presented in Table 4.7 and 4.8, respectively. The atomic coordinates and full list of bond lengths and angles are given in Appendix A.

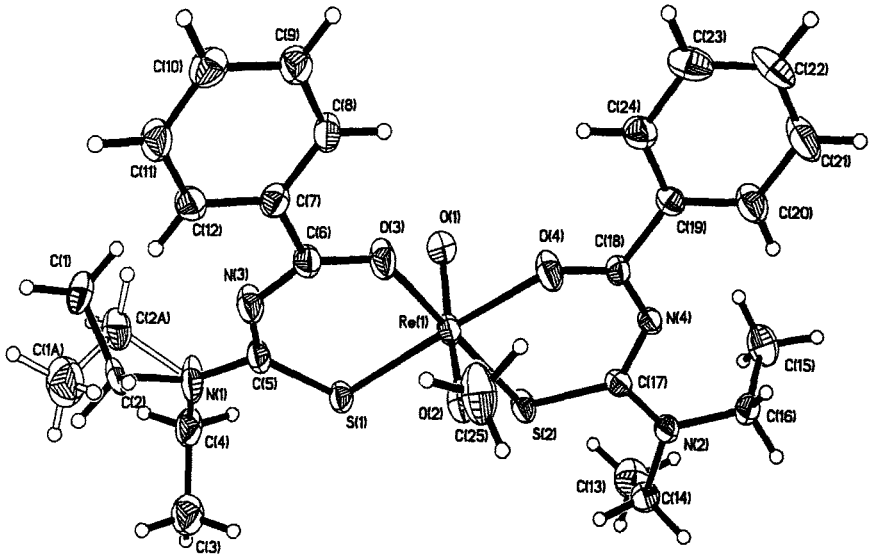

Figure 4.3. The molecular structure of [ReO(L)(OMe)] **(1)**, showing the atom numbering scheme adopted.

In the molecular structure of $[ReO(L)_2(OMe)]$, the Re(V) ion has a slightly distorted octahedral geometry with the S and O donor atoms of the chelated ligands coordinated in a *cis* arrangement

in the equatorial positions of the octahedron. The oxo and alkoxy ligands occupy the axial positions and are *trans* to each other. The bond angle CH_3O-Re=O is not linear but less than 180°. The molecular structures of complexes **(4)** and **(6)** are very similar to that of complex **(1)**.

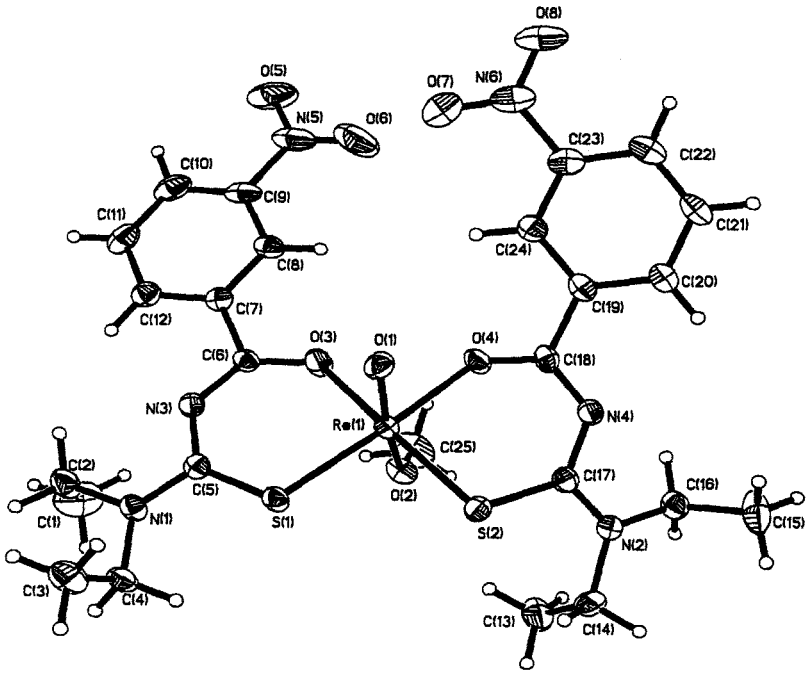

Figure 4.4. The molecular structure of $[ReO(LNO_2)_2(OMe)]$ **(4)**, showing the numbering scheme adopted.

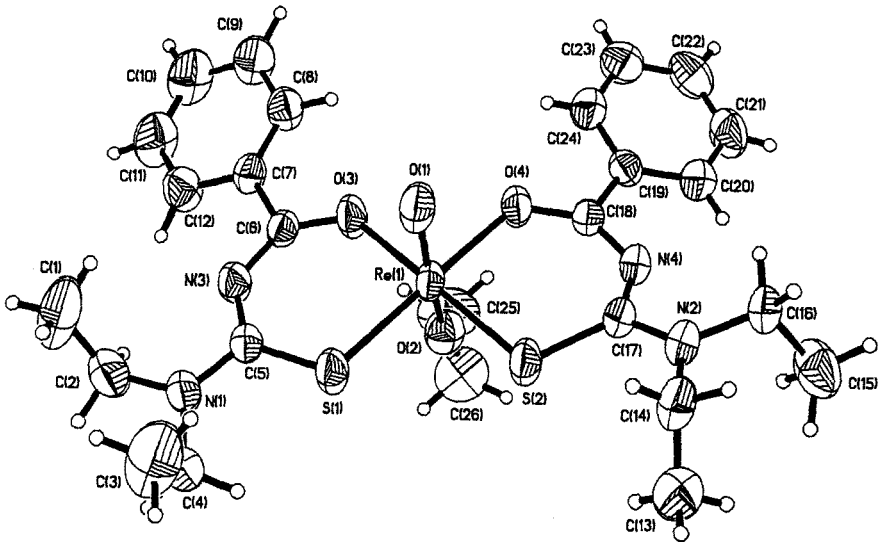

Figure 4.5. The molecular structure of $[ReO(L)_2(OEt)]$ **(6),** showing the atom numbering scheme adopted.

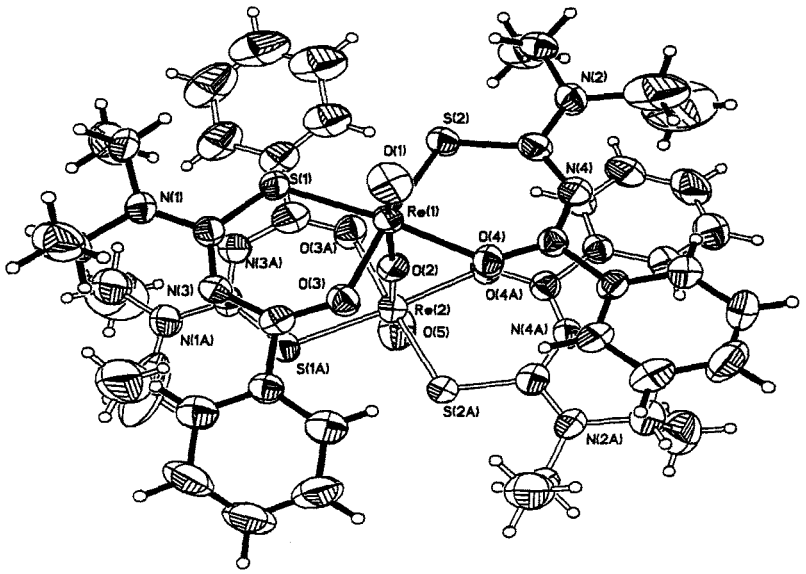

Figure 4.6. The molecular structure of $[(L)_2ORe\text{-}O\text{-}Re(O)(L)_2]$ **(15)**, showing the atom numbering scheme adopted.

The structure of complex **(15)** involves two Re(V)-oxo cores bridged by a single oxygen atom. Each half of the dimer adopts an octahedral configuration with the two acylthiourea ligands forming the equatorial plane of the octahedron in a *cis* arrangement. In each half of the dimer the oxo ligand and the bridging oxygen atom occupy the axial positions *trans* to each other with the Re-O-Re bond angle of 175.2°. The conformation in this complex is such that the acylthiourea ligands in one half of the dimer are not eclipsed with respect to the corresponding ligands in the other half presumably due to steric effects.

Table 4.6. Crystal data, structure refinement determination for complexes **(1), (4), (6)** and **(15)**.

Parameters	$[ReO(L)_2(OMe)]$ **(1)**	$[ReO(LNO_2)_2(OMe)]$ **(4)**	$[ReO(L)_2(OEt)]$ **(6)**	$[(L)_2ORe\text{-}O\text{-}ReO(L)_2]$ **(15)**
Emperical formula	$C_{25}H_{33}N_4O_4ReS_2$	$C_{25}H_{31}N_6O_8ReS_2$	$C_{26}H_{35}N_4O_4ReS_2$	$C_{48}H_{60}N_8O_7Re_2S_4$
Formula weight	703.87	793.88	717.90	1361.68
Temperature	173(2) K	173(2) K	298(2) K	298(2) K
Wavelength	0.71073 Å	0.71073 Å	0.71073 Å	0.71073 Å
Crystal system, space group	Monoclinic,C2/c	Triclinic, P1 bar	Triclinic, P1 bar	Monoclinic, P2(1)/n
Unit cell dimensions	a =31.6112 (14) Å α=90°	a =7.2723(4) Å α= 96.201(10)°	a =9.4859(11)Å α=81.195(2)°	a=16.7383(11) Å α = 90°
	b =11.3391(5) Å β =110.025 (0)°	b =143282(8) Å β =98.717(10)°	b=10.7123(13)Å β=79.018(2)°	b=16.0640(10) Å β = 108.73°
	c =15.9772(8) Å γ =90(2)°	c =15.5944(18) Å γ=94.881(10)°	c =15.5944(18)Å γ=67.429(2)°	c= 21.0911 (13) Å γ = 90°
Volume	5380.7 (4) $Å^3$	1522.44(14) $Å^3$	1430(3) $Å^3$	5370.7(6) $Å^3$
Z, Calculated density	8, 1.738 Mg/m^3	2, 1.732 Mg/m^3	2, 1.666 Mg/m^3	4, 1.684 Mg/m^3
Absorption coeffficient	4.710 mm^{-1}	4.184 mm^{-1}	4.430 mm^{-1}	4.715 mm^{-1}
F(000)	2800	788	716	2696
Crystal size	0.20 x 0.10 x 0.08 mm	0.22 x 0.08 x 0.06 mm	0.36 x 0.11 x 0.08 mm	0.26 x 0.05 x 0.05 mm
θ range for data collection	1.37 to 28.28°	5.62 to 28.29°	5.73 to 28.32°	1.36 to 28.36°
Limiting indices	-30≤ h ≤ 41, -15≤ k ≤ 14, -21 ≤ l ≤11	-9≤ h ≤ 9 , -18≤ k ≤ 19, -19 ≤ l ≤19	-12≤ h ≤ 12 ,-14≤ k ≤ 14,-20 ≤ l ≤17	-22 ≤ h ≤ 22 , -21≤ k ≤ 21, -28 ≤ l ≤28

Table 4.6 Continued.

Parameters	$[ReO(L)_2(OMe)]$ **(1)**	$[ReO(LNO_2)_2(OMe)]$ **(4)**	$[ReO(L)_2(OEt)]$ **(6)**	$[(L)_2ORe\text{-}O\text{-}ReO(L)_2]$ **(15)**
Reflections collected / unique	16897 / 6139 [R(int) = 0.0357]	16766 / 7377 [R(int) = 0.0292]	11776 / 6959 [R(int) = 0.0286]	60057 / 13363 [R(int) = 0.1553]
Completeness to $\theta = 28.36$	91.9 %	97.6 %	97.5 %	99.4 %
Max. and min. transmission	0.7044 and 0.4526	0.7874 and 0.4596	0.7182 and 0.2985	0.7984 and 0.3736
Refinement method	Full-matrix least-squares on F^2	Full-matrix least-squares on F^2	Full-matrix least-squares on F^2	Full-matrix least-squares on F^2
Data / restraints / parameters	6139 / 0 / 349	7377 / 0 / 384	6959 / 0 / 414	13363 / 0 / 622
Goodness-of-fit on F^2	1.078	1.025	0.909	0.917
Final R indices [$I > 2\sigma(I)$]	R1 = 0.0366, wR2 = 0.0683	R1 = 0.0270, wR2 = 0.0589	R1 = 0.0319, wR2 = 0.0598	R1 = 0.0467, wR2 = 0.0810
R indices (all data)	R1 = 0.0505, wR2 = 0.0736	R1 = 0.0322, wR2 = 0.0619	R1 = 0.0550, wR2 = 0.0660	R1 = 0.1177, wR2 = 0.1002
Largest diff. Peak and hole	2.243 and -1.670 e.Å^{-3}	1.274 and -0.941 e.Å^{-3}	0.737 and -0.622 e.Å^{-3}	1.307 and -1.145 e.Å^{-3}

Table 4.7. Selected bond lengths [Å] for compounds **(1)**, **(4)**, **(6)** and **(15)**.

Bond	(1)	(4)	(6)	(15)
Re(1)-O(1)	1.701 (14)	1.699 (2)	1.687 (3)	1.685 (5)
Re(1)-O(2)	1.897 (4)	1.903 (2)	1.899 (3)	1.893 (4)
Re(1)-O(3)	2.129 (3)	2.096 (2)	2.121 (3)	2.095 (4)
Re(1)-O(4)	2.118 (3)	2.144 (2)	2.134 (3)	2.092 (4)
Re(1)-S(1)	2.331 (11)	2.333 (8)	2.321 (11)	2.338 (17)
Re(1)-S(2)	2.324 (11)	2.360 (8)	2.328 (10)	2.342 (17)
S(1)-C(5)	1.744 (5)	1.756 (3)	1.741 (4)	1.753 (7)
S(2)-C(17)	1.759 (5)	1.771 (3)	1.758 (4)	1.269 (7)
O(3)-C(6)	1.273 (5)	1.272 (4)	1.268 (4)	1.274 (8)
O(4)-C(18)	1.268 (5)	1.285 (4)	1.271 (4)	1.301 (8)
Re(2)-O(5)				1.691 (5)
Re(2)-O(2)				1.917 (40
Re(2)-O(3A)				2.113 (4)
Re(2)-O(4A)				2.113 (4)
Re(2)-S(1A)				2.336 (19)
Re(2)-S(2A)				2.328 (18)
S(1A)-C(5A)				1.737 (7)
S(2A)-C(17)				1.757 (7)
O(3A)-C(6A)				1.254 (8)
O(4)-C(18A)				1.267 (8)

Table 4.8. Table of selected bond angles [Degrees] for compounds **(1)**, **(4)**, **(6)** and **(15)**.

Angle	(1)	(4)	(6)	(15)
O(1)-Re(1)-O(2)	163.05 (16)	164.94 (11)	162.58 (15)	171.2 (2)
O(3)-Re(1)-S(1)	92.55 (9)	92.72 (7)	92.05 (8)	91.91 (13)
O(4)-Re(1)-S(2)	92.30 (9)	94.10 (6)	91.61 (8)	91.66 (14)
O(3)-Re(1)-O(4)	84.51 (12)	81.63 (9)	86.79 (11)	84.15 (17)
S(1)-Re(1)-S(2)	90.15 (4)	91.09 (3)	89.17 (4)	91.63 (6)
O(3)-Re(1)-S(2)	174.07 (11)	171.57 (7)	174.85 (10)	172.77 (14)
O(4)-Re(1)-S(1)	173.90 (11)	173.52 (7)	175.49 (9)	172.97 (14)
Re(1)-O(2)-Re(2)				175.2 (2)
O(5)-Re(2)-O(2)				167.9 (2)
O(3A)-Re(2)-S(1A)				91.84 (14)
O(4A)-Re(2)-S(2A)				92.16 (13)
O(3A)-Re(2)-O(4A)				85.82 (18)
S(1A)-Re(2)-S(2A)				89.28 (6)
O(3A)-Re(2)-S(2A)				172.53 (15)
O(4A)-Re(2)-S(1A)				172.67 (14)

4.2.2. Solution state chemistry.

All the benzoylthiourea-alkoxy mixed ligand monorhenium complexes **(1)** - **(14)** exhibited an unusual property in that the colour of the solution changed from maroon or brown to green in deuterated chloroform ($CDCl_3$). Moreover ^1H NMR spectra for all the benzoylthiourea-alkoxy mixed ligand monorhenium complexes **(1)** - **(14)** in $CDCl_3$ show two sets of resonances of different intensities suggesting the presence of two species in solution. For example the ^1H NMR

spectrum of complex **(1)** is illustrated in figure 4.7 (spectrum 1). The two sets of signals in the ^{1}H NMR spectra of these complexes have been referred to as the minor and major species according to their respective integral intensities. The full ^{1}H NMR data of the synthesized complexes are given in Tables 4.9 - 4.15 and the assignment of the peaks is according to the numbering scheme given for each complex. In the case of complexes **(8)-(14)** the minor species is negligible hence only the assignment of the signals for the major species are given.

On the other hand only one set of resonances is observed for complex **(15)**, as shown by spectrum 2 in figure 4.7, and also no colour change was observed. The chemical shift positions for the protons in this complex correspond to those of the major species for the acylthiourea-alkoxy mixed ligand complexes **(1) - (14)**, suggesting that the major species present in solution is the corresponding Re-O-Re complex and the minor species is the mixed ligand monorhenium complex.

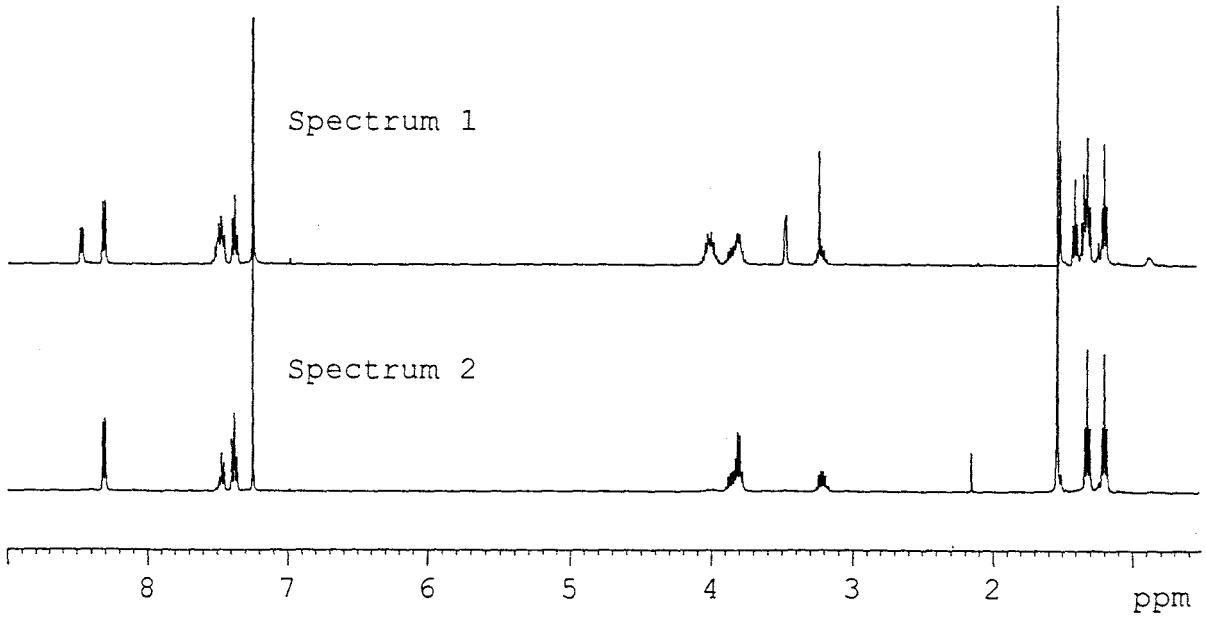

Figure 4.7. The ^{1}H NMR spectra of $[ReO(L)_2(OMe)]$ and $[(L)_2ORe\text{-}O\text{-}ReO(L)_2]$ shown as spectrum 1 and 2, respectively.

In the ^{1}H NMR spectra for the benzoylthiourea-methoxy mixed ligand complexes **(1)** - **(5)**, a singlet (within the 3.20 - 3.26 ppm range) assignable to the protons ($OC\mathbf{H}_3$) of the methoxy ligand is observed and its integral intensity corresponds to the integral intensity of the minor species. There is another singlet which is consistently found at 3.48 ppm for the benzoylthiourea-methoxy mixed ligand complexes **(1)-(5)** and **(9)-(14)** and the integral intensity of this signal corresponds to the integral intensity of the major species. This signal is in the methanol region [10] and it provides evidence for the displacement of the methoxy ligand from these complexes as free methanol.

Similarly for the benzoylthiourea-ethoxy mixed ligand complex **(6)**, two sets of signals consisting of two quartets at 3.53 ppm and 3.70 ppm and two overlapping triplets at 1.20 ppm are observed. The integral intensity of the quartet at 3.53 ppm corresponds to the integral intensity of the minor species and it is assignable to the protons ($OC\mathbf{H}_2$) of the ethoxy ligand. The quartet at 3.70 ppm is in the region of the ethyl protons ($HOC\mathbf{H}_2CH3$) of free ethanol[9] and its integral intensity corresponds to the integral intensity of the acylthiourea ligand of the major species. The overlapping triplets at 1.20 ppm are assignable to the methyl protons ($-CH_2C\mathbf{H}_3$) of ethanol and the ethoxy ligand.

In the case of the benzoylthiourea-(*iso*-propoxy) mixed ligand complex **(7)**, the chemical shifts for the protons of the *iso*-propoxy ligand and those of the free *iso*-propanol are overlapping. Moreover, the chemical shifts of O**C**H protons of the *iso*-propoxy and free *iso*-propanol (within the 3.98 - 4.06 ppm range) overlap with the chemical shifts of the methylene protons, ($\mathbf{H}_{(\alpha'\alpha \text{ and } \alpha'\alpha)}$), of the benzoylthiourea ligand in this complex and hence could not be unambiguously assigned. The doublet at 1.98 ppm is assigned to the $OCH(C\mathbf{H}_3)_2$ protons of both the *iso*-propoxy and free *iso*-propanol.

A green complex was isolated from the NMR sample solution of $[ReO(L)_2(OMe)]$ in $CDCl_3$ by drying under vacuum and was characterized by ^{1}H NMR and infrared spectroscopy. The IR and ^{1}H NMR spectra of this complex corresponded to that of the $[(L)_2ORe\text{-}O\text{-}ReO(L)_2]$ complex which is the complex obtained when $[ReO_2(py)_4]Cl$ was reacted with LH in acetonitrile and when

$[ReO(L)_2(OMe)]$ was recrystallized from acetone or ethylacetate. Moreover, the ^{1}H NMR spectrum of this complex corresponds to that of the major species in the original spectrum of $[ReO(L)_2(OMe)]$. These results suggest that a monorhenium complex undergoes dimerization in $CDCl_3$, in which the two alkoxy ligands have been replaced by a bridging oxygen to form a dirhenium complex $[(L)_2ORe\text{-}O\text{-}ReO(L)_2]$. This dimerization is thus associated with the observed colour change from maroon/brown to green when the benzoylthiourea-alkoxy mixed ligand complexes are dissolved in $CDCl_3$.

The ^{1}H NMR spectrum of the benzoylthiourea-chloro mixed ligand complex, $[ReO(L)_2Cl]$ **(1b)**, also consisted of two sets of resonances but of equivalent intensities. The two sets of resonances are in this case due to the unsymmetrical coordination of two benzoylthiourea ligands in this complex.

Table 4.9. ^{1}H NMR chemical shift data (ppm) for complexes [ReO(L-R')$_2$(OMe)], $CDCl_3$ at 300 K.

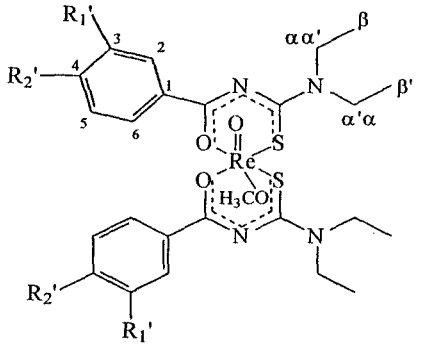

Complex	$H_{(\beta)}$	$H_{(\beta')}$	$H_{(R')}$	$H_{(OCH_3)}$	H(α)	$H_{(\alpha')}$	$H_{(\alpha)}$	$H_{(\alpha')}$	$H_{(2)}$	$H_{(3)}$	$H_{(4)}$	$H_{(5)}$	$H_{(6)}$
(1) : R_1' = H, R_2' = H													
Minor	1.34	1.43	-------	3.25	4.00 -4.04	4.00 -4.04	4.00 -4.04	4.00 -4.04	8.47	7.47	7.50	7.47	8..47
Major	1.21	1.33	-------	3.48*	3.20 - 3.25	3.80 - 3.88	3.80 - 3.88	3.80 -3.88	8.31	7.38	7.47	7.38	8.31
(2): R_1' = H, R_2' = CH_3													
Minor	1.35	1.41	2.44	3.21	3.95 - 4.04	3.95 - 4.04	3.95 - 4.04	3.95 - 4.04	7.27	8.36	--------	8.36	7.27
Major	1.21	1.32	2.44	3.48*	3.21- 3.27	3.78 -3.87	3.78 -3.87	3.78 -3.87	7.16	8.19	--------	8.19	7.16

Table 4.9. Continued.

Complex	$H_{(\beta)}$	$H_{(\beta')}$	$H_{(R')}$	$H_{(OCH_3)}$	H(α)	$H_{(\alpha')}$	$H_{(\alpha)}$	$H_{(\alpha')}$	$H_{(2)}$	$H_{(3)}$	$H_{(4)}$	$H_{(5)}$	$H_{(6)}$
(3): $R_1' = OCH_3$, $R_2' = H$													
Minor	1.35	1.41	3.92	3.23	3.97 - 4.09	3.97 - 4.09	3.97 - 4.09	3.97 - 4.09	8.07	------	8.05	7.35	7.13
Major	1.23	1.28	3.83	3.48*	3.31 - 3.36	3.65 - 3.70	3.89 - 3.97	3.89 - 3.97	7.87	------	7.89	7.23	6.94
(4): $R_1' = NO_2$, $R_2' = H$													
Minor	1.28	1.35	-------	3.23	3.78 -3.87	3.78 -3.87	3.89 - 4.03	3.89 - 4.03	8.99	------	8.99	7.61	8.31
Major	1.38	1.43	-------	3.48*	3.48 -3.49	4.03 - 4.10	4.03 - 4.10	4.03 - 4.10	9.27	------	8.90	7.71	8.39
(5): $R_1' = Cl$, $R_2' = H$													
Minor	1.37	1.42	-------	3.22	4.01 - 4.15	4.01 -4.15	4.01 - 4.15	4.01 - 4.15	8.47	------	8.41	7.43	7.45
Major	1.23	1.32	-------	3.48*	3.35 - 3.40	3.77 - 3.80	3.84 - 3.90	3.92 - 3.97	8.26	------	8.17	7.31	7.43
(15)	1.21	1.32	-------	--------	3.20 - 3.26	3.78 - 3.89	3.78 - 3.89	3.78 - 3.89	8.30	7.38	7.47	7.38	8.30

* free methanol peak.

Table 4.10. The ^{1}H NMR chemical shift data (ppm) for complex $[ReO(L)_2Cl]$ **(1b)**, $CDCl_3$ at 300K.

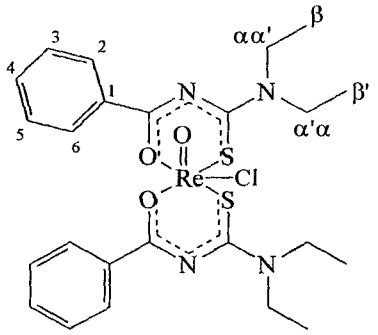

Complex	$H_{(\beta)}$	$H_{(\beta')}$	$H_{(\alpha)}$	$H_{(\alpha')}$	$H_{(2)}$	$H_{(3)}$	$H_{(4)}$	$H_{(5)}$	$H_{(6)}$
(1b)	1.38, 1.39	1.47, 1.52	3.83 - 3.91, 3.93 - 3.95	4.24 - 4.29 4.35 -4.43	8.43	7.44, 7.51	6.99, 7.24	7.44, 7.51	8.43

Table 4.11. The ^{1}H NMR chemical shift data (ppm) for complex $[ReO(L)_2(OEt)]$ **(6)**, $CDCl_3$ at 300 K.

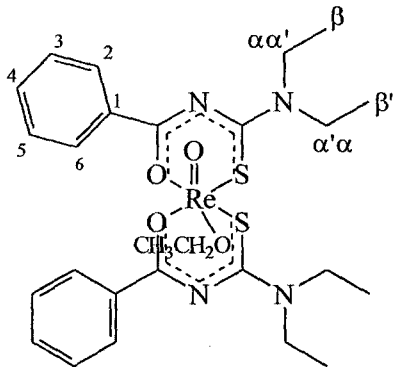

Complex	$H_{(\beta)}$	$H_{(\beta')}$	$H_{(OCH_2)}$	$H_{(CH_2CH_3)}$	$H_{(\alpha)}$	$H_{(\alpha')}$	$H_{(\alpha)}$	$H_{(\alpha')}$	$H_{(2)}$	$H_{(3)}$	$H_{(4)}$	$H_{(5)}$	$H_{(6)}$
Minor	1.34	1.39	3.53	1.20	3.99 -4.04	3.99 -4.04	3.99 -4.04	3.99 -4.04	8.45	7.45	7.51	7.45	8.45
Major	1.21	1.30	3.70*	1.20*	3.21-3.25	3.79 -3.86	3.79 -3.86	3.79 -3.86	8.31	7.36	7.45	7.36	8.31

* free ethanol peaks

Table 4.12. ^{1}H NMR chemical shift data (ppm) for complex [ReO(L)$_2$(O*i*Pr)] **(7),** $CDCl_3$ at 300 K.

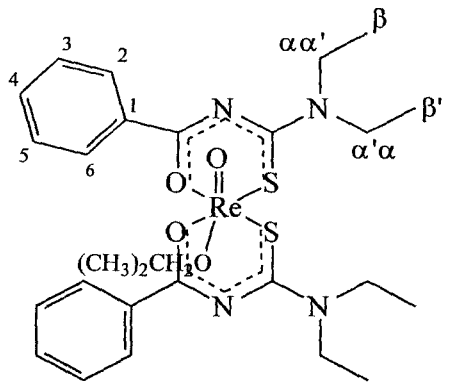

Complex	$H_{(\beta)}$	$H_{(\beta')}$	$H_{(OCH)}$	$H_{(OCHCH_3)}$	$H_{(OCHCH_3)}$	$H_{(\alpha)}$	$H_{(\alpha')}$	$H_{(\alpha)}$	$H_{(\alpha')}$	$H_{(2)}$	$H_{(3)}$	$H_{(4)}$	$H_{(5)}$	$H_{(6)}$
Minor	1.22	1.42	3.98 - 4.06	1.98	1.98	3.98 - 4.06	3.98 - 4.06	3.98 - 4.06	3.98 - 4.06	8.44	7.47	7.49	7.47	8.44
Major	1.20	1.32	3.98 - 4.06*	1.98*	1.98*	3.19 - 3.25	3.78 - 3.89	3.78 - 3.89	3.78 - 3.89	8.30	7.38	7.47	7.38	8.30

* free *iso*-propanol peaks.

Table 4.13. The ^{1}H NMR chemical shift data (ppm) for complex $[(L)_2ORe\text{-}O\text{-}ReO(L)_2]$**(15),** $CDCl_3$ at 300 K.

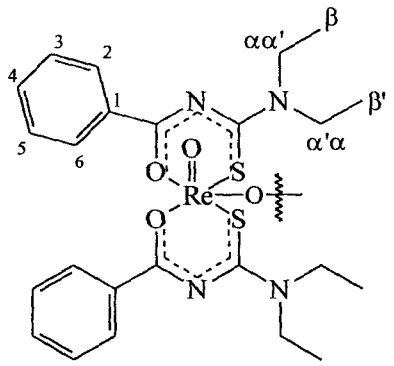

$H_{(\beta)}$	$H_{(\beta)}$	$H_{(\alpha)}$	$H_{(\alpha')}$	$H_{(\alpha)}$	$H_{(\alpha')}$	$H_{(2)}$	$H_{(3)}$	$H_{(4)}$	$H_{(5)}$	$H_{(6)}$
1.2	1.32	3.18 - 3.26	3.78 - 3.88	3.78 - 3.88	3.78 - 3.88	8.31	7.35	7.47	7.35	8.31

Table 4.14. The ^{1}H NMR chemical shift data (ppm) for complexes [ReO(morph-L-R')$_2$(OMe)], $CDCl_3$ at 300 K.

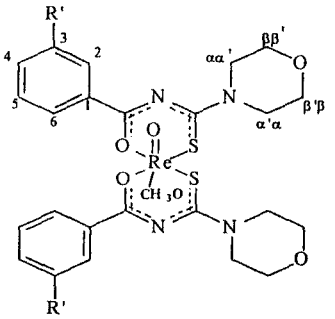

Complex	$H_{(\beta)}$	$H_{(\beta')}$	$H_{(\beta)}$	$H_{(\beta')}$	$H_{(OCH3)}$	$H_{(R')}$	$H_{(\alpha)}$	$H_{(\alpha')}$	$H_{(\alpha)}$	$H_{(\alpha')}$	$H_{(2)}$	$H_{(3)}$	$H_{(4)}$	$H_{(5)}$	$H_{(6)}$
(8): $R_1' = H$, $R_2' = H$															
Major	3.72 - 3.78	4.41 - 4.48	4.32 - 4.35	4.32 - 4.35	3.48*	-------	3.47 - 3.51	3.59 - 3.66	3.65 - 3.63	3.69 - 3.74	7.92	7.52	7.65	7.52	7.92
(9): $R_1' = CH_3$, $R_2' = H$															
Major	3.71 - 3.76	4.46 - 4.49	4.33 - 4.37	4.33 - 4.37	3.48*	2.39	3.44 - 3.50	3.62 - 3.69	3.62 - 3.69	3.62 - 3.69	8.31	------	7.31	7.29	8.01

Table 4.14. Continued

Complex	$H_{(\beta')}$	$H_{(\beta)}$	$H_{(\beta')}$	$H_{(\beta)}$	$H_{(OCH3)}$	$H_{(7)}$	$H_{(\alpha)}$	$H_{(\alpha')}$	$H_{(\alpha)}$	$H_{(\alpha')}$	$H_{(2)}$	$H_{(3)}$	$H_{(4)}$	$H_{(5)}$	$H_{(6)}$
(10): $R_1' = OCH_3$, $R_2' = H$															
Major	3.73 - 3.74	3.73 - 3.74	4.31 - 4.33	4.49 - 4.52	3.48*	3.91	4.45 - 3.51	3.57 - 3.65	3.57 - 3.65	3.57 - 3.65	7.94	------	7.05	7.29	7.84
(11): $R_1' = NO_2$, $R_2' = H$															
Major	3.63 - 3.67	3.63 - 3.67	4.44 - 4.49	4.44 - 4.49	3.48*	--------	3.49 - 3.55	3.75 - 3.85	3.75 - 3.85	3.75 - 3.85	8.29	------	8.12	7.36	7.51
(12): $R_1' =$, $R_2' = H$															
Major	3.77 - 3.89	3.77 - 3.89	4.44 - 4.52	4.44 - 4.52	3.48*	---------	3.62 - 3.71	3.62 - 3.71	3.77 - 3.89	3.77 - 3.89	9.00	------	8.56	7.68	8.85

* free methanol peak

Table 4.15. The ^1H NMR chemical shift data for complexes [ReO(spiro-L-R')$_2$(OMe)], $CDCl_3$ at 300 K.

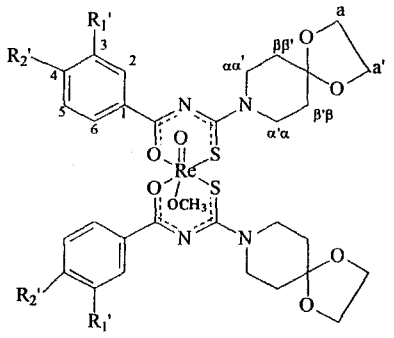

Complex	$H_{(\beta')}$	$H_{(\beta)}$	$H_{(\beta)}$	$H_{(\beta')}$	$H_{(OCH3)}$	$H_{(a)}$	$H_{(a')}$	$H_{(\alpha)}$	$H_{(\alpha')}$	$H_{(\alpha)}$	$H_{(\alpha')}$	$H_{(2)}$	$H_{(3)}$	$H_{(4)}$	$H_{(5)}$	$H_{(6)}$
(13): R_1' = H, R_2' = H																
Major	1.54 - 1.75	1.54 - 1.75	1.75 - 1.83	1.75 - 1.83	3.48*	3.96 - 4.01	3.96 - 4.01	3.68 - 3.75	3.96 - 4.01	4.49 - 4.55	4.49 - 4.55	7.37	8.24	7.47	8.24	7.37
(14): R_1' = NO_2, R_2' = H																
Major	1.27- 1.79	1.27- 1.79	1.84 - 1.91	1.84 - 1.91	3.48*	3.98- 4.02	3.98 - 4.02	3.78 - 3.84	3.98 - 4.02	3.98 - 4.02	3.98 - 4.02	8.95	-----	8.57	7.62	8.25

* free methanol peaks.

4.3. ^{1}H NMR kinetic studies of dimerization: Results.

The conversion of a monorhenium complex to a dirhenium complex is observed by a gradual colour change of the solution from maroon/brown to green and it is also indicated by the increase in the integral intensity of the major species and decrease in integral intensity of the minor species in the ^{1}H NMR spectrum with time.

4.3.1. The effect of the alkoxy ligand on the rate of the dimerization.

It has been observed that the rate of the colour change of the solution, which is associated with the dimerization, differs from one complex to another depending on the type of alkoxy ligand in the complex. Hence ^{1}H NMR kinetic studies of the three alkoxy complexes, $[ReO(L)_2(OMe)]$, $[ReO(L)_2(OEt)]$ and $[ReO(L)_2(O\textit{i}Pr)]$ were carried out in order to compare, qualitatively, the effect of the chain length and bulkiness of the alkoxy ligand on the rate of dimerization. For each complex, the concentrations of the two species in solution, at certain time intervals were determined by integration of the phenyl $H_{(2/6)}$proton. The rate of decrease in the integral intensity for the minor species and the increase in the integral intensity for the major species were then compared for these three complexes. Full details of the experimental procedure are given in the experimental section (Chapter 6) and the tabulated results are given in Appendix B. Graphical representations of the concentrations of the two species against time for each of the complexes are given in figures 4.8 - 4.10.

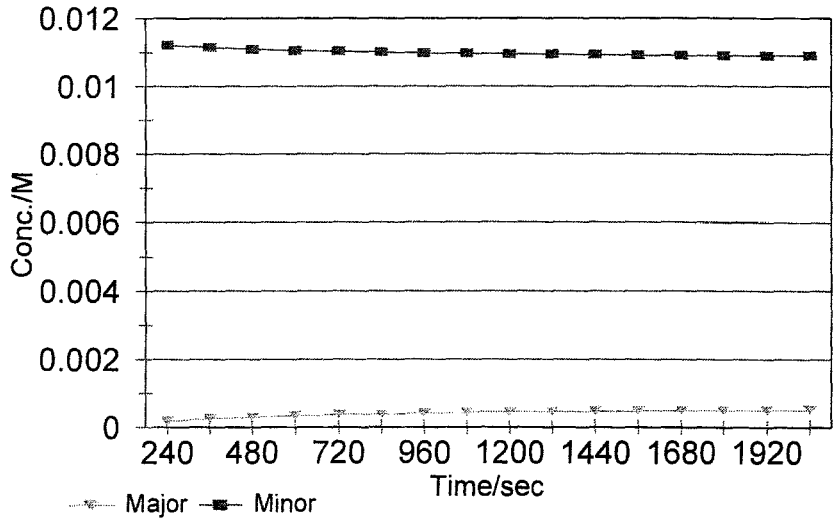

Figure 4.8. The graphical representation of $[ReO(L)_2(OMe)]$ (minor) → $[(L)_2ORe\text{-}O\text{-}ReO(L)_2]$ (major).

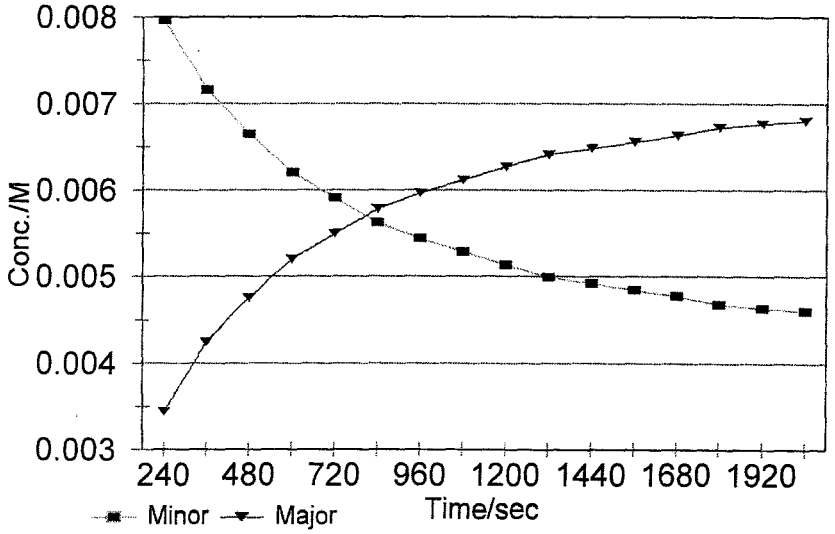

Figure 4.9. The graphical representation of $[ReO(L)_2(OEt)]$ (minor) → $[(L)_2ORe\text{-}O\text{-}ReO(L)_2]$ (major)

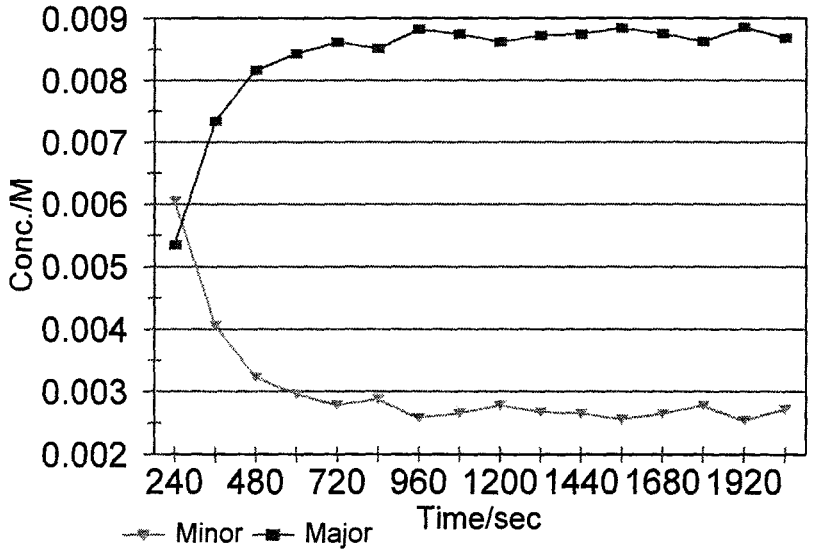

Figure 4.10. The graphical representation of [ReO(L)$_2$(O*i*Pr)] (minor) → [(L)$_2$ORe-O-ReO(L)$_2$] (major).

These results suggest that the rate of dimerization is fastest for the [ReO(L)$_2$(*i*OPr)] complex and slowest for the [ReO(L)$_2$(OMe)] complex. The rates of the colour change of the solutions of these three complexes also follow the same order.

4.3.2.The effect of the thioamide functionality on the rate of the dimerization.

Different rates in the change of colour of the solutions of the complexes with different thioamide functionalities were also observed, suggesting that the thioamide functionality also plays a role in the rate of dimerization. Due to time constraints, this factor could not be examined in any detail. Comparison of the rate of dimerization for different thioamide functionalities was however carried out by monitoring the change in colour of the solutions of [ReO(L)$_2$(OMe)], [ReO(morph-L)$_2$(OMe)] and [ReO(spiro-L)$_2$(OMe)] of the same concentrations in $CDCl_3$. The times taken for each solution to turn completely green in colour are shown in Table 4.16.

Table 4.16. Shows different times taken for each solution to turn green

Complex solution	Time/min.
$[ReO(L)_2(OMe)]$	40
$[ReO(morph\text{-}L)_2(OMe)]$	10
$[ReO(spiro\text{-}L)_2(OMe)]$	8

These results suggest that the more bulky the thioamide, the faster the rate of dimerization. Thus, $[ReO(spiro\text{-}L)_2OMe]$ complex undergoes dimerization the fastest followed by $[ReO(morph\text{-}L)_2OMe]$ and then the $[ReO(L)_2OMe]$ complex.

4.4. Discussion.

4.4.1. Synthetic chemistry.

4.4.1.1. Precursor studies.

The precursor studies have shown that the same complex, $[ReO(L)_2(OMe)]$, is obtained when the three different Re(V)-oxo precursor complexes, $ReOCl_3(PPh_3)_2$, $[ReO_2(py)_4]Cl$ and $[n\text{-}Bu_4N][ReOCl_4]$, are reacted with *N,N*-diethyl-*N'*-benzoylthiourea under basic conditions. Hence, the preparation of the mixed ligand Re(V)-oxo complexes containing acylthiourea and alkoxy ligands does not depend on the type of Re(V)-oxo precursor complex used for the reaction.

However, different percentage yields are obtained when the different Re(V)-oxo precursor complexes are used. The results have shown that the best product yield, calculated directly from the commercial rhenium(V) source ($KReO_4$), is obtained when $[ReO_2(py)_4]Cl$ is used. The low product yield obtained when using $ReOCl_3(PPh_3)_2$ could be accounted for by the fact that reactions involving $ReOCl_3(PPh_3)_2$ tend to be complicated by the presence of the triphenylphosphines which usually result in a mixture of products. The isolation of the target product from this mixture requires further separation techniques which could result in the loss of some of the product.

Although the reaction of $[n\text{-}Bu_4N][ReOCl_4]$ with *N,N*-diethyl-*N'*-benzoylthiourea ligand yields a pure product, which does not need any further purification, $[n\text{-}Bu_4N][ReOCl_4]$ is moisture sensitive and decomposes very rapidly and this could explain why a lower yield was obtained when this complex salt was used as a precursor.

4.4.1.2. Base studies.

The reaction of $[ReO_2(py)_4]Cl$ with *N,N*-diethyl-*N'*-benzoylthiourea in the absence of a base yielded a mixture of compounds, the characterization of which could not be carried out due to the small amounts of these compounds. However, the reaction between $[n\text{-}Bu_4N][ReOCl_4]$ and *N,N*-diethyl-*N'*-benzoylthiourea, in the absence of a base and under an inert atmosphere, resulted in the formation of the neutral chloro complex $[ReO(L)_2Cl]$.

As mentioned above, the addition of a base to the reaction mixture resulted in the formation of the mixed ligand complex $[ReO(L)_2(OMe)]$ in all cases. The present studies have also shown that the use of triethylamine and sodium acetate leads to the formation of the same product in virtually the same percentage yields.

4.4.1.3. Solvent studies.

These studies have shown that the solvent used for the reaction determines the composition of the resultant complex. The three different alkoxy complexes $[ReO(L)_2(OMe)]$, $[ReO(L)_2(OEt)]$ and $[ReO(L)_2(O\textit{i}Pr)]$ are obtained when using methanol, ethanol and *iso*-propanol, respectively. However, the use of acetonitrile resulted in the formation of an oxygen bridged dirhenium complex $[(L)_2ORe\text{-}O\text{-}ReO(L)_2]$.

4.4.2. Characterization.

4.4.2.1. Molecular configuration of the synthesized complexes.

As shown in figure 4.11, two molecular configurations, A and B, for Re(V)-oxo complexes with bidentate acylthiourea ligands are possible.

Figure 4.11. Two possible molecular configurations of Re(V)-oxo complexes with bidentate acylthiourea ligands.

In configuration A, the two acylthiourea ligands form the equatorial plane of the octahedron, with Re=O occupying the axial position. The monodentate ligand, X, which completes the octahedral geometry is situated *trans* to the oxo ligand. The two acylthiourea ligands in configuration B are perpendicular to each other forming a nonsymmetrical arrangement about the Re=O, with X situated *cis* to the oxo ligand. The configuration of the resultant complex depends on relative *trans* influences of the donor atoms in the coordination sphere. It is well-established that due to the strong *trans* influence of the Re=O bond, the binding of a hard donor atom *trans* to the Re=O group is preferred.[9,15] Hence, in configuration B, X has a greater *trans* influence than the oxygen donor atom of the bidentate ligand, whereas the oxygen donor atom of the chelate ligand has a greater *trans* influence than X in configuration A. In all the configurations the sulfur and oxygen donor atoms are *cis* to each other.

Both the solid and solution state studies have shown that complexes with the molecular configuration A are obtained in the present studies, with the exception of complex **(1b)** which has configuration B. This shows that the alkoxy ligand in these complexes has a smaller *trans* influence than the oxygen donor atom of the chelate ligand. In the dirhenium complex **(15)** both halves of the molecule also have the A configuration.

4.4.2.2. Solid state chemistry.

The IR spectra of all the complexes show a shifting and reduction in intensity of the carbonyl

stretch due to the reduction of the double bond character when the oxygen donor atom binds to the rhenium metal upon complex formation. There is also a disappearance of the N-H stretching peak in the IR spectra for all complexes which indicates the deprotonation of the benzoylthiourea ligand upon complex formation. A very strong band between 890 and 950 cm^{-1} indicates the presence of the Re=O bond in all complexes. Complexes **(1) - (14)**, with the exception of **(1b)**, have a strong band in the 400 - 600 cm^{-1} region which is due to a ν(Re-OR") stretch. The appearance of two very strong bands at 650 and 665 cm^{-1}, which are characteristic of Re-O-Re stretches, and the disappearance of strong bands in the range 400 - 600 cm^{-1}, which is the region for Re-OR" stretches, provides evidence for the formation of the dirhenium complex **(15).**

A closer examination of the Re=O bond stretches for the alkoxy complexes **(1) - (14)**, which are given in Table 4.17, shows that there is a significant difference (approximately 10 cm^{-1}) in the position of the ν(Re=O) band for the two rhenium complexes $[ReO(LNO_2)_2(OMe)]$ and $[ReO(LCH_3)_2(OMe)]$.

Table.4.17. Shows the trend in ν(Re=O) as the substituent (R') on the phenyl ring is changed.

R'	ν(Re=O)/cm^{-1}		
	Diethyl Ligand	Morpholine Ligand	Spiro Ligand
NO_2,	937	938	936
$-OCH_3$	946	940	------
H	942	941	946
Cl	945	941	------
$-CH_3$	946	941	------

This difference can be explained in terms of the electron withdrawing/donating nature of the R' substituents on the phenyl ring of the *N,N*-dialkyl-*N'*-(substituted)benzoylthiourea ligands. The NO_2 substituent is an electron withdrawing group and could thus reduce the electron density

on the rhenium metal ion, thereby reducing the π-back-bonding character of this metal to the oxo ligand. This would result in a slight reduction in the double bond character of the Re=O bond. On the other hand, the electron donating group, CH_3, could increase the electron density on the rhenium metal ion hence enhancing the π-back-bonding character of the rhenium metal to the oxo ligand. The overall result is that the ν(Re=O) band in $[ReO(LNO_2)_2(OMe)]$ should be expected at lower wavenumbers compared to the ν(Re=O) band for $[ReO(LCH_3)_2(OMe)]$, and this agrees with the results observed.

A similar explanation could be given to explain the difference (approximately 10 cm^{-1}) in the position of the ν(Re=O) bands for the $[ReO(spiro\text{-}LNO_2)_2(OMe)]$ and $[ReO(spiro\text{-}L)_2(OMe)]$ complexes. The difference in the position of the ν(Re=O) bands for $[ReO(morph\text{-}LNO_2)_2(OMe)]$ and $[ReO(LCH_3)_2(OMe)]$ is however smaller, but this difference could also be due to electronic effects.

As shown in Table 4.18, the ν(Re-OR") frequencies increase with an increase in the number of carbon atoms of the alkoxy ligand.

Table 4.18. The ν(Re=O) and ν(Re-R") IR stretches and their corresponding bond lengths.

Complex	R"	IR stretches/cm^{-1}		Bond lengths/Å	
		ν(Re=O)	ν(Re-R")	Re=O	Re-R"
(1)	$-OCH_3$	942	495	1.701(14)	1.897(4)
(6)	$-OCH_2CH_3$	948	584	1.687(3)	1.899(3)
(7)	$-OCH(CH_3)_2$	933	592	---------	---------
(15)	Re	891	651, 665	1.685(5)	1.893(4)
				1.691(5)[a]	1.917(4)[a]

[a] Bond length values for the second half of the dirhenium complex.

These results can be explained in terms of the different electronic properties of the alkoxy ligands due to the inductive effect of the groups attached to the alkoxy oxygen donor atom. The electron donating ability of the oxygen donor atom increases with the increase in the carbon chain length of the alkoxy group.[11] It is therefore expected that the electron donating character will be highest in the $(CH_3)_2CH_2O$- ligand and lowest in the CH_3O- ligand as shown in figure 4.12.

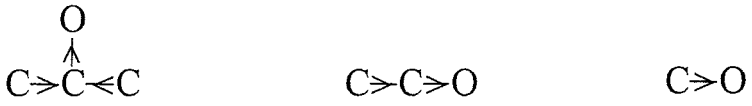

Figure 4.12. Shows the inductive effect in iso-propanol, ethanol and methanol.

The increase in electron density on the oxygen donor atom of the alkoxy ligand will allow it to bind more strongly to the metal ion and as a result the Re-OR" bond strength should decrease in the order $[ReO(L)_2(OiPr)]$ **(7)** > $[ReO(L)_2(OEt)]$ **(6)** > $[ReO(L)_2(OMe)]$ **(1)**. This trend is reflected in the ν(Re-OR") stretching frequencies, which decrease in the order **(7)** (592 cm^{-1}) > **(6)** (584 cm^{-1}) > **(1)** (496 cm^{-1}), which corresponds to a decrease in the Re-OR" bond strength.

According to the molecular configuration A (see figure 4.12), the alkoxy ligand is situated *trans* to the Re=O moiety. In this configuration the different R" groups are expected to lead to different Re-OR" bond strengths which in turn will exert different degrees of *trans* influences on the Re=O moiety. The stronger the Re-OR" bond, the weaker the Re=O bond should be and this should be seen as a decrease in the ν(Re=O) wavenumber. This trend is observed for complexes **(6)** and **(7)** in that the ν(Re=O) band in $[ReO(L)_2(OiPr)]$ is at a lower wavenumber compared to the ν(Re=O) band in $[ReO(L)_2(OEt)]$. However this trend does not include the $[ReO(L)_2(OMe)]$ complex and this could be due to differences in the vibrational coupling in the three complexes.[12]

The ν(Re-OR") stretching frequencies for the dirhenium complex **(15)** indicate that the bridging oxygen atom binds strongly to the rhenium metal ions. The ν(Re=O) band in the dirhenium complex has shifted to a lower stretching frequency (890 cm^{-1}) relative to the ν(Re=O) moiety

stretching frequencies in the monorhenium complexes. This suggests that the μO ligand exerts a higher *trans* influence on the Re=O relative to the alkoxy ligands and is in agreement with the fact that the μO ligand binds more strongly relative to the alkoxy ligands.

The X-ray crystal structures of $[ReO(L)_2(OMe)]$ **(1)**, $[ReO(LNO_2)_2(OMe)]$ **(4)** and $[ReO(L)_2(OEt)]$ **(6)** have confirmed that these complexes adopt configuration A, as shown in figure 4.11. In these complexes the rhenium metal has a slightly distorted octahedral geometry. The two ligands are in a symmetrical environment and are arranged *cis* to each other in the equatorial plane. In the dirhenium complex **(15)**, the metal ion adopts a similar geometry, however, the ligands of the one half are not eclipsed with respect to the ligands in the other half.

The S(1)-Re(1)-S(2) angles, in all four complexes, are virtually right angles with values ranging between 89.17(4) and 91.63(6)°. On the other hand the O(3)-Re(1)-O(4) angles formed by the oxygen donors atoms from the two ligands, are slightly smaller with values ranging between 81.63(9) and 86.79(11)°. This angle has been found to be even smaller in the chloro complex reported by Dilworth *et al.* (79.3(2)°).[1]

In the alkoxy complexes **(1)**, **(4)** and **(6)**, the angle formed by the oxo ligand and the oxygen donor atom of the alkoxy ligand, O(1)-Re(1)-O(2), ranges from 163.05(16) to 164.94(11)°. In the chloro complex, this angle formed by the oxo ligand, the rhenium centre and the oxygen donor atom of one of the acylthiourea ligands, is greater (169.8(3)°).[1] In complex **(15)**, these bond angles, O(1)-Re(1)-O(2) and O(5)-Re(2)-O(2), formed by the oxo ligands, the rhenium centres and the bridging oxygen are closely related to that in the chloro complex and they amount to 171.2(2) and 167.9(2)°, respectively. The Re(1)-O(2)-Re(2) is 175.2(2)° and together with the O(1)-Re(1)-O(2) and O(5)-Re(2)-O(2) bond angles, these three bond angles make the O(1)-Re(1)-O(2)-Re-O(5) system quasi linear.

The Re=O bond lengths in complexes **(1)**, **(4)**, **(6)** and **(15)** are closely related (see Table 4.18) and they average 1.693 Å. It was expected that the Re=O bond lengths in complexes **(1)**, **(6)**, **(15)** would differ significantly according to different *trans* influences exerted by the different

ligands in the *trans* position to the Re=O. However the results show that there are no significant differences in the Re=O bond lengths for these complexes and these bond lengths fall within the range reported for related complexes (range: 1.677(6) - 1.723(7) Å).[4, 5, 12, 13, 14, 15] The Re-OR" bond lengths in complexes **(1)**, **(4)**, **(6)** and **(15)** are also closely related (see Table 4.18, average1.898 Å) and they are comparable to the estimated Re-O single bond length (2.04 Å) using Pauli's covalent radii.[16] The Re-O bond lengths for the bonds between the rhenium metal ion and the oxygen donor atoms of the chelate ligands are slightly longer and average 2.111 Å.

The average Re-S single bond length in complexes **(1)**, **(4)**, **(6)** and **(15)** is 2.336 Å. These Re-S bond lengths are similar to the Re-S single bond lengths reported for the $[ReO(L)_2Cl]$ and [ReO(TATU)] (TATU = thiol-amide-thiourea) complexes (range: 2.269(5) - 2.409(4) Å)[1,14] and they are also comparable to the average Re-S bond length in the rhenium complex with the monodentate thiourea ligand, $[ReO(H_2O)Cl_2(SCN_2H_4)_2]$ (2.356(5) Å).[17]

The C-S, C-O, and C-N bond lengths in the chelate ring of all the complexes show partial double bond character due to the delocalization of electrons in the ring. The delocalization of electrons in the ring also extends to the thioamide bond, (C(S)-N), rendering this bond partial double bond character with average bond lengths of 1.332 Å in all four complexes (see Appendix A). This extensive delocalization of electrons is also manifested in the ^{1}H NMR spectrum as a separation of the resonance shifts for the $-CH_{2(\alpha)}$ protons due to the restricted rotation around this bond.

4.4.2.3. Solution state chemistry.

All the complexes were found to be air stable in the solid state, however, studies of the complexes in solution have shown that all the alkoxy complexes dimerize to give a dirhenium complex. This is indicated by the two sets of resonances and the appearance of the free alcohol signals in the ^{1}H NMR spectra of all the alkoxy complexes. Furthermore this dimerization is accompanied by a colour change of all the solutions for the monorhenium complexes from brown/maroon to green in $CDCl_3$. It was possible to isolate a green crystalline material by slow evaporation of $CDCl_3$ from the NMR sample of the $[ReO(L)_2(OMe)]$ complex. The ^{1}H NMR and IR spectra of these

green coloured crystals corresponded to the one for the complex obtained from the reaction of LH with $[ReO_2(py)_4]Cl$ in acetonitrile and the recrystallization of $[ReO(L)_2(OMe)]$ from acetone (i.e complex **(15)**).

For both the monorhenium and dirhenium complexes, a single set of proton signals is observed which means the chelated acylthiourea ligands are in the same chemical environment as suggested by the symmetrical molecular configuration A. The ^1H NMR spectroscopy shows the expected disappearance of the N-H peak (between 8 and 12 ppm) in all the complexes. The disappearance of the N-H peak is also accompanied by a general downfield shift of the proton resonances due to the altered electronic properties of the ligand upon binding to the rhenium metal. The alteration of the electronic properties of the ligand upon complexation includes among other factors the delocalization of the electrons within the six membered chelate ring of the acylthiourea ligand.

Besides the general shifting of the proton resonances of the acylthiourea ligands upon complexation, the proton resonances of the complexes are better resolved than the corresponding proton resonances of the unbound acylthiourea ligands and this is more pronounced in the dialkyl functionality. This enhanced resolution is attributed to the delocalization of electrons within the six membered chelate ring which in turn extends to the thioamide C-N bond, rendering it a partial double bond and hence slowing down the rotation about this bond.

Although this dimerization was not observed with the closely related $[ReO(L)_2Cl]$ complex, it has been previously observed for a number of other mixed ligand rhenium complexes with different ligand structures from the one used presently. As an example, van Bommel *et al.* reported the dimerization of the [ReO(salpd)(OAlk)] complex to [(salpd)ORe-O-ReO(salpd)] (salpd = *O,N,N,O*-tetradentate Schiff base ligands).[9]

Both present and previous studies[9, 13] have suggested that the dimerization from a monorhenium to a dirhenium complex is facilitated by the presence of traces of water and the absence of alcohol. Van Bommel *et al.* proposed that the formation of the μO bond probably occurs because the alkoxy moieties exchange with water from the air to form an $[ReO(L)_2OH]$ intermediate, which

dimerizes with the elimination of a water molecule as shown in Scheme 4.3.[9]

$$ReO(alkoxy)(L)_2 + H_2O \longrightarrow HO\text{-}ReO(L)_2 + alcohol \quad (a)$$

$$HO\text{-}ReO(L)_2 + HO\text{-}ReO(L)_2 \longrightarrow (L)_2ORe\text{-}O\text{-}Re(O)(L)_2 + H_2O \quad (b)$$

Scheme 4.3. The proposed scheme for dimerization (L = benzoylthiourea ligand).

The present studies have shown that this reaction is reversible in the presence of alcohol. This was indicated by the change in colour of the solution of the dirhenium complex in $CDCl_3$ from green back to brown on addition of methanol to the solution, which is in agreement with the two sets of resonances observed in the ^1H NMR spectrum. This suggests that an equilibrium exists between the monorhenium and the dirhenium complexes. Preliminary ^1H NMR kinetic studies were carried out in order to examine this dimerization in a bit more detail.

4.4.3. Preliminary ^1H NMR kinetics studies of dimerization.

Graphical representations of the dimerization for the three complexes $[ReO(L)_2(O\textit{i}Pr)]$, $[ReO(L)_2(OEt)]$ and $[ReO(L)_2(OMe)]$ in figures 4.8 - 4.10, clearly show the decrease in the concentration of the mononuclear species as the concentration of the dinuclear species increases. The flattening of the curves (clearly seen in figure 4.10) before the monorhenium complex is completely converted to a dirhenium complex, confirms the suggested reversibility of this reaction.

This study has also shown that the rate of dimerization changes as the type of the alkoxy ligand is changed. This is clearly shown in figure 4.13 where the increase in the concentration of the dirhenium complex in the ^1H NMR samples for complexes $[ReO(L)_2(O\textit{i}Pr)]$, $[ReO(L)_2(OEt)]$ and $[ReO(L)_2(OMe)]$ was plotted against time. These results have shown qualitatively that the rate of dimerization increases with the increase in the carbon chain length and bulkiness of the alkoxy ligand (i.e. $[ReO(L)_2(O\textit{i}Pr)] > [ReO(L)_2(OEt)] > [ReO(L)_2(OMe)]$.

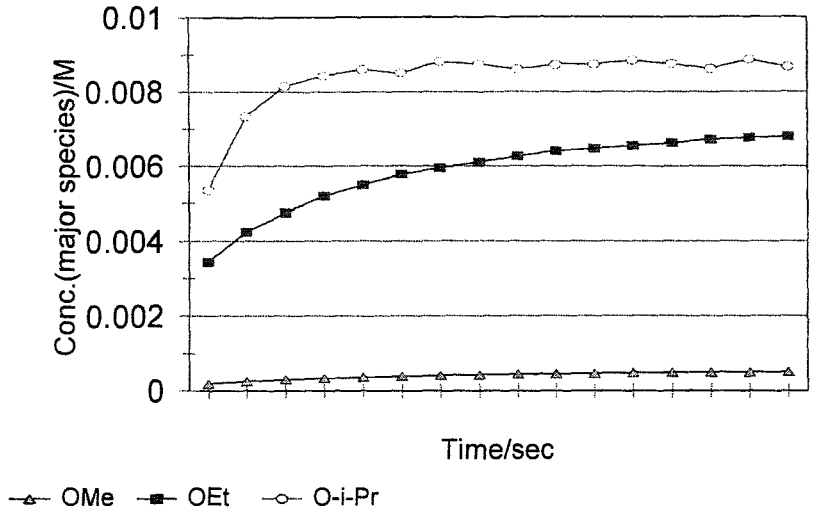

Figure 4.13. Comparison of the rate of dimerization for the three different alkoxy complexes: $[ReO(L)_2(OMe)]$, $[ReO(L)_2(OEt)]$ and $[ReO(L)_2(O\textit{i}Pr)]$.

These results were somewhat unexpected because according to the IR data discussed above the Re-$OCH(CH_3)_2$ bond is the strongest and the hydrolysis thereof was expected to be the slowest. It is possible that the rate of this nucleophilic substitution could be increased by steric effects due to the increased bulkiness of the alkoxy ligand. These results could, perhaps, also be explained in terms of the different stabilities of the alcohols, which can be compared by considering their pK_a values.

The pK_a values of *iso*-propanol, ethanol and methanol are 18.00, 16.00 and 15.54, respectively.[11] These values indicate that protonation of *iso*-propoxy to *iso*-propanol is most favoured, which in turn would favour the dimerization reaction proposed in Scheme 4.2. A comparison of the colour of change of complexes $[ReO(L)_2(OMe)]$, $[ReO(morph\text{-}L)_2(OMe)]$ and $[ReO(spiro\text{-}L)_2(OMe)]$, with time, suggests that the rate of dimerization increases in the following order: $[ReO(L)_2(OMe)] < [ReO(morph\text{-}L)_2(OMe)] < [ReO(spiro\text{-}L)_2(OMe)]$. This suggests that the rate of dimerization increases with the increase in the bulkiness of the thioamide functionality.

REFERENCES

1. R. Dilworth, J. S. Lewis, J. R. Miller, Y. Zheng, *Polyhedron*, **12**, 221, (1993).
2. K. Nakamoto, *Infrared and Raman Spectra of Inorganic Coordination Compounds, 3rd ed.*, John and Wiley Inc., New York (1978).
3. T. N. Rao, D. Adhikesavalu, A. Camerman, A. R. Fritzberg, *J. Am. Chem. Soc.*, **112**, 5798, (1990).
4. L. G. Marzilli, M. G. Banasczyk, L. Hansen, Z. Kuklenyik, R. Cini, A. Taylor, Jr, *Inorg. Chem.*, **33**, 4850, (1994).
5. L. Hansen, R. Cini, A. Taylor, Jr, L. G. Marzilli, *Inorg. Chem.*, **31**, 2801, (1992).
6. R. W. Adams, R. L. Martin, G. Winter, *Aust. J. Chem.*, **20**, 773 (1967).
7. G. N. Holder, L. A. Bottomley, *Inorg. Chimica. Acta*, **194**, 133, (1992).
8. G. Wilkinson (editor-in chief), *Comprehensive Coordination Chemistry*, **4**, 125 Pergamon Press, Great Britain, (1987).
9. K. J. C. van Bommel, W. Verboom, H. Kooijman, A. L. Spek, D. N. Reinhoudt., *Inorg. Chem.*, **37**, 4197, (1998).
10. C. J. Pouchert, *The Aldrich Library of NMR Spectra, 2nd ed.*, Aldrich Chemical Company Inc., USA, (1983).
11. J. McMurry, *Organic Chemistry, 3rd ed.*, Brooks/Cole, Pacific Grove, California, (1992).
12. P. A. Skoog, D. M. West, *Principles of Instrumental Analysis, 2nd ed.*, 218, H. Sounders, New York, (1981).
13. S. R. Fletcher, A. C. Skapski, *J. Chem. Soc. Dalton Trans.*, 1073, (1972).
14. M. Lipowska, B. L. Hayes, L. Hansen, A. Taylor, Jr., L. G. Marzilli, *Inorg. Chem.*, **35** 4227, (1996).
15. W. A. Herrmann, M. U. Rouch, G. R. J. Artus, *Inorg. Chem.*, **35**, 1988, (1996).
16. F. A. Cotton, S. J. Lippard, *Inorg. Chem.*, **5**, 416, (1966).
17. T. Lis, *Acta Cryst.*, **B 32**, 2707, (1976).

CHAPTER 5

Tc(V)-oxo COMPLEXES WITH THE BENZOYLTHIOUREA LIGANDS.

Introduction

Dilworth *et al.* have briefly mentioned the formation of the square pyramidal cationic complex $[TcO(DEBT)_2]^+$ in their study on the neutral pseudo-octahedral rhenium complex $[ReO(DEBT)_2Cl]$.[1] This is, to the best of our knowledge, the only existing information on the complexation reaction of technetium(V) with *N,N*-diethyl-*N'*-benzoylthiourea in the literature. Details of the reaction conditions used for the preparation of the complex $[TcO(DEBT)_2]^+$ were also not discussed.

Unfortunately, due to time constraints, the complexation reaction of technetium(V) with all other ligands, described in Chapter 2, could not be investigated and only the complexation reaction of $[n\text{-}Bu_4N][TcOCl_4]$ with *N,N*-diethyl-*N'*-benzoylthiourea (LH) could be examined in some detail. These studies were done using the ground state technetium isotope (^{99}Tc) and the results have suggested that a square pyramidal complex $[TcO(L)_2]Cl$ (see figure 5.1) is obtained under the reaction conditions discussed below. Due to the unavailability of the necessary facilities and equipment required for handling radioactive material at Rhodes University, these studies were carried out at the Atomic Energy Corporation of South Africa in Pelindaba.

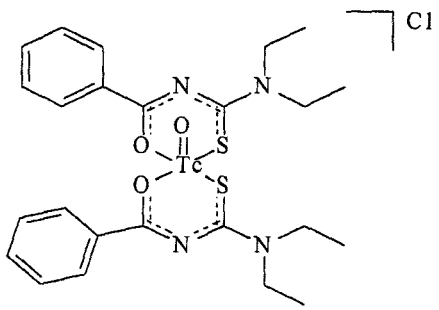

Figure 5.1. The structural formula of $[TcO(L)_2]Cl$.

5.1. Results and discussion.

5.1.1. Complexation of Tc(V)-oxo with LH.

A Tc(V)-oxo complex with LH was obtained by the reaction of [*n*-Bu_4N][$TcOCl_4$] with the ligand in the presence of triethylamine, as shown by equation 5.1.

$$[n\text{-}Bu_4N][TcOCl_4] \quad + \quad 2\,LH \xrightarrow[MeOH]{2\,Et_3NH} [TcO(L)_2]Cl \quad \textbf{(5.1)}$$

The sequence in which thereactants are added was found to be very important. When the solution of [*n*-Bu_4N][$TcOCl_4$] in methanol was added to a mixture of the ligand and base in methanol, a black precipitate was obtained possibly due to the formation of [$TcO_2.xH_2O$]. The addition of the ligand to a mixture of [*n*-Bu_4N][$TcOCl_4$] and triethylamine also resulted in the formation of [$TcO_2.xH_2O$]. On the other hand, the [$TcO(L)_2$]Cl complex was obtained as green coloured crystals when a solution of [*n*-Bu_4N][$TcOCl_4$] was slowly added to a solution of the ligand followed by the slow addition of triethylamine.

5.1.1.1. The effect of the base on the reaction.

In the absence of triethylamine the reaction according to equation 5.1 did not occur as no colour change was observed. When the reaction, described above, was carried out in the presence of sodium acetate, the colour of the reaction mixture turned black. The TLC of this reaction mixture indicated the presence of five compounds and an attempt to separate these compounds using flash chromatography was unsuccessful. Hence the complex [$TcO(L)_2$]Cl could only be obtained when triethylamine was used for the complexation reaction instead of sodium acetate.

5.1.2.Characterization.

5.1.2.1. Solid state chemistry.

The elemental analysis of the complex [$TcO(L)_2$]Cl is given in Table 5.1. The appearance of the

ν(Tc=O) at 928 cm^{-1} and the shifting/disappearance of the ν(C=O) at 1600 cm^{-1} in the IR spectrum provides evidence for the formation of $[TcO(L)_2]Cl$ complex. The absence of a ν(Tc-OCH_3) between 300 and 600 cm^{-1}, which is the region where ν(M-OR) is normally observed, also provides evidence for the formation of the structural formula shown in figure 5.1, instead of the methoxy complex. The complete IR data set is given in the experimental section (Chapter 6).

Table 5.1. The elemental analysis data for $[TcO(L)_2]Cl$.

Complex	C %	H %	N %
$[TcO(L)_2]Cl$ **(16)**	47.97	5.31	8.69
	(46.54)[a]	(4.90)[a]	(9.00)[a]

[a] Calculated values are given in parentheses

5.1.2.2. Solution state chemistry.

The ^1H NMR spectrum of this complex shows the presence of two sets of resonances with different integral ratios which suggests that dimerization of the complex occurs in solution, similar to that observed for the Re(V)-oxo complexes with *N,N*-dialkyl-*N'*-(substituted)benzoylthiourea ligands. Due to overlapping of peaks, not all peaks could be unambiguously assigned, hence the ^1H NMR spectrum of the complex is shown in figure 5.2.

The absence of proton resonances due to a methoxy ligand in the ^1H NMR spectrum, provides further evidence that a methoxy complex is not formed. The duplication of the proton resonance peaks, as can be seen in figure 5.2, suggests that dimerization to the oxygen bridged dinuclear complex $[(L)_2OTc\text{-}O\text{-}TcO(L)_2]$ occurs in solution. The dimerization of Tc(V)-oxo complexes has been observed in many cases with other ligand systems and has been shown to take place in solution in the presence of water traces.[2] The fact that one set of resonances is observed for the mononuclear and the dinuclear species, suggests the symmetrical arrangement of the ligands around the technetium centre in each complex (mononuclear and binuclear) and is in accordance with the square pyramidal configuration in the mononuclear complex.

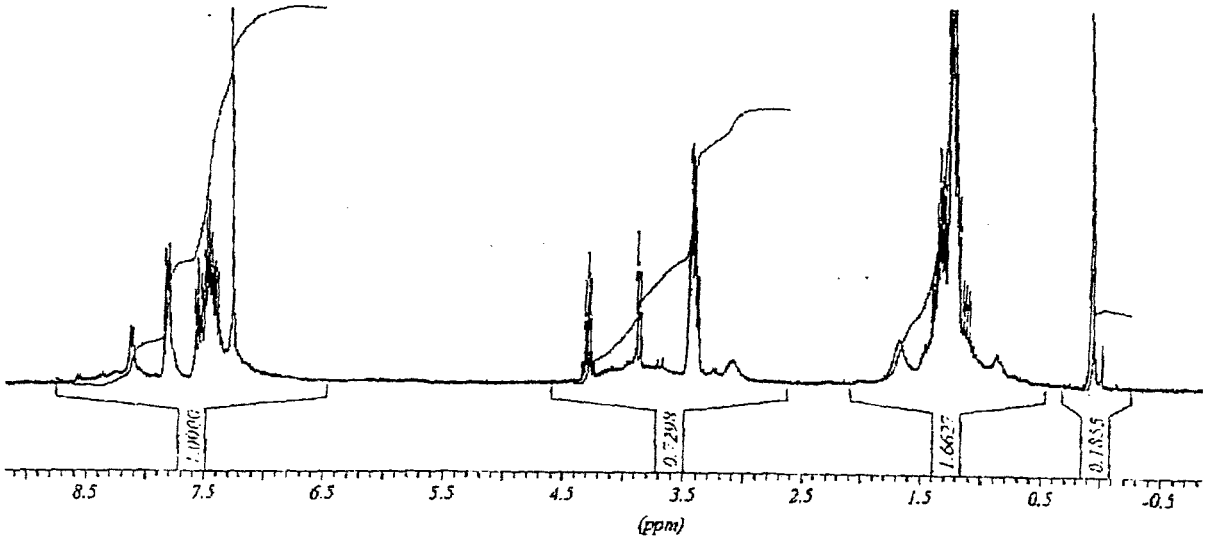

Figure 5.2. The ^{1}H NMR spectrum of $[TcO(L)_2Cl]$ in $CDCl_3$ at 303 K.

In summary, the preliminary studies done in the present study have indicated that the complexation chemistry of technetium(V) with the *N,N*-dialkyl-*N'*-benzoylthiourea is different to that of rhenium(V). The reaction between $[n\text{-}Bu_4N][TcOCl_4]$ and *N,N*-diethyl-*N'*-benzoylthiourea yielded the square pyramidal cationic complex $[TcO(L)_2]Cl$ under the conditions discussed above. By contrast the octahedral methoxy complex $[ReO(L)_2(OMe)]$ was obtained when the analogous Re(V)-oxo precursor, $[n\text{-}B_4N][ReOCl_4]$, was reacted with *N,N*-diethyl-*N'*-benzoylthiourea under the same reaction conditions. This presumably reflects the greater lability of the ligand *trans* to the oxo group on technetium.

REFERENCES

1 J. R. Dilworth, J. S. Lewis, J. R. Miller, Y. Zheng, *Polyhedron*, **12**, 221, (1993).

2. F. Tisato, F. Refosco, U. Mazzi, G. Bandoli A. Dolmella, *Inorg. Chim. Acta,* **164**, 127, (1989).

CONCLUDING REMARKS

The present study has shown that Re(V)-oxo complexes with *N,N*-dialkyl-*N'*-(substituted)benzoylthiourea ligands are obtained by the reaction of the ligands with different Re(V)-oxo precursor complexes, $ReOCl_3(PPh_3)_2$, $[ReO(py)_4]Cl$ and $[n\text{-}Bu_4N][ReOCl_4]$. This study has also shown that a Tc(V)-oxo complex with the *N,N*-diethyl-*N'*-benzoylthiourea ligand is afforded by the reaction of $[n\text{-}Bu_4N][TcOCl_4]$ with the ligand. However, this study has revealed that the synthesis of Re(V)-oxo complexes with *N,N*-dialkyl-*N'*-(substituted)benzoylthiourea ligand systems is not straight-forward and that different reaction conditions lead to the formation of different products.

It was found that the formation and composition of the resultant complex depends on the basicity and solvent of the reaction. While no characterizable product was obtained when $[ReO_2(py)_4]Cl$ was reacted with *N,N*-diethyl-*N'*-benzoylthiourea in the absence of a base, the reaction between $[n\text{-}Bu_4N][ReOCl_4]$ and *N,N*-diethyl-*N'*-benzoylthiourea in the absence of a base under an inert atmosphere gave the chloro complex $[ReO(L)_2Cl]$. However, the reaction of all three Re(V)-oxo precursor complexes $ReOCl_3(PPh_3)_2$, $[ReO_2(py)_4]Cl$ and $[n\text{-}Bu_4N][ReOCl_4]$ with *N,N*-diethyl-*N'*-benzoylthiourea carried out in methanol, in the presence of sodium acetate, resulted in the formation of the methoxy complex $[ReO(L)_2(OMe)]$. The formation of the different alkoxy complexes when *N,N*-diethyl-*N'*-benzoylthiourea was reacted with $[ReO_2(py)_4]Cl$ using different solvents is an indication of the dependence of the resultant complex on the solvent used for the reaction.

This study has also shown that the alkoxy ligand is displaced in the presence of water to give the oxygen bridged dirhenium complex. This indicates that the alkoxy ligands could be displaced by other donor ligands in solution. Thus it can be expected that biological moieties with suitable donor atoms could displace the alkoxy ligand and hence bind directly to the metal. Ligand exchange reactions of this type have been explored by van Bommel *et al.* using a cholesteroxy ligand.[1] In the present study, the ^1H NMR kinetic study of the dimerization has shown that the bulkier the alkoxy ligand, the faster the rate of dimerization. This means that in order to

synthesize complexes for attachment to biologically active moieties, the use of bulky alcohols should be considered.

Due to time constraints, the complexation reactions of Tc(V)-oxo precursor complex with these ligand structures could not be extensively studied. However, preliminary studies carried out suggest that the coordination chemistry of Tc(V)-oxo with *N,N*-dialkyl-*N'*-(substituted)benzoylthiourea is different to that of Re(V)-oxo.

While the initial and developing objectives have been addressed in the present study, various possibilities for future research have been identified and these include the following:

1. Synthesis of water soluble complexes through derivatization of the *N,N*-dialkyl-*N'*-(substituted)benzoylthiourea ligands.
2. Synthesis of Re(V)-oxo and Tc(V)-oxo complexes of *N,N*-dialkyl-*N'*-acylthiourea ligands which contain suitable substituents for the potential binding of biologically active moieties.
3. Synthesis of complexes of Re(V)-oxo and Tc(V)-oxo complexes with tetradentate acylthiourea ligands, which could be expected to be more stable.
4. To study the kinetics of the dimerization in more detail in order to elucidate the reaction mechanism involved. In addition, ligand exchange reactions with biologically active ligands could be explored.

REFERENCES

1. K. J. C. van Bommel, W. Verboom, H. Kooijman, A. L. Spek, D. N. Reinhoudt., *Inorg. Chem.*, **37**, 4197, (1998).

CHAPTER 6

EXPERIMENTAL.

6.1. Physical Methods.

Thin-layer chromatography (TLC) was performed on silica sheets $60F_{254}$ (Merck, Darmstadt). Flash chromatography was performed on silica gel 60. Melting points of all compounds were recorded on a Reichert hot-stage microscope and are uncorrected. ^{1}H NMR spectra were recorded at 400.13 MHz on a Bruker 400AMX spectrometer, except for the ^{1}H NMR spectrum of $[TcO(L)_2(Cl)]$ which was recorded on a Bruker (500 MHz) spectrometer at Pretoria University. All samples were prepared using deuterated chloroform ($CDCl_3$) purchased from Aldrich Chemical Company and 5 mm NMR sample tubes were used. Chemical shifts are given in parts per million (ppm) relative to the central line of the solvent proton resonance of known shifts relative to tetramethylsilane (TMS). The Infrared spectra were all recorded using nujol mulls between 400 and 4000 cm^{-1} on a Perkin-Elmer180 FT-IR spectrophotometer. The description of the relative intensities of the bands are given using the following abbreviations: w = weak, vw = very weak, s = strong and vs = very strong. The shapes of the bands are distinguished as sh = sharp, shld = shouldered and br = broad. The elemental analysis were carried out in the microanalytical unit of the University of Cape Town, South Africa.

6.2. Materials.

Benzoyl chloride was purchased from SaArchem, *p*-chlorobenzoyl chloride, *m*-methylbenzoyl chloride, *m*-methoxybenzoyl chloride, potassium perrhenate and chlorotrimethylsilane were all purchased from Aldrich Chemical Company and tetrabutylammonium chloride was purchased from Fluka. Diethylamine was distilled from 3 Å molecular sieves prior to use and all other chemicals were of commercial grade and were used as supplied. Acetone and methanol were purified and dried by standard procedures described by Perrin and Armarego.[1] Thus, acetone was distilled under N_2 from 3 Å molecular sieves, methanol was distilled under N_2 from magnesium methoxide, generated *in situ* by reacting methanol with magnesium turnings in the presence of iodine, 95%

absolute ethanol was distilled under N_2 from calcium hydride and hexane was distilled under N_2 over sodium. All other solvents were used without further purification or drying.

6.3. Preparative procedures.

6.3.1. Ligand synthesis.

Synthesis of N,N-diethyl-N'-benzoylthiourea : (LH).

KSCN (1.23 g, 12.7 mmol) was dissolved in acetone (50 ml) and to this solution was added, dropwise, a solution of benzoyl chloride (1.79 g, 12.7 mmol) in acetone (5 ml) whereupon a white precipitate of KCl separated out from the solution. This reaction mixture was refluxed for 1 h under nitrogen and then cooled to room temperature. A solution of *N,N*-diethylamine (0.93 g, 12.7 mmol) in acetone (5 ml) was added dropwise and the reaction mixture was refluxed under nitrogen for 30 min. and then poured into ice-water from which the product precipitated out. The precipitate was collected by filtration and recrystallized from ethanol to yield *N,N*-diethyl-*N'*-benzoylthiourea as white crystals.

Yield 76%, R_f 0.77, mp (ethanol) 95°C, IR (nujol mull): cm^{-1} 405.4 (vw), 444.6 (vw), 472.6 (w), 535.6 (vw), 616.4 (w), 649.9 (vs, sh), 666.9 (vw), 692.9 (vw), 714.9 (vs, sh), 797.1 (s, sh), 862.8 (vs, sh), 925.3 (s, sh), 974.4 (vw), 1001.9 (vw)1025.1 (w), 1064.1 (vs, shld), 1099.5 (vw), 1133.2 (vs, sh), 1173.3 (s, sh),1227.9 (vs, sh), 1284.0 (vs, shld), 1417.7 (s, sh), 1531.2 (vs, sh), 1578.0 (vw), 1596.9 (vw), *v*(C=O)1681.8 (vs, sh), *v*(N-H) 3205.7 (s, br). *Anal.* Found. C, 60.98, H, 6.91, N, 11.58, S, 13.64. *Calc.* for $C_{12}H_{16}N_2OS$: C, 60.98, H, 6.82, N, 11.86, S, 13.57.

Synthesis of N,N-diethyl-N'-(p-methylbenzoyl)thiourea: (LCH_3).

The same procedure as described above was followed except that *p*-methylbenzoyl chloride was used instead of benzoyl chloride.

Yield 81%, R_f 0.88, mp (ethanol) 94-95 °C, IR (nujol mull): cm^{-1} 409.5 (vw), 429.2 (w), 480.1 (vw), 504.7 (vw), 568.1 (vs), 700.4 (s, sh), 736.5 (vs), 790.0 (w), 838.3 (s, shld), 876.7 (s, sh), 918.9 (s, sh), 1076.6 (s, shld), 1096.2 (w), 1122.7 (w), 1139.7 (w), 1168.2 (vw), 1230.2 (vs, shld), 1276.5 (s, sh), 1524.0 (vs, shld), 1572.9 (s, sh), 1609.7 (s, sh), *v*(C=O) 1639.1 (vs, sh), *v*(N-H) 3292.9 (s, br). *Anal.* Found. C, 62.64, H, 7.50, N, 11.33, S, 12.21. *Calc.* for $C_{13}H_{18}N_2OS$: C, 62.36, H, 7.25, N, 11.19, S, 12.81.

Synthesis of N,N-diethyl-N'-(m-chlorobenzoyl)thiourea: (LCl).

The same procedure as described above was followed except that *m*-chlorobenzoyl chloride was used instead of benzoyl chloride.

Yield 65%, R_f 0.77, mp (ethanol) 94-96°C, IR (nujol mull): cm^{-1} 428.2 (vw), 490.0 (w), 547.0 (vw), 611.7 (w, sh), 650.0 (s, sh), 665.5 (s, sh), 686.5 (s, shld), 732.7 (vs, sh), 769.4 (s, sh), 809.6 (s, sh), 865.5 (vs, sh), 881.7 (s, sh), 931.8 (vw), 952.0 (vw), 1020.9 (w), 1061.4 (w), 1084.5 (vw), 1121.0 (vs, shld), 1172.4 (vw), 1224.5 (vs, sh), 1283.9 (s, sh), 1310.3 (w), 1348.4 (vw), 1531.7 (vs, sh), 1568.3 (vw), 1594.2 (vw), *v*(C=O) 1697.5 (vs, sh), *v*(N-H) 3153.5 (s, br). *Anal.* Found. C, 53.22, H, 5.65, N, 9.57, 11.04. *Calc.* for $C_{12}ClH_{14}N_2OS$: C, 53.22, H, 5.58, N,10.35, S, 11.82.

Synthesis of N,N-diethyl-N'-(m-methoxybenzoyl)thiourea: ($LOCH_3$).

The same procedure as described above was followed except that *m*-methoxybenzoyl chloride was used instead of benzoyl chloride.

Yield 51%, R_f 0.73, mp (ethanol) 90-91°C , IR (nujol mull): cm^{-1} 419.0 (s, sh), 491.4 (s, sh), 540.9 (w), 575.2 (w), 609.5 (w), 672.3 (vs, shld), 742.8 (vs, sh), 796.1 (s, sh), 819.0 (s, sh), 853.8 (vs, sh), 895.2 (vw), 942.8 (vw), 994.2 (vw), 1043.8 (w), 1062.8 (vw), 1116.1 (s, sh), 1184.7 (vw), 1215.2 (vs, shld), 1276.1 (s, sh), 1325.7 (vw), 1489.5 (vw), 1527.6 (vs, sh), 1596.1 (vs, sh), *v*(C=O) 1691.4 (vs, sh), *v*(N-H) 3183.2 (s, br). *Anal.* Found C, 59.33, H, 7.25, N, 9.80, S, 11.70.

Calc. for $C_{13}H_{16}N_2O_2S$: C, 58.62, H, 6.81, N, 10.52, S, 12.06.

6.3.2. Preparation of metal complexes.

6.3.2.1. Metal precursors.

Preparation of trichloroxobis(triphenylphosphine)rhenium(V): $ReOCl_3(PPh_3)_2$.[2]

$KReO_4$ (0.9 g, 2.0 mmol) was dissolved in 37% hydrochloric acid (7 ml). This solution was added to a suspension of triphenylphosphine (12 g, 48 mmol) in glacial acetic acid (250 ml) and stirred for 30 min. The resulting precipitate was filtered, washed sequentially with glacial acetic acid and ether and dried under vacuum to afford $ReOCl_3(PPh_3)_2$ as a yellowish-green coloured precipitate.

Yield 98%, mp (ether) 188-190°C, IR (nujol mull) :cm^{-1} 454.7 (w), 506.2 (s, shld), 522.8 (s, sh), 693.6 (vs, db), 748.0 (vs, sh), 847.8 (vw), ν(Re=O) 969.1 (s, sh), 998.6 (w), 1029.5 (vw), 1092.8 (s, sh), 1160.6 (vw) 1191.7 (m, br), 1377.2 (s, sh), 1434.8 (s, sh), 1482.2 (w) and 1714.7 (w).

Preparation of dioxotetrapyridinerhenium(V)chloride: $[ReO_2(py)_4]Cl$.[3]

$ReOCl_3(PPh_3)_2$ (1.0 g, 1.2 mmol) was dissolved in acetone/water (9:1, v/v) (10 ml) and to this solution was added dropwise a solution of pyridine (4.9 g, 62 mol) in acetone/water (5 ml). The mixture was refluxed for 2 h whereupon the volume was reduced by rotary evaporation to 10 ml and allowed to cool. The precipitate was washed with toluene (2 x 5ml) and diethyl ether (2 x 5 ml) and dried under vacuum overnight to yield $[ReO_2(py)_4]Cl$ as orange coloured crystals.

Yield 92%, mp (ethanol/ diethyl ether)188-191°C, IR (nujol mull) : cm^{-1} 3382(s, sh), 3063(m, sh), 1604(m, br), 1477(s, sh), 1345(m, br), 1209(m, sh), 1150(w, br), 1068(m, br), ν(Re=O) 821(s, sh), 1778(s), 704(s, sh) and 468(m, br).

Preparation of tetrabutylammonium tetraoxorhenate(VII): [n-Bu_4N][ReO_4].[4]

$KReO_4$ (1.0 g, 3.7 mmol) was dissolved in dimineralized water (50 ml) in a 250 ml conical flask. The solution was stirred and heated to 60°C and then added to a warm solution (60°C) of tetrabutylammonium chloride (1.3 g, 4.6 mmol) in demineralized water (50 ml) in a 250 ml conical flask. The solution was left to stir for 30 min. at room temperature. The white solid which formed was collected by filtration using a No. 3 sintered-glass filter tube and washed sequentially with distilled water (4 x 20 ml) and diethyl ether (4 x 30 ml) and dried under vacuum for 5 h at 56°C to yield [*n*-Bu_4N][ReO_4].

Yield 67%, mp (water/diethyl ether) 238-240°C, IR (nujol mull): cm^{-1} 523.0 (vw), 737.3 (m, shld), 793.3 (vw), ν(Re=O) 905.8 (vs, br), 1012.3 (vw),1035.1 (w), 1069.9 (w), 1110.0 (vw), 129.3 (vw), 1164.6 (m, br), 1242.0 (vw), 1319.9 (vw), 1464.0 (vs, sh) and 1810.8 (vw).

Preparation of tetrabutylammonium tetrachlorooxorhenate(V): [n-Bu_4N][$ReOCl_4$].[4]

A 100 ml two-necked round-bottomed flask, fitted with a nitrogen inlet and a tightly fitted septum was charged with a solution of [*n*-Bu_4N][ReO_4] (0.83 g, 1.68 mmol) in dry distilled chloroform (6.00 ml). The solution was stirred and cooled in an ice bath and trimethylchlorosilane (4.9 ml, 39 mmol) was added slowly using a pre-dried constant pressure funnel over a period of 5 min. to give a dark brown coloured solid. Dry degassed methanol (1.6 ml, 39 mmol) was added and the solution was stirred in the ice bath for 3 h. The volume of the solution was then reduced to 2 ml by rotary evaporation. Dry absolute ethanol (10 ml) mixed with trimethylchlorosilane was added to the round-bottomed flask and the solution shaken vigorously for 1 min. The solution was stirred at room temperature for 1 h and the volume was reduced to 10 ml by rotary evaporation, after which the concentrated solution was placed in a deep freezer for 15 h. The product was collected as yellow-green coloured crystals under nitrogen, washed with ice-cold dry deoxygenated hexane (4 x 30 ml) and dried under vacuum for 5 h at 56 °C.

Yield 72 %, mp (hexane) 118-121 °C, IR (nujol mul): cm^{-1} 532.7 (w), 735.5 (vs,sh), 800.0 (w),

880.8 (vs, sh), 924.9 (m, sh), 1002.4 (vs, sh), ν(Re=O) 1030.2 (vs, sh), 1066.6 (vw), 1085.7 (vw), 1104.7 (vw) 1168.2 (s, sh), 1238.0 (m).

6.3.2.2. Metal complexes of acylthiourea ligands.

Preparation of $[ReO(L)_2(OMe)]$ from $[ReOCl_3(PPh_3)_2]$.

A solution of trichloroxobis(triphenylphosphine)rhenium(V) (83 mg, 0.10 mmol) in methanol (6 ml) was added, dropwise, to a solution of *N,N*-diethyl-*N'*-benzoylthiourea (50 mg, 0.20 mmol) in methanol (5 ml). To this mixture was added, dropwise, a 1 M solution of sodium acetate (0.2 ml, 0.2 mmol). This mixture was then heated to reflux for 30 min. during which time the mixture turned dark brown.. TLC showed the presence of four compounds which were separated by flash chromatography (hexane/dichloromethane, (1:9, v/v)) to afford a colourless fraction, a pink coloured fraction, a brown fraction and a bright-green coloured fraction. The collected fractions were concentrated to dryness by rotary evaporation and characterized by ^{1}H NMR and IR spectroscopy. The brown coloured fraction proved to be $[ReO(L)_2(OMe)]$, the colourless fraction proved to be the unreacted ligand and the other two components were present in very small amounts hence could not be fully characterized. The brown coloured fraction was further recrystallized by dissolving it in chloroform followed by a small addition of methanol to afford the pure $[ReO(L)_2(OMe)]$ as purple coloured crystals.

Yield 11%, mp (chloroform/methanol)167-171°C, IR(nujol mull): cm^{-1} 420.0 (w), 468.5 (vw), 496.0 (m), 581.0 (vw), 544.7 (vw), 670.4 (m), 712.3 (s, sh), 773.3 (vw), 800.0 (vw), 819.0 (w), 887.6 (m), ν(Re=O) 941.1 (s, sh), 1003.6 (vw), 1024.7 (vw), 1092.3 (vs), 1135.2 (m), 1169.5 (s, sh), 1200.0 (m,sh), 1245.9 (m, sh), 1303.9 (w, shld), 1347.5 (s, shld), 1348.5 (s, sh) and 1496.7 (s, br).

Preparation of [ReO(L)$_2$(OMe)] from [ReO$_2$(py)$_4$]Cl in the presence of sodium acetate.

N,N-diethyl-*N'*-benzoylthiourea (61.1 mg, 0.33 mmol) was dissolved in methanol (6 ml) at room temperature and to this was added, dropwise, a 1 M solution of sodium acetate in methanol (0.13 ml, 0.33 mmol) while stirring. A solution of dioxotetrapyridinerhenium(V)chloride (100 mg, 0.165 mmol) in methanol (6 ml) was added slowly to the mixture and the mixture was refluxed for 30 min. during which time the reaction mixture became purple in colour. The product separated out from solution as small purple coloured crystals. The crystalline product was collected by filtration and recrystallized by dissolving it in chloroform followed by a small addition of methanol to give the pure product as purple coloured crystals.

Yield 62%, mp (chloroform/methanol) 166-168°C, IR(nujol mull):cm^{-1} 419.0 (w), 468.5 (vw), 495.2 (m), 518.0 (vw), 544.7 (vw), 670.4 (m), 712.3 (s, sh), 773.3 (vw), 800.0 (vw), 819.0 (w), 887.6 (m,sh), *ν*(Re=O) 940.9 (s, sh), 1001.9 (vw), 1024.7 (vw), 1093.3 (vs, br), 1135.2 (m), 1169.5 (s, sh), 1200.0 (m), 1245.7 (m), 1302.8 (w), 1348.5 (s, shld), 1348.5 (s, sh) and 1497.1 (s, br). *Anal.* Found: C, 42.63; H, 4.65; N, 7.97; S, 9.11. *Calc.* for $ReC_{25}H_{33}N_4O_4S_2$: C, 42.65; H, 4.72; N, 7.76; S, 9.11.

Preparation of [ReO(L)$_2$(OMe)] from [ReO$_2$(py)$_4$]Cl in the presence of triethylamine.

N,N-diethyl-*N'*-benzoylthiourea (61.1 mg, 0.33 mmol) was dissolved in methanol (6 ml) at room temperature and to this was added, dropwise, triethylamine (33.0 mg, 0.33 mmol) while stirring. A solution of dioxotetrapyridinerhenium(V)chloride (100 mg, 0.165 mmol) in methanol (6 ml) was added slowly to the mixture and the mixture was refluxed for 30 min. during which time the reaction mixture became purple in colour. At the end of the reaction the mixture was concentrated by rotary evaporation to a volume of 5 ml and left to cool to room temperature. The product separated out from solution as small purple coloured crystals. The crystalline product was collected by filtration and recrystallized by dissolving it in chloroform followed by a small addition of methanol to give the pure product as purple coloured crystals.

Yield 61%, mp (chloroform/methanol) 167-170°C, IR(nujol mull):cm^{-1} 420.2.0 (w), 468.5 (vw), 495.2 (m), 517.8 (vw), 545.5 (vw), 670.4 (m), 712.3 (s, sh), 773.3 (vw), 800.0 (vw), 819.0 (w), 887.6 (m,sh), ν(Re=O) 941.1 (s, sh), 1002.1 (vw), 1025.4 (vw), 1093.3 (vs, br), 1135.2 (m), 1169.5 (s, sh), 1200.0 (m), 1245.6 (m), 1302.6 (w), 1348.5 (s, shld), 1348.5 (s, sh) and 1497.1 (s, br)

Preparation of $[ReO(L)_2(OMe)]$ from $[n\text{-}Bu_4N][ReOCl_4]$ at room temperature in the presence of sodium acetate and under atmospheric conditions.

N,N-diethyl-*N'*-benzoylthiourea (40 mg, 0.17 mmol) was dissolved in methanol (5 ml) and to this solution was added, dropwise, a 1M solution of sodium acetate in methanol (0.17 ml, 0.17 mmol). A solution of tetrabutylammoniumtetrachlorooxorhenate(V) (50.0 mg, 0.085 mmol) in methanol (6 ml) was added dropwise and the colour of the reaction mixture changed from bright green to purple and then to brown-green. The reaction mixture was stirred for 30 min. and during this period a maroon-brown coloured crystalline product started forming. The crystalline product was collected by filtration and recrystallized by dissolving it in chloroform followed by a small addition of methanol to yield the pure product as brown-purple coloured crystals.

Yield 51%, mp (chloroform/methanol) 165-168°C, IR(nujol mull): cm^{-1} 419.5 (w), 469.2 (vw), 496.2 (m, sh), 518.0 (vw), 544.7 (vw), 670.4 (m), 712.3 (s, sh), 773.3 (vw), 800.0 (vw), 819.0 (w), 887.9 (m), ν(Re=O) 940.5 (s, sh), 1002.1 (vw), 1024.7 (vw), 1093.3 (vs, br), 1134.2 (m), 1169.5 (s, sh), 1200.0 (m), 1245.7 (m), 1301.9 (w, shld), 1348.5 (s, shld), 1348.5 (s, sh) and 1498.1 (s, br).

Preparation of $[ReO(L)_2(OMe)]$ from $[n\text{-}Bu_4N][ReOCl_4]$ at room temperature in the presence of sodium acetate and under an inert atmosphere.

The same procedure as described above was followed except that the reaction was carried out under N_2 an dry solvents were used.

Yield 54%, mp (chloroform/methanol) 165 -168°C, IR(nujol mull): cm^{-1} 418.9 (w), 469.5 (vw),

495.7 (m, sh), 518.6 (vw), 544.9 (vw), 670.4 (m), 712.3 (s, sh), 773.3 (vw), 800.0 (vw), 819.0 (w), 887.9 (m), ν(Re=O) 940.4 (s, sh), 1003.1 (vw), 1024.7 (vw), 1093.3 (vs, br), 1134.2 (m), 1169.1 (s, sh), 1201.0 (m), 1245.7 (m), 1301.9 (w, shld), 1348.5 (s, shld), 1348.5 (s, sh) and 1499.9 (s, br).

Preparation of [ReO(L)$_2$Cl] from [n-Bu$_4$N][ReOCl$_4$] at room temperature under N$_2$ in the absence of a base.[4]

N,N-diethyl-*N'*-benzoylthiourea (40.0 mg, 0.17 mmol) was dissolved in dry degassed methanol (5ml) and to this solution was added dropwise a solution of tetrabutylammonium tetrachlorooxorhenate(V) (50 mg, 0.085 mmol) in dry degassed methanol (6 ml). The resulting blue green mixture was stirred at room temperature under N_2 for 2 h during which time a blue-green coloured solid material was formed. The solid material was collected by filtration, washed with methanol and diethyl ether and dried under vacuum.

Yield 60%, mp (methanol/diethyl ether) 169-170 °C, IR(nujol mull) cm^{-1}: 510.3 (w), 548.4 (vw), 569.5 (vw), 671.1 (s, sh), 702.9 (vs, sh), 717.7 (vs, sh), 796.0 (w), 827.7 (s, sh), 891.2 (w), ν(Re=O) 973.7 (vs, shld), 1003.4 (vw), 1024.5 (vw), 1069.0 (w), 1083.8 (w), 1096.5 (w), 1136.7 (s, sh), 1168.5 (s, sh), 1200.2 (s, sh), 1242.5 (s, sh), 1303.9 (vw), 1365.3 (vs, shld), 1458.4 (vs, sh), 1492.3 (vs, sh), 1534.6 (vs, sh), 1583.3 (w), 1596.0 (vw), 2671.7 (vw), 2717.5 (vw). *Anal.* Found: C, 40.82, H, 4.53, N, 8.01, S, 9.23. *Calc.* for $C_{24}H_{30}N_4O_3ClS_2Re$: C, 40.74, H, 4.32, N, 7.91, S, 9.12.

Preparation of [ReO(LNO$_2$)$_2$(OMe)] from [ReO$_2$(py)$_4$]Cl.

N,N-diethyl-*N'*-(*m*-nitrobenzoyl)thiourea (89 mg, 0.33 mmol) was dissolved in methanol (6 ml) at room temperature and to this was added, dropwise, a 1 M solution of sodium acetate in methanol (0.5 ml, 0.5 mmol). A solution of dioxotetrapyridinerhenium(V)chloride (100 mg, 0.165 mmol) in methanol (6 ml) was added slowly to the mixture, which was then refluxed for 30 min. The reaction mixture became brown in colour and small brown coloured crystals started to form.

At the end of the reaction the mixture was concentrated by rotary evaporation to a volume of 5 ml and left to cool for 5 h during which time more of the product separated out from the reaction mixture as brown coloured crystals. The crystals were collected by filtration and recrystallized by dissolving them in chloroform followed by a small addition of methanol and the pure product was collected by filtration as maroon-brown coloured crystals.

Yield 72%, mp (methanol/chloroform) 170-172°C, IR(nujol mull): cm^{-1} 419.0 (w), 468.5 (vw), 495.2 (m), 518.0 (vw), 544.7 (vw), 670.4 (m, 712.3 (s, sh), 773.3 (vw), 800.0 (vw), 819.0 (w), 887.6 (m), *v*(Re=O) 940.9 (s, sh), 1001.9 (vw), 1024.7 (vw), 1093.3 (vs), 1135.2 (m, sh), 1169.5 (s, sh), 1200.0 (m), 1245.7 (m), 1302.8 (w), 1348.5 (s, shld), 1348.5 (s, sh) and 1497.1 (s, br). *Anal.* Found: C, 38.02; H, 3.91; N, 10.63; S, 8.28. *Calc.* for $ReC_{25}H_{31}N_6O_8S_2$: C, 37.82; H, 3.93; N, 10.59; S, 8.08.

Preparation of [ReO(LCH$_3$)$_2$(OMe)] from [ReO$_2$(py)$_4$]Cl.

N,N-diethyl-*N'*-(*p*-methylbenzoyl)thiourea (74.0 mg, 0.33 mmol) was dissolved in methanol (6 ml) at room temperature and to this was added, dropwise, a 1 M solution of sodium acetate in methanol (0.5 ml, 0.5 mmol). A solution of dioxotetrapyridinerhenium(V)chloride (100 mg, 0.165 mmol) in methanol (6 ml) was added slowly to the mixture and the mixture was refluxed for 30 min. during which time the mixture became deep red in colour. At the end of the reaction the mixture was concentrated by rotary evaporation to a volume of 5 ml and left to cool to room temperature. The product separated out from solution as deep red small crystals. The crystalline product was collected by filtration and recrystallized by dissolving them in chloroform followed by a small addition of methanol to give the pure product as deep red crystals.

Yield 60%, mp 157-159°C, IR (nujol mull): cm^{-1} 420.2 (w, br), 500.6 (m, br, shld), 638.7 (vw, sh), 657.8 (vw, sh), 694.1 (w, sh), 751.6 (s, sh), 787.9 (m, sh), 840.9 (m, shld), 890.7 (m, sh), *v*(Re=O) 946.2 (vs, sh), 1002.5 (vw, sh), 1089.5 (m, shld), 1113.5 (s, sh), 1137.5 (m, sh), 1174.7 (s, sh), 1206.1 (m, sh), 1251.2 (s, sh), 1353.9 (s, sh), 1376.9 (w, sh), 1423.1 (vs, br), 1505.6 (vs, shld), 1579.2 (m, sh), 1608.9 (m, sh) and 2806.9 (m, shld). *Anal.* Found. C, 47.02, H, 4.98, N,

8.15, S, 9.33. *Calc.* for $C_{27}H_{41}N_4O_4S_2Re$: C, 44.14, H, 5.14, N, 7.71, S, 8.76.

Preparation of $[ReO(L)_2(OEt)]$ from $[ReO_2(py)_4]Cl$ in ethanol.

N,N-diethyl-*N'*-benzoylthiourea (61.1 mg, 0.33 mmol) was dissolved in ethanol (6 ml) at room temperature and 1 M sodium acetate (0.50 ml, 0.50 mmol) was added to the stirred solution. A solution of dioxotetrapyridinerhenium(V)chloride (100 mg, 0.165 mmol) in ethanol (6 ml) was added, dropwise, to the reaction mixture. The reaction was refluxed for 30 min during which time the colour of the solution turned maroon and maroon coloured crystals separated out from the solution. The crystalline product was collected by filtration and recrystallized by from chloroform/ethanol to give the product as maroon coloured crystals. Suitable crystals for crystallography were grown by dissolving the crystals in chloroform followed by a slow addition of ethanol to form a double layer of solvents.

Yield 63%, mp(ethanol/chloroform) 176-178 °C, IR (nujol) : cm^{-1} 470.0 (vw), 514.1 (vw), 550.0 (vw), 583.8 (s, sh), 671.1 (w), 687.9 (vw), 716.0 (vs, sh), 771.3 (vw), 803.0 (vw), 816.9 (w), 887.7 (s, sh), 912.4 (s, sh), 947.6 (vs, sh), 972.9 (vw), 1000.1 (vw), 1026.2 (vw), 1068.3 (s, sh), 1085.7 (w), 1105.6 (vw), 1135.6 (w), 1170.4 (w), 1202.8 (w), 1246.9 (w), 1299.9 (vw), 1352.1 (s, sh), 1376.8 (vs, sh), 1425.3 (vs, sh), 1497.8 (vs, sh), 1585.6 (s, sh), 2725.2 (vw). *Anal.* Found. C, 41.41; H,4.60, N, 8.32; S, 7.32. *Calc.* for $C_{26}H_{35}N_4O_4S_2Re$: C,43.50, H, 4.94, N, 8.93 S, 7.810.

Preparation of $[(L)_2ORe\text{-}O\text{-}ReO(L)_2]$ from $[ReO_2(py)_4]Cl$ in acetonitrile.

N,N-diethyl-*N'*-benzoylthiourea (61.1 mg, 0.33 mmol) was dissolved in acetonitrile (6 ml) at room temperature and to this was added, dropwise, a 1 M solution of sodium acetate in acetonitrile (0.5 ml, 0.50 mmol). A solution of dioxotetrapyrinerhenium(V)chloride (100 mg, 0.165 mmol) in acetonitrile (6 ml) was added dropwise to the reaction mixture. The reaction mixture was refluxed for 28 min. during which time the colour of the solution changed from orange to brown then to green. After refluxing for further 7 min, the mixture was concentrated by rotary evaporation to

a volume of 5 ml and left in a fridge for 24 h. during which time the product separated out from the solution as green coloured crystals. The crystalline product was collected by filtration and recrystallized from chloroform/acetonitrile to give $[(L)_2ORe\text{-}O\text{-}ReO(L)_2]$ as green coloured fine crystals.

Yield 32%, mp(chloroform/acetonitrile) 202 - 204 °C, IR (nujol mull): cm^{-1} 426.7 (w), 543.6 (w), 657.2 (vs), 724.2 (vs, sh), 775.2 (vw), 798.6 (vw), 819.8 (w), ν(Re=O) 890.0 (s, sh), 944.2 (vw), 998.3 (vw), 1023.8 (vw)1136.5 (s, sh), 1168.3 (w), 1247.0 (s, sh), 1376.6 (vs, sh 1519.0 (vs, sh), 1584.8 (vs, sh), 2664.1 (vw), 2717.5 (vw). *Anal*: Found: C, 42.22, H, 4.19, N, 7.31, S, 8.93. *Calc.* for $C_{48}H_{60}N_8O_7S_4Re_2$: C, 42.31, H, 4.43, N, 8.24 S, 9.40.

Preparation of $[(L)_2ORe\text{-}O\text{-}ReO(L)_2]$ from the recrystallization of $[ReO(L)_2(OMe)]$ from acetone.

$[ReO(L)_2(OMe)]$ (100 mg, 0.14 mmol) was dissolved in a minimum amount of boiling acetone to give a maroon coloured solution. The colour of the solution changed to green upon cooling to room temperature. The product started to separate out as green coloured crystals and the solution was placed in a deep freezer for 24 h during which time more of the product separated out. The crystalline product was collected by filtration, washed with ice-cold acetone and dried under vacuum for 24 h. Suitable crystals for crystallography were grown by dissolving the green coloured crystals in chloroform followed by the slow addition of acetone.

Yield 53%, mp(chloroform/acetone) 203 °C, IR (nujol mull): cm^{-1} 427.2 (w, sh), 451.2 (vw), 547.1 (w), 657.1 (vs, sh), 698.8-710.0 (vs, shld), 776.2 (vw), 799.5 (vw), 820.1 (w), 850.2 (vw, sh), 891.5 (s, sh), 935.4 (vw), 953.4 (vw), 999.9 (w), 1025.7 (vw) 1076.4 (s, shld), 1135.8 (s, sh), 1168.5 (s, sh), 1168.5 (s, sh), 1247.9 (s, sh), 1299.5 (vw), 1352.4 (w), 1415.0 (vw), 1493.8 (w), 1518.8 (vw), 1585.8 (vs, sh). *Anal.* Found. C, 42.90, H, 4.46, N, 8.34, S, 9.57. *Calc.* for $C_{48}H_{60}N_8O_5S_4Re_2$: C, 43.00, H, 4.43, N, 8.24, S, 9.40.

Preparation of $[(L)_2ORe\text{-}O\text{-}ReO(L)_2]$ from the recrystallization of $[ReO(L)_2(OMe)]$ from ethylacetate.

The same procedure as described above was followed except that ethylacetate was used instead of acetone.

Yield 51%, mp (chloroform/ethylacetate) 203 °C, IR (nujol mull): cm^{-1} 426.9 (w, sh), 451.3 (vw), 547.1 (w), 657.1 (vs, sh), 698.8-710.0 (vs, shld), 776.2 (vw), 799.5 (vw), 820.1 (w), 850.2 (vw, sh), 891.5 (s, sh), 935.4 (vw), 953.4 (vw), 999.9 (w), 1025.7 (vw) 1076.4 (s, shld), 1135.8 (s, sh), 1168.5 (s, sh), 1168.5 (s, sh), 1247.9 (s, sh), 1299.5 (vw), 1352.4 (w), 1415.0 (vw), 1493.8 (w), 1518.8 (vw), 1585.8 (vs, sh). *Anal.* Found. C, 43.60, H, 4.87, N, 8.11, S, 9.52. *Calc.* for $C_{48}H_{60}N_8O_5S_4Re_2$: C, 42.31, H, 4.43, N, 8.24 S, 9.40.

Preparation of $[ReO(L)_2(OiPr)]$ from $[ReO_2(py)_4]Cl$ in iso-propanol.

N,N-diethyl-*N'*-benzoylthiourea (61.1 mg, 0.33 mmol) was dissolved in *iso*-propanol (6 ml) at room temperature and to this was added, dropwise, a 1 M solution of sodium acetate in *iso*-propanol (0.5 ml, 0.5 mmol). A solution of dioxotetrapyridinerhenium(V)chloride (100 mg, 0.165 mol) in *iso*-propanol (6 ml) was added slowly to the mixture. The reaction mixture was refluxed for 30 min. during which time the colour of the solution changed from orange to brick-red. At the end of the reaction, the solution was concentrated by rotary evaporation to a volume of 5 ml and left to cool to room temperature whereupon brown crystals started to separate out from the solution. The crystalline product was collected by filtration and recrystallized from chloroform/*iso*-propanol to give the pure product as brick-red coloured crystals.

Yield 43%, mp (chloroform/*iso*-propanol)194-195 °C, IR (nujol mull): cm^{-1} 415.7 (w), 434.6 (vw), 466.2 (w), 497.7 (vw), 532.4 (vw, shld), 589.2 (s, sh), 661.8 (w), 715.5 (vs, sh), 797.5 (w), 819.6 (w), 844.9 (w), 882.7 (w), 930.1 ν(Re=O), 999.5 (s, sh), 1075.3 (s, sh),1204.7 (s, sh), 318.3 (vw),1507.6 (vs, sh), 1586.5 (s, sh), 2666.9 (vw), 2717.7 (vw). *Anal.* Found. C, 44.00, H, 5.01, N, 7.63, S, 8.63. *Calc.* for $C_{27}H_{37}N_4O_3S_2$: C, 44.30, H, 5.10, N, 7.66, S, 8.76.

Preparation of [ReO(LCl)(OMe)] from $[ReO_2(py)_4]Cl$.

N,N-diethyl-*N'*-(*m*-chlorobenzoyl)thiourea (121 mg, 0.33 mmol) was dissolved in methanol (10 ml) at room temperature and to this was added, dropwise, a 1 M solution of sodium acetate in methanol (0.50 ml, 0.50 mmol). A solution of dioxotetrapyridinerhenium(V)chloride (0.10 mg, 0.165 mmol) in methanol (6 ml) was added slowly to the mixture. The mixture was refluxed for 30 min. and during this period the colour of the solution turned deep red. At the end of the reaction the volume of the mixture was reduced to about 5ml by rotary evaporation and the solution was placed in a deep freezer overnight. The resultant precipitate was collected by filtration, recrystallized from chloroform/methanol and dried under vacuum to yield the pure product as brown coloured fine crystals.

Yield 59%, mp (methanol) 92-96°C, IR (nujol mull) cm^{-1}: 480.0 (vs, sh), 506.0 (s, sh), 560.0 (s, sh), 655.2 (vs, sh), 647.2 (s, sh), 727.6 (vs, db), 754.2 (vs, sh), 771.1 (s, sh), 803.8 (s, sh), 830.4 (w), 899.0 (s, sh), ν(R=O) 944.7 (vs, sh), 998.0 (m), 1093.3 (s, shld), 1139.0 (w), 1158.0 (vw), 1200.0 (s, sh), 1245.7 (m) 1264, 7 (w) 1348.5-1523.8 (vs, shld) and 1577.1 (w). *Anal.* Found: C, 38.89, H, 3.94, N, 6.25, S, 8.08, *Calc.* for $ReC_{27}ClH_{35}N_4O_6S_2$: C, 38.85, H, 4.04, N, 7.25, S, 8.29.

Preparation of $[ReO(LOCH_3)_2(OMe)]$ from $[ReO_2(py)_4]Cl$.

The same procedure as above was followed except that *N,N*-diethyl-*N'*-(*m*-methoxybenzoyl)thiourea was used instead of *N,N*-diethyl-*N'*-(*m*-chlorobenzoyl)thiourea. The product was recrystallized from chloroform/methanol and dried under vacuum to yield the pure product as maroon coloured fine crystals.

Yield 73%, mp (chloroform/methanol) 122-125°C, IR (nujol mull): cm^{-1}) 419.0 (w), 499.0 (m), 662.8 (m), 750.4 (vs, sh), 792.3 (s, sh), 853.3 (w), 906.6 (vw), ν(Re=O) 937.1 (vs, sh), 998.0 (vw) 1040.0 (s, sh), 1089.5 (vs, shld), 1131.4 (vw), 1154.2 (vw) 1173.3 (vw), 1196.1 (w), 1230.4 (m, sh) 1257.1 (s, sh) 1283.8 (m), 1310.4 (vw) 1352.3 (s, sh)1375.2 (w), 1413.3 (vs, shld) 1455.2

(vs, shld) 1497.1 (vs, sh) and 1600.0 (vw, shld). *Anal.* Found: C, 42.58, H, 5.02, N, 6.55, S, 8.37, *Calc.* for $ReC_{27}H_{37}N_4O_6S_2$: C, 42.44, H, 4.88, N, 7.33, 8.39.

Preparation of [ReO(morph-L)$_2$(OMe)] from [ReO$_2$(py)$_4$]Cl.

The same procedure as above was followed except that *N*-morpholino-*N'*-benzoylthiourea was used instead of *N,N*-diethyl-*N'*-(*m*-chlorobenzoyl)thiourea. The product was recrystallized from chloroform/methanol and dried under vacuum to yield the pure product as grey-green coloured fine crystals.

Yield 52%, mp (chloroform/methanol) 180-182°C, IR(nujol mull): cm^{-1} 605.7 (w), 651.4 (vw), 678.0 (w) 712.3 (vs, shld), 803.8 (vw, db), 849. 5 (vw), 895.2 (s, sh), *v*(Re=O) 937.1 (vs, sh), 998.0 (vw), 1024.7 (vs, sh), 1059.0 (w), 1108.5 (vs, db), 1165.7 (m), 1203.8 (s, sh), 1222.8 (s, sh), 1260.9 (s, sh), 1299.0 (br), 1344.7 (s, sh) 1375.2 (vs, sh) 1417.1 (vs, shld),1508.5 (vs, shld) and 1584.7 (w). *Anal.* Found: C, 38.33, H, 3.62, N, 6.38, S, 8.92. *Calc.* for $ReC_{25}H_{33}N_4O_6S_2$: C, 40.80, H, 3.99, N,7.60, S, 8.76.

Preparation of [ReO (morph-LCH$_3$)$_2$)(OMe)] from [ReO$_2$(py)$_4$]Cl.

The same procedure as above was followed except that *N*-morpholino-*N'*-(*m*-methylbenzoyl)thiourea was used instead of *N,N*-diethyl-*N'*-(*m*-chlorobenzoyl)thiourea. The product was recrystallized from chloroform/methanol and dried under vacuum to yield the pure product as dark brown coloured fine crystals.

Yield 70%, mp(chloroform/methanol) 168-171°C, IR (nujol mull): cm^{-1}) 499.0 (s, sh), 540.9 (vw), 605.7 (w), 647.6 (vw), 678.0 (vw), 712.3 (vs, shld), 761.9 (vw), 803.8 (w), 845.7 (vw, br), 895.2 (s, sh), *v*(Re=O) 937.1 (vs, shld), 998.0 (vw), 1024.7 (vs, sh), 1059.0 (w), 1108.5(s, sh), 1165.7 (w, shld), 1203.8 (s, sh), 1222.8 (s, sh), 1257.1 (s, sh), 1299.0 (w), 1348.5 (s, sh), 1375.2 (vs, sh) and 1584.7 (w,). *Anal.* Found: C, 42.09, H, 4.37, N, 6.41, S, 8.22. *Calc.* for $ReC_{27}H_{37}N_4O_6S_2$: C, 42.44, H, 4.88, N, 7.33, S, 8.39.

Preparation of [ReO(morph-LOCH$_3$)$_2$(OMe)] from [ReO$_2$(py)$_4$]Cl.

The same procedure as above was followed except that *N*-morpholino-*N'*-(*m*-methoxylbenzoyl)thiourea was used instead of *N,N*-diethyl-*N'*-(*m*-chlorobenzoyl)thiourea. The product was recrystallized from chloroform/methanol and dried under vacuum to yield the pure product as brown fine coloured crystals.

Yield 79%, mp(chloroform/methanol) 154-156°C, IR (nujol mull): cm^{-1}) 416.6 (w), 487.6 (s, sh), 525.7 (w), 609.5 (w), 647.6 (m) 670-680.4 (s, br), 720.0 (w), 746.6 (vs, sh), 784.7 (s, sh), 834.2 (m, sh), 872.3 (vs, sh), *ν*(Re=O) 940.9 (vs, sh), 1020.9 (vs, sh), 1059.0 (m), 1108.5 (vs, sh), 1234.2 (vs, shld), 1260.9 (vs, sh) 1280.0 (vw), 1299.0 (vw), 1318.0 (vw) 1348.5 (s, sh), 1379.0 (vs, sh) 1384.5-1472.8 (vs, br, shld), 1516.1 (vs, sh) and 1596.1 (m). *Anal.* Found: C, 40.90, H, 4.20, N, 6.94, S, 7.87, *Calc.* for $ReC_{27}H_{33}N_4O_8S_2$: C, 41.05, H, 4.21, N, 7.10, S, 8.12.

Preparation of [ReO(morph-LCl)$_2$(OMe)] from [ReO$_2$(py)$_4$]Cl.

The same procedure as above was followed except that *N*-morpholino-*N'*-(*m*-chlorobenzoyl)thiourea was used instead of *N,N*-diethyl-*N'*-(*m*-chlorobenzoyl)thiourea. The product was recrystallized from chloroform/methanol and dried under vacuum to yield the pure product as dark brown fine coloured crystals.

Yield 83%, mp(chloroform/methanol) 169-172°C, IR (nujol mull): cm^{-1} 419.0 (s, sh, shld), 441.9 (w, sh), 544.7 (s, sh), 605.7 (vs, sh), 647.6 (s, sh), 662.8 (s, sh), 685.7 (s, sh), 735.2 (vs, sh), 754.2 (vs, sh), 807.6 (s, shld), 860.9 (vs, sh), 899.0 (vs, sh), *ν*(Re=O) 933.3 (vs, sh), 1020.9 (vs, shld), 1062.8 (m), 1104.7 (vs, sh), 1180.9 (m, sh), 1213.3 (vs, shld), 1257.1 (vs, sh), 1344.7-1516.1 (vs, br, shld) and 1573.3 (w). *Anal.* Found: C, 37.71, H, 3.66, N, 6.87, S, 7.87. *Calc.* for $ReC_{25}ClH_{31}N_4O_6S_2$: C, 37.59, H, 3.41, 7.02, S, 8.03.

Preparation of [ReO(morph-LNO$_2$)$_2$(OMe)] from [ReO$_2$(py)$_4$]Cl.

The same procedure as above was followed except that *N*-morpholino-*N'*-(*m*-nitrobenzoyl)thiourea was used instead of *N,N*-diethyl-*N'*-(*m*-chlorobenzoyl)thiourea. The product was recrystallized from chloroform/methanol and dried under vacuum to yield the pure product as brown coloured fine crystals.

Yield 90%, mp (methanol) > 270°C, IR (nujol mull): cm^{-1} (s, sh), 537.1 (w), 601.9 (w), 651.4 (w), 681.9 (vw), 712.3 (vs, shld), 735.2 (s, sh), 769.5 (w), 807.6 (w), 822.8 (vw), 841.9 (w), 880.0 (vw), *ν*(Re=O) 938.1 (vs, sh), 1024.7 (vs, sh), 1072.4 (s, shld), 1108.5 (vs, sh), 1023.8 (m), 1226.6 (s, sh), 1257.1 (s, sh), 1299.0 (m, sh), 1240.9 (m, sh), 1375.2-1531.4 (vs, shld), 1580.9 (m, sh) and 1611.4 (w). *Anal.* Found. C, 36.31, H, 3.25, N, 9.46, S, 7.61. *Calc.* for $ReC_{25}H_{31}N_6O_{10}S_2$: C, 36.40, H, 3.80, N, 10.20, S, 7.82.

Preparation of [ReO(spiro-L)$_2$(OMe)] from [ReO$_2$(py)$_4$]Cl.

The same procedure as above was followed except that 8-(*N*-benzoylcarbamoyl)-1,4-dioxa-8-azaspiro[4.5]decane was used instead of *N,N*-diethyl-*N'*-(*m*-chlorobenzoyl)thiourea. The product was recrystallized from chloroform/methanol and dried under vacuum to yield the pure product as dark-brown coloured fine crystals.

Yield 61 %, mp(chloroform/methanol) 188-190°C, IR (nujol mull): cm^{-1} 475.7 (vw), 496.4 (w), 519.1 (vw), 591.2 (w), 660.9 (w), 700.1 (s, sh), 720.3 (vs, sh), 770.4 (vw), 797.5 (w), 884.6 (s, sh), 918.2 (s, sh), *ν*(Re=O) 945.5 (vs, sh), 1028.8 (s, shld), 1102.3 (vs, sh), 1145.5 (s, shld), 1212.5 (s, sh), 1238.0 (m, br), 1259.3 (w) 1275.9 (vw), 1333.3 (vw), 1358.3 (s, shld), 1504.8 (vs, shld) and 1585.1 (m, sh). *Anal.* Found, C, 42.61, H, 4.60, N, 6.34, S, 7.65. *Calc*, for $C_{32}H_{40}N_4O_{12}S_2$ Re, C , 42.69, H,4.42, N, 6.64, S, 7.60.

Preparation of [ReO(spiro-LNO$_2$)$_2$(OMe)] from [ReO$_2$(py)$_4$]Cl.

The same procedure as above was followed except that 8-(*N*-(m-nitrobenzoyl)carbamoyl)-1,4-dioxa-8-azaspiro[4.5]decane was used instead of *N,N*-diethyl-*N'*-(*m*-chlorobenzoyl)thiourea. The product was recrystallized from chloroform/methanol and dried under vacuum to yield the pure product as maroon coloured fine crystals.

Yield 67 %, mp (methanol) 174 -176°C, IR (nujol mull): cm^{-1} 426.6 (w), 476.1 (vw), 499.0 (s, sh), 601.9 (m, sh), 655.2 (s, sh), 685.7 (vw), 712.3 (vs, sh), 735.2 (vs, sh), 769.5 (w), 792.3 (vw), 811.4 (m, br), 906.6 (s, sh), *v*(Re=O) 933.3 (vs, sh), 1028.5 (m), 1089.5 (vs, shld), 1142.8 (vs, sh), 1211.4 (m, br), 1241.8 (m, br), 1272.3 (w), 1348.5-1527.6 (vs, shld), 1584.7 (vs, sh) and 1611.4 (m, br). *Anal.* Found. C, 39.73, H, 3.61, N, 8.84, S, 6.56. *Calc.* for $C_{32}H_{38}N_6O_{12}S_2Re$: C, 39.75, H, 4.20, N, 9.02, 6.85.

Synthesis of [TcO(L)$_2$]Cl from [n-Bu$_4$N][TcOCl$_4$].

[*n*-Bu$_4$N][TcOCl$_4$] (50.0 mg, 0.10 mmol) was dissolved in methanol (4 ml) and this was added, dropwise, to a solution of *N,N*-diethyl-*N'*-benzoylthiourea (22.6 mg, 0.20 mmol) in methanol (5 ml). The mixture was stirred for 2 min. and triethylamine (30.3 mg, 0.30 mmol) was slowly added. The colour of the solution changed from light green to dark green and a dark green solid material started to separate out from the solution. The reaction mixture was stirred for a further 25 min. and then the solid material was collected by filtration, washed with methanol (3 x 5 ml) and ether (2 x5 ml), and then dried in air overnight.

Yield 41%, mp (ether) 153 - 156 °C IR (KBr pellet): cm^{-1} 618 (w) 705 (s, sh), 800 (vw), 820 (w), 890 (s, sh), *v*(Tc=O) 828 (vs, sh), 1002 (vw), 1028 (w,), 1095 (vs, sh), 1140 (s, sh), 1175 (w), 1208 (s, sh) 1225 (vs, sh), 1308 (vw), 1356 (s, sh), 1378 (vw), 1410 - 1450 (vs, br), 1490 - 1500 (vs, br), 1585 (w), *Anal.* Found: C, 47.97, H, 5.31, N, 8.69, *Calc.* for $C_{24}H_{31}N_4O_4S_2Tc$: C, 47.94, H, 5.2, N 9.31.

6.4. Crystal structure determination.

The crystal structures were solved by Ms Leanne Cook at the University of the Witwatersrand. The experimental details for the crystallographic studies for each structure is given below. The atomic coordinates, complete tables of bond lengths, bond angles and torsion angles, hydrogen coordinates and anisotropic parameters are given in Appendix A.

The X-ray data set was collected on the novel 1K SMART Siemens [5] CCD area detector system using Mo radiation. X-rays were generated using a regular sealed tube and an X-ray generator operating at 50 kV 30 mA. The 9 cm wide CCD area detector was mounted 4.5 cm from the crystal and the data set collected at room temperature. A graphite monochromator followed by a 0.5 mm collimator was used.[6] The selected crystal was mounted on a thin glass fiber.

The determination of the unit cell parameters, crystal orientation and data collection were performed with the SMART.[5] The crystallographic raw data frames were integrated, all reflections extracted, reduced and Lp-corrected using the program SAINT.[7] The cell refinement using all data was performed by SAINT.[7] The program SHELXTL ver. 5.0.[8] was used for structure solution, refinement, molecular graphics and publication preparation.

Outline for the crystal structure determination of $[ReO(L)_2(OMe)]$ ***(1).***

In order to obtain an initial set of cell parameters and an orientation matrix for data collection, reflections 196 from three sets of 15 frames each were collected covering 3 perpendicular sectors of space. The data collection nominally covered over a hemisphere of reciprocal space, by a combination of 3 sets of exposures, 1321 frames. Each set had a different j angle for the crystal and each exposure covered 0.3° in w, with 10 sec. exposure time per frame.

In order to monitor crystal and instrument stability and to enable crystal decay corrections, the first 50 frames of the first set were measured again at the end of the data collection. Crystal decay was found to be negligible after analysing the duplicate reflections. The final data set after

internal scaling consisted of 16897 reflections to 0.9 Å resolution. Coverage of all data is 96.91% complete to at least 25° in q. The data collection took about 6 h.

Outline for the crystal structure determination of [ReO(L-NO_2)$_2$(OMe)] (**4**).

In order to obtain an initial set of cell parameters and an orientation matrix for data collection, reflections 125 from three sets of 15 frames each were collected covering 3 perpendicular sectors of space. The data collection nominally covered over a full sphere/hemisphere of reciprocal space, by a combination of 3 sets of exposures, 2169 frames. Each set had a different j angle for the crystal and each exposure covered 0.3° in w, with 20 sec. exposure time per frame.

In order to monitor crystal and instrument stability and to enable crystal decay corrections, the first 50 frames of the first set were measured again at the end of the data collection. Crystal decay was found to be negligible after analyzing the duplicate reflections. The final data set after internal scaling consisted of 16766 reflections to 0.9 Å resolution. Coverage of all data is 97.6% complete to at least 28.29° in q. The data collection took about 14 h.

Outline for crystal structure determination of [ReO(L)$_2$(OEt)] (**6**).

In order to obtain an initial set of cell parameters and an orientation matrix for data collection, reflections 180 from three sets of 15 frames each were collected covering 3 perpendicular sectors of space. The data collection nominally covered over a full sphere/hemisphere of reciprocal space, by a combination of 3 sets of exposures, 2169 frames. Each set had a different j angle for the crystal and each exposure covered 0.3° in w, with 20 sec. exposure time per frame.

In order to monitor crystal and instrument stability and to enable crystal decay corrections, the first 50 frames of the first set were measured again at the end of the data collection. Crystal decay was found to be negligible after analysing the duplicate reflections. The final data set after internal scaling consisted of 60057reflections to 0.9 Å resolution. Coverage of all data is 99.4% complete to at least 28.36° in q. The data collection took about 17 h.

*Outline for the crystal structure determination of [$(L)_2$ORe-O-ReO$(L)_2$] **(15)**.*

In order to obtain an initial set of cell parameters and an orientation matrix for data collection, reflections 97 from three sets of 15 frames each were collected covering 3 perpendicular sectors of space. The data collection nominally covered over a full sphere/hemisphere of reciprocal space, by a combination of 3 sets of exposures, 2169 frames. Each set had a different j angle for the crystal and each exposure covered 0.3° in w, with 10 sec. exposure time per frame.

In order to monitor crystal and instrument stability and to enable crystal decay corrections, the first 50 frames of the first set were measured again at the end of the data collection. Crystal decay was found to be negligible after analysing the duplicate reflections. The final data set after internal scaling consisted of 16143 reflections to 0.9 Å resolution. Coverage of all data is 98% complete to at least 28.36° in q. The data collection took about 6 h.

6.5. ^{1}H NMR kinetics studies of dimerization.

The ^{1}HNMR samples of $[ReO(L)_2(OMe)]$, $[ReO(L)_2(OEt)]$ and $[ReO(L)_2(O\textit{i}Pr)]$ of exactly the same concentrations (1×10^{-2}M) were prepared. The ^{1}H NMR acquistion parameter was set to acquire 30 scans at 30 sec. intervals for all samples. The ratio of the integral intensities of the phenyl-$H_{(2/6)}$ protons for both species in all samples at 30 sec. intervals were used to calculate the respective concentrations. The conversion of a monorhenium to a dirhenium complex is in a 1:1 stoichiometry. Taking into account that, there are two ligands in a monorhenium complex and four ligands in a dirhenium complex, every 1 proton integral unit for the monorhenium complex corresponds to 2 proton integral units for the dirhenium complex. Hence the concentrations for the two complexes in solution at various time intervals were calculated as follows:

[Dinuclear] = (integral dinuclear/2)/(integral dinuclear/2 + integral mononuclear) x 0.01 M and
[Mononuclear] = 0.01 M - [Dinuclear]
Tabulation of the results is given in Appendix B.

REFERENCES

1. D. D Perrin, W.L. F. Armarego, *Purification of laboratory Chemicals, 3rd ed.*, Pergamon Press, Oxford, (1988).
2. M. S. Ram, J. T. Hupp, *Inorg. Chem.*, **30**, 130, (1991).
3. N. P Johnson, C. J. L. Lock, G. Wilkinson, *J. Chem. Soc.*, 1054, (1964).
4. J. R. Dilworth, W. Hussain, A. J. Hutson, C. J. Jones, F. S. McQuillan, *Inorg. Synth.*, **31**, 257, (1997).
5. Siemens *ASTRO and SAINT. Data collection and Processing Software for the SMART system.* Siemens Analytical X-ray Instruments Inc., Madison, Wisconsin, USA, (1995).
6. Siemens *SMART Reference Manual.* Siemens Analytical X-ray Instruments Inc., Madison, Wisconsin, USA, (1996).
7. G. M. Sheldrick, *SADABS User Guide.* University of Göttingen, Germany, (1996).
8. Siemens *SHELXTL Version 5.0 (Dos version) – Structure determination programme.* Siemens Analytical X-ray Instruments Inc., Madison, Wisconsin, USA, (1995).

GLOSSARY

Alkylating agents	anticancer drugs whose mode of action is by cross-linking the opposing strands in the DNA double helix by bifunctional alkylation.
Anticancer drug	a drug designed to treat/cure cancer.
Antihormonal	anticancer drug whose mode of action is by interfering with the production or action of certain hormones which are responsible for the growth/division of cells in the area where cancer cells are found e.g estrone and oestradiol in breast cancer.
Antimetabolite	a drug with a structure similar to that of a naturally occurring molecule that it is designed to antagonise.
Benign	non-cancerous tumor which is localised in one area (does not spread to other areas of the body).
Biologically active moiety	the part of the biological molecule (e.g. protein) on which a drug can be attached for delivery to specific areas of the body.
Cancer	a term used for diseases in which abnormal cells divide without control and can invade nearby tissues through the bloodstream and lymphatic system hence spreading to other parts of the body.
Carcinogen	any substance that causes cancer.
Carcinogenesis	the origination of cancer.
Carcinoma	neoplasms arising in the epithelial cells.
Clinical trial	a research study that evaluates the effectiveness of new interventions in people designed to evaluate new methods of screening, prevention, diagnosis, or treatment of cancer.
Cytoplasm	the fluid part of the body cell.
Chemotherapy	the use of drugs in treatment of cancer.
Deshielding effect	an effect observed in nuclear magnetic resonance spectroscopy that causes a nucleus to absorb downfield (to the left of tetramethylsilane standard)

Dihydrofolate reductase	the enzyme responsible for the reduction of folate in the cell.
Dihydrosterone	a hormone that promotes the development and maintenance of male sex characteristics
Haematological toxicity	toxic to blood.
Leukemia	cancer of white corpuscles.
Lymphomas	tumors affecting structures pertaining the formation of the blood.
Lymph nodes	small organs located throughout the body along the channels of the lymphatic system.
Malignant	a tumor with a tendency to invade and destroy nearby tissue and spread to other parts of the body.
Marrow transplantation	temporary removal of the marrow from the bone during chemotherapy.
Metastases	the spread of cancer from one part of the body to another.
Monoclonal antibodies	laboratory produced substances that can locate and react to cancer cells wherever they are in the body.
Myelosupression	inhibition of the marrow cell production.
Mutation	any change in the base sequence of DNA which gives rise to a gene that is different from the original gene.
Nephrotoxicity	poisonous to the kidneys.
Neolplasm	swelling consisting of malignant tissues.
Neurological	of the nervous system
Nitrogenous base	part of the nucleotide which consists of a heterocyclic purine or pyrimidine structure.
Nucleotide	a monomer unit of DNA or RNA, consisting of a sugar residue bonded to a heterocyclic purine or pyrimidine base and to a phosphate group.
Pathogenesis	cellular mechanism of development.
Phenotype	any characteristic of an organism that can be detected in terms of appearance, structure, or some measurable property.

Sarcomas	neoplasms that originate from connective tissues, muscle, cartilage, fat or bone.
Secondary tumor	tumors following metastases.
Thymidylate synthetase	the enzyme which catalyzes the formation of thymidylic acid.
Tumor	an abnormal mass of tissue that results from excessive cell division.

Appendix A

Crystallographic data for $[ReO(L)_2(OMe)]$ **(1)**.

Table A1: Atomic coordinates.

Table A2: Bond lengths and angles.

Table A3: Anisotropic parameters.

Table A4: Hydrogen coordinates.

Table A1. Atomic coordinates (x 10^4) and equivalent isotropic displacement parameters ($Å^2$ x 10^3) for $[ReO(L)_2(OMe)]$ **(1)** U(eq)is defined as one third of the trace of the orthogonalized Uij tensor.

	x	y	z	U(eq)
Re(1)	6202(1)	7333(1)	6184(1)	26(1)
S(1)	6499(1)	5463(1)	6133(1)	27(1)
O(1)	6397(1)	7511(3)	7309(2)	40(1)
N(1)	7306(1)	4646(4)	6369(4)	53(2)
C(1)	8119(3)	5029(9)	6892(7)	33(2)
C(1A)	7962(5)	4416(13)	5987(9)	59(4)
S(2)	5507(1)	6499(1)	6024(1)	29(1)
N(2)	4689(1)	7339(3)	5702(2)	25(1)
C(2)	7726(3)	4686(8)	6069(8)	29(2)
C(2A)	7830(4)	4680(9)	6777(9)	37(2)
O(2)	6063(1)	7582(3)	4944(2)	34(1)
O(3)	6805(1)	8186(3)	6203(3)	41(1)
N(3)	7297(1)	6617(3)	6204(3)	37(1)
C(3)	6908(2)	2837(5)	5631(4)	46(1)
O(4)	5943(1)	9068(3)	6100(3)	38(1)
N(4)	5204(1)	8808(3)	6090(2)	22(1)
C(4)	7135(2)	3482(4)	6493(4)	41(1)
C(5)	7064(2)	5636(4)	6240(3)	30(1)
C(6)	7170(2)	7728(4)	6187(3)	27(1)
C(7)	7527(1)	8601(4)	6184(3)	26(1)
C(8)	7484(2)	9790(4)	6377(3)	30(1)
C(9)	7827(2)	10578(4)	6454(4)	33(1)
C(10)	8215(2)	10212(4)	6309(4)	35(1)
C(11)	8256(2)	9048(4)	6083(4)	35(1)
C(12)	7919(2)	8245(4)	6039(3)	30(1)
C(13)	4485(2)	5416(5)	6227(4)	50(2)
C(14)	4525(2)	6129(4)	5455(4)	33(1)
C(15)	4336(2)	8498(5)	6619(4)	40(1)
C(16)	4344(1)	8231(4)	5689(3)	28(1)
C(17)	5122(1)	7654(4)	5926(3)	23(1)
C(18)	5577(1)	9398(4)	6188(3)	22(1)
C(19)	5560(2)	10685(4)	6394(3)	23(1)
C(20)	5152(2)	11233(4)	6311(4)	38(1)
C(21)	5140(2)	12425(4)	6484(4)	50(2)

C(22)	5529(2)	13076(5)	6759(4)	47(2)
C(23)	5934(2)	12552(4)	6844(4)	44(1)
C(24)	5947(2)	11352(4)	6650(3)	34(1)

Table A2. Bond lengths [Å] and angles/° for [ReO(L)$_2$(OMe)] **(1)**.

Re(1)-O(1)	1.701(4)
Re(1)-O(2)	1.897(4)
Re(1)-O(4)	2.118(3)
Re(1)-O(3)	2.129(3)
Re(1)-S(2)	2.3243(11)
Re(1)-S(1)	2.3317(11)
S(1)-C(5)	1.744(5)
N(1)-C(5)	1.334(6)
N(1)-C(4)	1.464(6)
N(1)-C(2A)	1.558(12)
N(1)-C(2)	1.560(11)
C(1)-C(2)	1.517(15)
C(1A)-C(2A)	1.491(16)
S(2)-C(17)	1.759(4)
N(2)-C(17)	1.340(5)
N(2)-C(14)	1.471(6)
N(2)-C(16)	1.480(5)
O(2)-C(25)	1.413(6)
O(3)-C(6)	1.273(5)
N(3)-C(6)	1.318(6)
N(3)-C(5)	1.346(6)
C(3)-C(4)	1.507(8)
O(4)-C(18)	1.268(5)
N(4)-C(18)	1.320(5)
N(4)-C(17)	1.342(5)
C(6)-C(7)	1.503(6)
C(7)-C(12)	1.393(6)
C(7)-C(8)	1.401(6)
C(8)-C(9)	1.377(6)
C(9)-C(10)	1.388(7)
C(10)-C(11)	1.386(7)
C(11)-C(12)	1.384(6)
C(13)-C(14)	1.516(8)
C(15)-C(16)	1.526(7)
C(18)-C(19)	1.501(6)
C(19)-C(24)	1.375(6)
C(19)-C(20)	1.398(6)
C(20)-C(21)	1.383(7)
C(21)-C(22)	1.371(8)
C(22)-C(23)	1.376(8)
C(23)-C(24)	1.399(7)

O(1)-Re(1)-O(2)	163.05(16)
O(1)-Re(1)-O(4)	87.08(16)
O(2)-Re(1)-O(4)	81.32(14)
O(1)-Re(1)-O(3)	86.21(16)
O(2)-Re(1)-O(3)	80.43(15)
O(4)-Re(1)-O(3)	84.51(12)
O(1)-Re(1)-S(2)	98.64(12)
O(2)-Re(1)-S(2)	94.16(10)
O(4)-Re(1)-S(2)	92.30(9)
O(3)-Re(1)-S(2)	174.07(11)
O(1)-Re(1)-S(1)	98.07(12)
O(2)-Re(1)-S(1)	92.94(10)
O(4)-Re(1)-S(1)	173.90(11)
O(3)-Re(1)-S(1)	92.55(9)
S(2)-Re(1)-S(1)	90.15(4)
C(5)-S(1)-Re(1)	107.76(15)
C(5)-N(1)-C(4)	124.0(4)
C(5)-N(1)-C(2A)	120.9(5)
C(4)-N(1)-C(2A)	110.7(5)
C(5)-N(1)-C(2)	115.6(5)
C(4)-N(1)-C(2)	117.4(5)
C(2A)-N(1)-C(2)	40.0(5)
C(17)-S(2)-Re(1)	107.86(15)
C(17)-N(2)-C(14)	123.6(4)
C(17)-N(2)-C(16)	120.0(4)
C(14)-N(2)-C(16)	116.4(3)
C(1)-C(2)-N(1)	105.7(9)
C(1A)-C(2A)-N(1)	101.9(10)
C(25)-O(2)-Re(1)	137.0(4)
C(6)-O(3)-Re(1)	128.8(3)
C(6)-N(3)-C(5)	128.7(4)
C(18)-O(4)-Re(1)	128.0(3)
C(18)-N(4)-C(17)	128.5(4)
N(1)-C(4)-C(3)	113.3(5)
N(1)-C(5)-N(3)	114.2(4)
N(1)-C(5)-S(1)	115.7(4)
N(3)-C(5)-S(1)	130.1(3)
O(3)-C(6)-N(3)	131.2(4)
O(3)-C(6)-C(7)	114.7(4)
N(3)-C(6)-C(7)	114.0(4)
C(12)-C(7)-C(8)	118.4(4)
C(12)-C(7)-C(6)	121.4(4)
C(8)-C(7)-C(6)	120.1(4)
C(9)-C(8)-C(7)	120.7(4)

Appendix

C(8)-C(9)-C(10)	120.3(4)
C(11)-C(10)-C(9)	119.7(4)
C(12)-C(11)-C(10)	120.1(4)
C(11)-C(12)-C(7)	120.8(4)
N(2)-C(14)-C(13)	113.5(4)
N(2)-C(16)-C(15)	112.3(4)
N(2)-C(17)-N(4)	115.0(4)
N(2)-C(17)-S(2)	116.0(3)
N(4)-C(17)-S(2)	128.8(3)
O(4)-C(18)-N(4)	130.5(4)
O(4)-C(18)-C(19)	114.5(4)
N(4)-C(18)-C(19)	114.9(4)
C(24)-C(19)-C(20)	118.8(4)
C(24)-C(19)-C(18)	120.3(4)
C(20)-C(19)-C(18)	120.8(4)
C(21)-C(20)-C(19)	120.1(5)
C(22)-C(21)-C(20)	120.6(5)
C(21)-C(22)-C(23)	120.1(5)
C(22)-C(23)-C(24)	119.6(5)
C(19)-C(24)-C(23)	120.7(5)

Symmetry transformations used to generate equivalent atoms:

Table A3. Anisotropic displacement parameters ($A^2 \times 10^3$) for $[ReO(L)_2(OMe)]$ **(1)**.
The anisotropic displacement factor exponent takes the form:
$-2\pi^2[h^2 a^{*2} U11 + ... + 2h k a^* b^* U12]$

	U11	U22	U33	U23	U13	U12
Re(1)	20(1)	19(1)	40(1)	-4(1)	14(1)	1(1)
S(1)	21(1)	19(1)	41(1)	-2(1)	10(1)	2(1)
O(1)	30(2)	42(2)	45(2)	-13(2)	9(2)	5(2)
N(1)	24(2)	22(2)	115(5)	-7(2)	28(3)	4(2)
C(1)	20(5)	35(6)	49(7)	11(5)	16(5)	2(4)
C(1A)	50(8)	79(10)	58(9)	-2(7)	29(7)	8(7)
S(2)	24(1)	17(1)	51(1)	-3(1)	18(1)	0(1)
N(2)	19(2)	25(2)	31(2)	-4(2)	10(2)	-1(2)
C(2)	27(5)	22(5)	46(7)	-3(4)	23(5)	7(4)
C(2A)	36(6)	29(6)	47(8)	9(5)	16(6)	11(5)
O(2)	34(2)	28(2)	47(2)	8(2)	21(2)	7(1)
O(3)	23(2)	23(2)	82(3)	-8(2)	25(2)	-3(1)
N(3)	26(2)	20(2)	68(3)	-5(2)	22(2)	0(2)
C(3)	39(3)	31(3)	64(4)	0(3)	15(3)	5(2)
O(4)	27(2)	19(2)	74(3)	-3(2)	25(2)	0(1)
N(4)	19(2)	19(2)	30(2)	-5(2)	11(2)	-2(1)
C(4)	28(3)	22(2)	68(4)	0(2)	11(3)	6(2)
C(5)	23(2)	22(2)	45(3)	-5(2)	12(2)	6(2)
C(6)	23(2)	25(2)	36(3)	-3(2)	13(2)	0(2)
C(7)	21(2)	26(2)	30(3)	2(2)	9(2)	0(2)
C(8)	22(2)	28(2)	41(3)	3(2)	12(2)	5(2)
C(9)	29(2)	25(2)	45(3)	0(2)	13(2)	1(2)
C(10)	28(3)	32(3)	43(3)	5(2)	11(2)	-7(2)
C(11)	26(2)	33(3)	50(3)	-1(2)	21(2)	-1(2)
C(12)	29(2)	28(2)	36(3)	-6(2)	15(2)	-2(2)
C(13)	49(3)	29(3)	74(4)	3(3)	24(3)	-5(2)
C(14)	22(2)	27(2)	49(3)	-8(2)	10(2)	-8(2)
C(15)	45(3)	39(3)	47(3)	5(2)	29(3)	8(2)
C(16)	20(2)	29(2)	34(3)	0(2)	7(2)	3(2)
C(17)	24(2)	21(2)	26(2)	-4(2)	12(2)	-1(2)
C(18)	20(2)	22(2)	24(2)	0(2)	9(2)	2(2)
C(19)	28(2)	18(2)	26(2)	-1(2)	12(2)	-2(2)
C(20)	35(3)	24(2)	60(4)	-1(2)	21(3)	1(2)
C(21)	53(3)	26(3)	79(4)	-5(3)	32(3)	10(3)

C(22)	72(4)	19(2)	60(4)	-8(2)	35(3)	1(3)
C(23)	53(3)	29(3)	51(3)	-8(2)	20(3)	-16(2)
C(24)	31(3)	29(3)	42(3)	-6(2)	14(2)	-5(2)

Table A4. Hydrogen coordinates (x 10^4) and isotropic displacement parameters (A^2 x 10^3) for [ReO(L)$_2$(OMe)] **(1)**.

	x	y	z	U(eq)
H(1A)	8072	5829	7075	50
H(1B)	8399	5003	6756	50
H(1C)	8140	4475	7375	50
H(1A1)	7857	3625	5764	89
H(1A2)	8291	4450	6158	89
H(1A3)	7826	4998	5519	89
H(2A)	7779	3905	5846	34
H(2B)	7683	5275	5589	34
H(2A1)	7938	5467	7028	44
H(2A2)	7946	4075	7247	44
H(3A)	6655	3307	5251	69
H(3B)	6798	2073	5756	69
H(3C)	7125	2712	5324	69
H(4A)	6917	3578	6809	49
H(4B)	7389	2998	6874	49
H(8)	7215	10056	6456	36
H(9)	7797	11376	6607	39
H(10)	8451	10756	6364	42
H(11)	8515	8801	5959	42
H(12)	7955	7442	5908	36
H(13A)	4783	5333	6686	75
H(13B)	4364	4633	6015	75
H(13C)	4282	5820	6480	75
H(14A)	4733	5719	5210	40
H(14B)	4226	6165	4979	40
H(15A)	4289	7765	6900	61
H(15B)	4090	9049	6574	61
H(15C)	4623	8853	6980	61
H(16A)	4044	7942	5310	33
H(16B)	4407	8968	5420	33
H(20)	4881	10785	6135	46
H(21)	4860	12796	6411	60
H(22)	5518	13891	6890	57
H(23)	6204	13002	7034	53
H(24)	6226	10994	6696	41
H(25A)	6056	9260	4622	81
H(25B)	5896	8389	3784	81
H(25C)	6419	8489	4369	81

Crystallographic data for [ReO(LNO$_2$)$_2$(OMe)] **(4)**.

Table A5: Atomic coordinates.

Table A6: Bond lengths and angles.

Table A7: Anisotropic parameters.

Table A8: Hydrogen coordinates.

Table A5 Atomic coordinates (x 10^4) and equivalent isotropic displacement parameters ($Å^2$ x 10^3) for [ReO(LNO_2)$_2$(OMe)] **(4)**. U(eq)is defined as one third of the trace of the orthogonalized Uij tensor.

	x	y	z	U(eq)
Re(1)	5403(1)	7538(1)	7240(1)	19(1)
S(2)	4611(1)	6560(1)	8327(1)	23(1)
S(1)	3643(1)	6490(1)	6056(1)	22(1)
O(3)	6513(3)	8366(2)	6338(2)	29(1)
O(4)	7242(3)	8528(2)	8226(2)	24(1)
O(2)	7642(3)	6955(2)	7173(2)	26(1)
O(1)	3800(3)	8321(2)	7355(2)	27(1)
N(4)	6763(4)	7934(2)	9568(2)	22(1)
N(3)	5096(4)	7656(2)	4881(2)	23(1)
N(2)	7392(4)	6413(2)	9685(2)	24(1)
N(1)	3673(4)	6218(2)	4282(2)	23(1)
C(5)	4224(4)	6829(2)	5031(2)	21(1)
C(6)	6063(4)	8327(2)	5478(2)	20(1)
C(17)	6410(4)	7010(2)	9246(2)	21(1)
C(18)	7034(4)	8610(2)	9068(2)	22(1)
C(20)	7837(5)	9798(3)	10469(2)	26(1)
C(8)	7579(4)	9975(2)	5674(2)	25(1)
C(7)	6773(4)	9176(2)	5083(2)	22(1)
C(24)	6750(4)	10318(2)	9015(2)	26(1)
C(12)	6624(4)	9190(2)	4143(2)	26(1)
C(4)	2618(5)	5289(2)	4262(2)	27(1)
C(19)	7229(4)	9593(2)	9534(2)	23(1)
C(16)	8983(5)	6761(3)	10406(2)	28(1)
C(14)	7131(6)	5385(3)	9417(3)	34(1)
C(23)	6872(5)	11221(3)	9459(3)	29(1)
C(3)	536(5)	5344(3)	3980(3)	36(1)
C(11)	7260(5)	9989(3)	3789(3)	34(1)
C(22)	7502(5)	11449(3)	10384(3)	31(1)
C(10)	8073(5)	10790(3)	4371(3)	36(1)
C(2)	4026(5)	6460(3)	3383(2)	33(1)
C(9)	8211(5)	10760(2)	5295(3)	31(1)
C(21)	7999(5)	10726(3)	10886(3)	31(1)
C(25)	9530(5)	7245(3)	7139(4)	48(1)
C(15)	8454(6)	6763(4)	11352(3)	47(1)
C(13)	8313(7)	5117(3)	8697(3)	47(1)
C(1)	5927(7)	6221(4)	3195(4)	56(1)

O (8)	6563(4)	12795(2)	9273(3)	49(1)
O(5)	9720(5)	12279(2)	5589(3)	62(1)
N(6)	6242(5)	11972(2)	8915(3)	39(1)
N(5)	9045(5)	11607(2)	5918(3)	45(1)
O(6)	9026(6)	11607(2)	6726(3)	66(1)
O(7)	5383(6)	11740(3)	8141(2)	66(1)

Table A6. Bond lengths [Å] and angles/° for $ReO(LNO_2)_2(OMe)]$ **(4)**.

Re(1)-O(1)	1.699(2)
Re(1)-O(2)	1.903(2)
Re(1)-O(3)	2.096(2)
Re(1)-O(4)	2.144(2)
Re(1)-S(1)	2.3333(8)
Re(1)-S(2)	2.3602(8)
S(2)-C(17)	1.771(3)
S(1)-C(5)	1.756(3)
O(3)-C(6)	1.272(4)
O(4)-C(18)	1.285(4)
O(2)-C(25)	1.410(4)
N(4)-C(18)	1.305(4)
N(4)-C(17)	1.349(4)
N(3)-C(6)	1.312(4)
N(3)-C(5)	1.353(4)
N(2)-C(17)	1.324(4)
N(2)-C(16)	1.469(4)
N(2)-C(14)	1.472(4)
N(1)-C(5)	1.331(4)
N(1)-C(4)	1.474(4)
N(1)-C(2)	1.477(4)
C(6)-C(7)	1.494(4)
C(18)-C(19)	1.489(5)
C(20)-C(19)	1.392(5)
C(20)-C(21)	1.393(5)
C(8)-C(9)	1.387(5)
C(8)-C(7)	1.394(4)
C(7)-C(12)	1.395(5)
C(24)-C(23)	1.378(5)
C(24)-C(19)	1.399(5)
C(12)-C(11)	1.386(5)
C(4)-C(3)	1.520(5)
C(16)-C(15)	1.520(5)
C(14)-C(13)	1.513(6)
C(23)-C(22)	1.384(5)
C(23)-N(6)	1.480(5)
C(11)-C(10)	1.391(6)
C(22)-C(21)	1.385(6)
C(10)-C(9)	1.376(6)
C(2)-C(1)	1.512(6)
C(9)-N(5)	1.472(5)
O(8)-N(6)	1.229(4)

O(5)-N(5)	1.227(5)
N(6)-O(7)	1.224(5)
N(5)-O(6)	1.210(5)
O(1)-Re(1)-O(2)	164.94(11)
O(1)-Re(1)-O(3)	88.68(11)
O(2)-Re(1)-O(3)	81.52(11)
O(1)-Re(1)-O(4)	85.02(11)
O(2)-Re(1)-O(4)	82.27(10)
O(3)-Re(1)-O(4)	81.63(9)
O(1)-Re(1)-S(1)	98.10(8)
O(2)-Re(1)-S(1)	93.78(7)
O(3)-Re(1)-S(1)	92.72(7)
O(4)-Re(1)-S(1)	173.52(7)
O(1)-Re(1)-S(2)	98.23(8)
O(2)-Re(1)-S(2)	90.72(8)
O(3)-Re(1)-S(2)	171.57(7)
O(4)-Re(1)-S(2)	94.10(6)
S(1)-Re(1)-S(2)	91.09(3)
C(17)-S(2)-Re(1)	99.05(11)
C(5)-S(1)-Re(1)	107.17(11)
C(6)-O(3)-Re(1)	129.3(2)
C(18)-O(4)-Re(1)	120.3(2)
C(25)-O(2)-Re(1)	137.1(3)
C(18)-N(4)-C(17)	124.7(3)
C(6)-N(3)-C(5)	128.7(3)
C(17)-N(2)-C(16)	120.7(3)
C(17)-N(2)-C(14)	123.2(3)
C(16)-N(2)-C(14)	115.8(3)
C(5)-N(1)-C(4)	124.4(3)
C(5)-N(1)-C(2)	120.8(3)
C(4)-N(1)-C(2)	114.8(3)
N(1)-C(5)-N(3)	114.2(3)
N(1)-C(5)-S(1)	117.0(2)
N(3)-C(5)-S(1)	128.8(2)
O(3)-C(6)-N(3)	130.3(3)
O(3)-C(6)-C(7)	114.7(3)
N(3)-C(6)-C(7)	115.0(3)
N(2)-C(17)-N(4)	117.5(3)
N(2)-C(17)-S(2)	119.2(2)
N(4)-C(17)-S(2)	123.2(2)
O(4)-C(18)-N(4)	127.6(3)
O(4)-C(18)-C(19)	115.6(3)
N(4)-C(18)-C(19)	116.7(3)
C(19)-C(20)-C(21)	120.1(3)

C(8)-C(7)-C(12)	119.6(3)
C(8)-C(7)-C(6)	118.8(3)
C(12)-C(7)-C(6)	121.6(3)
C(23)-C(24)-C(19)	118.1(3)
C(11)-C(12)-C(7)	120.9(3)
N(1)-C(4)-C(3)	110.5(3)
C(20)-C(19)-C(24)	120.0(3)
C(20)-C(19)-C(18)	121.5(3)
C(24)-C(19)-C(18)	118.5(3)
N(2)-C(16)-C(15)	111.9(3)
N(2)-C(14)-C(13)	110.2(3)
C(24)-C(23)-C(22)	123.3(3)
C(24)-C(23)-N(6)	117.7(3)
C(22)-C(23)-N(6)	119.0(3)
C(12)-C(11)-C(10)	120.1(4)
C(21)-C(22)-C(23)	117.8(3)
C(9)-C(10)-C(11)	118.1(3)
N(1)-C(2)-C(1)	111.9(3)
C(10)-C(9)-C(8)	123.4(3)
C(10)-C(9)-N(5)	118.6(3)
C(8)-C(9)-N(5)	118.0(4)
C(22)-C(21)-C(20)	120.7(3)
O(7)-N(6)-O(8)	123.4(4)
O(7)-N(6)-C(23)	118.3(3)
O(8)-N(6)-C(23)	118.2(4)
O(6)-N(5)-O(5)	123.3(4)
O(6)-N(5)-C(9)	118.5(4)
O(5)-N(5)-C(9)	118.2(4)

Symmetry transformations used to generate equivalent atoms:

Table A7. Anisotropic displacement parameters ($Å^2 \times 10^3$) for $ReO(LNO_2)_2(OMe)$] **(4)**. The anisotropic displacement factor exponent takes the form: $-2\pi^2 [h^2 a^{*2} U11 + ... + 2hk a^* b^* U12]$

	U11	U22	U33	U23	U13	U12
Re(1)	19(1)	19(1)	18(1)	1(1)	3(1)	1(1)
S(2)	24(1)	22(1)	21(1)	5(1)	1(1)	-1(1)
S(1)	21(1)	22(1)	21(1)	1(1)	3(1)	-5(1)
O(3)	35(1)	28(1)	21(1)	2(1)	6(1)	-12(1)
O(4)	27(1)	22(1)	21(1)	-3(1)	3(1)	-5(1)
O(2)	19(1)	27(1)	31(1)	-3(1)	4(1)	2(1)
O(1)	32(1)	26(1)	25(1)	6(1)	5(1)	11(1)
N(4)	24(1)	23(1)	19(1)	0(1)	2(1)	5(1)
N(3)	24(1)	22(1)	21(1)	3(1)	3(1)	-2(1)
N(2)	28(1)	22(1)	20(1)	3(1)	1(1)	3(1)
N(1)	22(1)	25(1)	21(1)	0(1)	5(1)	-2(1)
C(5)	15(1)	24(2)	23(2)	3(1)	1(1)	2(1)
C(6)	19(1)	19(2)	22(2)	1(1)	3(1)	3(1)
C(17)	22(1)	23(2)	20(2)	1(1)	6(1)	4(1)
C(18)	18(1)	27(2)	19(2)	-1(1)	0(1)	2(1)
C(20)	24(2)	28(2)	24(2)	-2(1)	4(1)	1(1)
C(8)	19(1)	20(2)	34(2)	-1(1)	1(1)	2(1)
C(7)	16(1)	21(2)	28(2)	4(1)	3(1)	1(1)
C(24)	24(2)	25(2)	27(2)	1(1)	4(1)	3(1)
C(12)	23(2)	25(2)	31(2)	7(1)	3(1)	2(1)
C(4)	30(2)	21(2)	27(2)	-3(1)	3(1)	-6(1)
C(19)	18(1)	26(2)	24(2)	-2(1)	3(1)	1(1)
C(16)	27(2)	30(2)	26(2)	2(1)	-2(1)	6(1)
C(14)	43(2)	22(2)	34(2)	8(1)	-6(2)	8(2)
C(23)	21(2)	26(2)	41(2)	4(2)	10(1)	4(1)
C(3)	28(2)	35(2)	41(2)	0(2)	6(2)	-8(2)
C(11)	30(2)	37(2)	38(2)	19(2)	5(2)	2(2)
C(22)	26(2)	25(2)	40(2)	-7(2)	10(1)	-2(1)
C(10)	24(2)	29(2)	56(2)	21(2)	5(2)	0(1)
C(2)	44(2)	32(2)	21(2)	-1(1)	9(1)	-8(2)
C(9)	22(2)	16(2)	53(2)	4(2)	3(2)	1(1)
C(21)	31(2)	32(2)	28(2)	-10(1)	7(1)	1(2)
C(25)	17(2)	51(3)	73(3)	-7(2)	13(2)	0(2)
C(15)	48(2)	67(3)	23(2)	-2(2)	-2(2)	20(2)
C(13)	68(3)	37(2)	34(2)	-5(2)	-7(2)	30(2)

C(1)	69(3)	52(3)	61(3)	13(2)	47(3)	10(2)
O(8)	42(2)	22(1)	85(2)	10(1)	12(2)	5(1)
O(5)	49(2)	23(2)	107(3)	15(2)	-7(2)	-11(1)
N(6)	35(2)	26(2)	60(2)	9(2)	14(2)	9(1)
N(5)	33(2)	21(2)	74(3)	-2(2)	-2(2)	1(1)
O(6)	81(3)	37(2)	67(3)	-19(2)	3(2)	-13(2)
O(7)	99(3)	47(2)	51(2)	14(2)	-4(2)	26(2)

Table A8. Hydrogen coordinates (x 10^4) and isotropic displacement parameters (Å^2 x 10^3) for ReO(LNO$_2$)$_2$(OMe)] **(4)**.

	x	y	z	U(eq)
H(20)	8143	9304	10824	31
H(8)	7693	9981	6316	30
H(24)	6354	10191	8374	31
H(12)	6079	8645	3741	31
H(4A)	2847	5076	4874	32
H(4B)	3057	4822	3826	32
H(16A)	9446	7411	10322	34
H(16B)	10010	6358	10354	34
H(14A)	5796	5184	9174	40
H(14B)	7493	5058	9957	40
H(3A)	98	5798	4419	54
H(3B)	-143	4721	3967	54
H(3C)	310	5550	3372	54
H(11)	7140	9990	3147	41
H(22)	7592	12082	10665	37
H(10)	8521	11341	4137	43
H(2A)	3943	7143	3361	40
H(2B)	3048	6111	2901	40
H(21)	8455	10863	11521	38
H(25A)	9768	7116	6512	72
H(25B)	10341	6898	7539	72
H(25C)	9793	7923	7343	72
H(15A)	7463	7178	11413	70
H(15B)	9552	6993	11813	70
H(15C)	8004	6120	11439	70
H(13A)	7913	5419	8153	71
H(13B)	8160	4430	8539	71
H(13C)	9630	5329	8935	71
H(1A)	6902	6593	3649	84
H(1B)	6088	6368	2584	84
H(1C)	6024	5547	3229	84

Crystallographic data for $[ReO(L)_2(OEt)]$ **(6)**.

Table A9: Atomic coordinates.

Table A10: Bond lengths and angles.

Table A11: Anisotropic parameters.

Table A12: Hydrogen coordinates.

Table A9. Atomic coordinates (x 10^4) and equivalent isotropic displacement parameters ($Å^2$ x 10^3) [ReO(L)2(OEt)] **(6)**. U(eq) is defined as one third of the trace of the orthogonalized Uij tensor.

	x	y	z	U(eq)
Re(1)	1949(1)	2833(1)	2526(1)	44(1)
S(1)	644(1)	3264(1)	3931(1)	56(1)
O(1)	888(4)	2066(3)	2222(2)	69(1)
N(1)	842(4)	1983(4)	5502(2)	58(1)
C(1)	738(8)	-189(7)	6222(5)	112(2)
S(2)	572(1)	5065(1)	2041(1)	54(1)
O(2)	3638(3)	3244(3)	2714(2)	57(1)
N(2)	276(4)	6396(3)	479(2)	54(1)
C(2)	1438(7)	839(5)	6178(3)	74(1)
O(3)	3375(4)	852(3)	2962(2)	62(1)
N(3)	2578(4)	677(3)	4488(2)	48(1)
C(3)	-1963(8)	3212(7)	5886(6)	126(3)
O(4)	3298(4)	2457(3)	1265(2)	61(1)
N(4)	2519(4)	4570(3)	447(2)	46(1)
C(4)	-410(7)	3225(5)	5837(3)	81(2)
C(5)	1434(5)	1862(4)	4655(3)	48(1)
C(6)	3410(4)	268(4)	3733(3)	41(1)
C(7)	4583(4)	-1144(4)	3796(3)	43(1)
C(8)	5260(5)	-1815(5)	3053(3)	57(1)
C(9)	6310(6)	-3140(5)	3111(4)	76(2)
C(10)	6705(6)	-3772(6)	3912(5)	86(2)
C(11)	6069(7)	-3108(6)	4649(5)	82(2)
C(12)	4979(6)	-1794(5)	4607(4)	64(1)
C(13)	-1184(9)	8383(7)	1336(5)	79(2)
C(14)	-1250(6)	7296(5)	880(4)	64(1)
C(15)	1250(9)	7867(8)	-670(5)	85(2)
C(16)	678(7)	6712(5)	-469(3)	64(1)
C(17)	1205(5)	5314(4)	915(3)	45(1)
C(18)	3448(5)	3303(4)	621(3)	44(1)
C(19)	4777(5)	2760(4)	-79(3)	44(1)
C(20)	5185(6)	3605(6)	-763(3)	60(1)
C(21)	6381(7)	3051(7)	-1417(4)	71(2)
C(22)	7144(7)	1679(7)	-1418(4)	72(2)
C(23)	6754(6)	843(6)	-743(4)	66(1)

C (24)	5600 (6)	1386 (5)	-75 (3)	57 (1)
C(25)	5254(6)	2685(7)	2592(5)	98(2)
C(26)	5967(7)	3522(7)	2853(5)	96(2)

Table A10. Bond lengths [Å] and angles/° $[ReO(L)_2(OEt)]$ **(6)**.

Re(1)-O(1)	1.687(3)
Re(1)-O(2)	1.899(3)
Re(1)-O(3)	2.121(3)
Re(1)-O(4)	2.134(3)
Re(1)-S(1)	2.3209(11)
Re(1)-S(2)	2.3283(10)
S(1)-C(5)	1.741(4)
N(1)-C(5)	1.338(5)
N(1)-C(4)	1.489(6)
N(1)-C(2)	1.495(6)
C(1)-C(2)	1.477(8)
S(2)-C(17)	1.758(4)
O(2)-C(25)	1.402(6)
N(2)-C(17)	1.337(5)
N(2)-C(16)	1.475(6)
N(2)-C(14)	1.478(6)
O(3)-C(6)	1.268(4)
N(3)-C(6)	1.319(5)
N(3)-C(5)	1.339(5)
C(3)-C(4)	1.466(9)
O(4)-C(18)	1.271(4)
N(4)-C(18)	1.324(5)
N(4)-C(17)	1.338(5)
C(6)-C(7)	1.496(5)
C(7)-C(8)	1.375(6)
C(7)-C(12)	1.390(6)
C(8)-C(9)	1.387(7)
C(9)-C(10)	1.373(8)
C(10)-C(11)	1.359(9)
C(11)-C(12)	1.392(7)
C(13)-C(14)	1.480(8)
C(15)-C(16)	1.502(8)
C(18)-C(19)	1.492(6)
C(19)-C(24)	1.376(6)
C(19)-C(20)	1.387(6)
C(20)-C(21)	1.382(7)
C(21)-C(22)	1.366(8)
C(22)-C(23)	1.366(8)
C(23)-C(24)	1.372(7)
C(25)-C(26)	1.452(8)
O(1)-Re(1)-O(2)	162.58(15)

O(1)-Re(1)-O(3)	85.69(14)
O(2)-Re(1)-O(3)	81.57(13)
O(1)-Re(1)-O(4)	85.81(14)
O(2)-Re(1)-O(4)	81.68(13)
O(3)-Re(1)-O(4)	86.79(11)
O(1)-Re(1)-S(1)	98.45(12)
O(2)-Re(1)-S(1)	93.84(10)
O(3)-Re(1)-S(1)	92.05(8)
O(4)-Re(1)-S(1)	175.49(9)
O(1)-Re(1)-S(2)	99.09(11)
O(2)-Re(1)-S(2)	93.36(9)
O(3)-Re(1)-S(2)	174.85(10)
O(4)-Re(1)-S(2)	91.61(8)
S(1)-Re(1)-S(2)	89.17(4)
C(5)-S(1)-Re(1)	109.08(15)
C(5)-N(1)-C(4)	123.9(4)
C(5)-N(1)-C(2)	120.4(4)
C(4)-N(1)-C(2)	115.8(4)
C(17)-S(2)-Re(1)	108.13(14)
C(25)-O(2)-Re(1)	139.3(3)
C(17)-N(2)-C(16)	121.1(4)
C(17)-N(2)-C(14)	123.5(4)
C(16)-N(2)-C(14)	115.3(4)
C(1)-C(2)-N(1)	111.3(5)
C(6)-O(3)-Re(1)	129.1(3)
C(6)-N(3)-C(5)	129.2(3)
C(18)-O(4)-Re(1)	129.0(3)
C(18)-N(4)-C(17)	129.3(3)
C(3)-C(4)-N(1)	113.6(5)
N(1)-C(5)-N(3)	114.8(4)
N(1)-C(5)-S(1)	116.0(3)
N(3)-C(5)-S(1)	129.2(3)
O(3)-C(6)-N(3)	131.3(3)
O(3)-C(6)-C(7)	114.4(3)
N(3)-C(6)-C(7)	114.3(3)
C(8)-C(7)-C(12)	119.5(4)
C(8)-C(7)-C(6)	120.1(4)
C(12)-C(7)-C(6)	120.4(4)
C(7)-C(8)-C(9)	120.3(5)
C(10)-C(9)-C(8)	119.9(5)
C(11)-C(10)-C(9)	120.3(5)
C(10)-C(11)-C(12)	120.6(6)
C(7)-C(12)-C(11)	119.3(5)
N(2)-C(14)-C(13)	113.8(5)

N(2)-C(16)-C(15)	113.1(5)
N(2)-C(17)-N(4)	116.1(4)
N(2)-C(17)-S(2)	116.0(3)
N(4)-C(17)-S(2)	127.9(3)
O(4)-C(18)-N(4)	129.0(4)
O(4)-C(18)-C(19)	115.7(3)
N(4)-C(18)-C(19)	115.0(3)
C(24)-C(19)-C(20)	118.2(4)
C(24)-C(19)-C(18)	120.2(4)
C(20)-C(19)-C(18)	121.6(4)
C(21)-C(20)-C(19)	119.6(5)
C(22)-C(21)-C(20)	121.2(5)
C(23)-C(22)-C(21)	119.4(5)
C(22)-C(23)-C(24)	119.8(6)
C(23)-C(24)-C(19)	121.7(5)
O(2)-C(25)-C(26)	114.0(5)

Symmetry transformations used to generate equivalent atoms:

Appendix

Table A11. Anisotropic displacement parameters ($Å^2 \times 10^3$) [$ReO(L)_2(OEt)$] **(6)**

The anisotropic displacement factor exponent takes the form:

$-2\pi^2 [h^2 a^{*2} U11 + ... + 2hk a^* b^* U12]$

	U11	U22	U33	U23	U13	U12
Re(1)	56(1)	35(1)	33(1)	7(1)	-3(1)	-13(1)
S(1)	60(1)	41(1)	41(1)	7(1)	3(1)	-1(1)
O(1)	101(2)	63(2)	50(2)	17(2)	-21(2)	-43(2)
N(1)	76(3)	46(2)	38(2)	2(2)	2(2)	-14(2)
C(1)	108(5)	87(4)	121(6)	38(4)	4(4)	-41(4)
S(2)	60(1)	43(1)	41(1)	11(1)	-2(1)	-6(1)
O(2)	51(2)	52(2)	60(2)	1(1)	-8(1)	-12(1)
N(2)	68(2)	41(2)	48(2)	10(2)	-14(2)	-18(2)
C(2)	95(4)	72(3)	46(3)	-2(2)	-6(3)	-25(3)
O(3)	84(2)	38(2)	36(2)	7(1)	2(2)	-1(1)
N(3)	54(2)	38(2)	38(2)	3(1)	-3(2)	-6(2)
C(3)	84(5)	86(5)	151(7)	18(4)	34(5)	-4(4)
O(4)	87(2)	41(2)	35(2)	3(1)	8(2)	-14(2)
N(4)	61(2)	40(2)	37(2)	5(1)	-5(2)	-22(2)
C(4)	121(5)	58(3)	50(3)	-7(2)	7(3)	-27(3)
C(5)	60(3)	40(2)	37(2)	2(2)	-2(2)	-16(2)
C(6)	44(2)	35(2)	40(2)	3(2)	-6(2)	-13(2)
C(7)	38(2)	42(2)	46(2)	5(2)	-6(2)	-12(2)
C(8)	55(3)	50(3)	52(3)	0(2)	-1(2)	-9(2)
C(9)	69(3)	51(3)	76(4)	-6(3)	19(3)	0(2)
C(10)	62(3)	54(3)	102(5)	8(3)	1(3)	10(3)
C(11)	73(4)	63(3)	85(4)	21(3)	-26(3)	1(3)
C(12)	70(3)	56(3)	53(3)	5(2)	-17(3)	-9(2)
C(13)	87(5)	66(4)	77(4)	-4(3)	-7(4)	-23(4)
C(14)	70(3)	52(3)	62(3)	15(2)	-15(3)	-19(3)
C(15)	109(5)	116(5)	55(4)	3(4)	-2(4)	-75(4)
C(16)	98(4)	50(3)	43(3)	13(2)	-23(3)	-26(3)
C(17)	58(3)	38(2)	40(2)	5(2)	-8(2)	-21(2)
C(18)	60(2)	41(2)	37(2)	2(2)	-12(2)	-23(2)
C(19)	50(2)	49(2)	36(2)	-2(2)	-8(2)	-23(2)
C(20)	75(3)	54(3)	50(3)	0(2)	-3(2)	-29(3)
C(21)	79(4)	89(4)	46(3)	3(3)	8(3)	-41(3)
C(22)	62(3)	96(5)	52(3)	-18(3)	9(3)	-25(3)
C(23)	65(3)	64(3)	63(3)	-14(3)	1(3)	-19(3)

C (24)	64 (3)	53 (3)	52 (3)	2 (2)	-3 (2)	-26 (2)
C(25)	58(3)	103(5)	129(6)	-37(4)	1(3)	-22(3)
C(26)	73(4)	101(5)	114(5)	-9(4)	-16(4)	-29(3)

Table A12. Hydrogen coordinates (x 10^4) and isotropic displacement parameters (A^2 x 10^3) [$ReO(L)_2(OEt)$] **(6)**.

	x	y	z	U(eq)
H(1A)	1141	-909	6661	168
H(1B)	978	-549	5663	168
H(1C)	-361	224	6371	168
H(2A)	2550	417	6037	89
H(2B)	1210	1191	6746	89
H(3A)	-2713	4040	6100	189
H(3B)	-2060	2455	6276	189
H(3C)	-2132	3131	5312	189
H(4A)	-256	3319	6418	97
H(4B)	-335	4011	5458	97
H(8)	4910(50)	-1330(50)	2510(30)	62(13)
H(9)	6730(70)	-3610(60)	2550(40)	103(19)
H(10)	7490(70)	-4710(70)	3980(40)	104(19)
H(11)	6350(70)	-3490(60)	5200(40)	95(19)
H(12)	4670(50)	-1310(50)	5110(30)	63(14)
H(13A)	-710(80)	8910(70)	940(50)	110(20)
H(13B)	-480(110)	7990(90)	1770(60)	170(30)
H(13C)	-2260(80)	8990(70)	1520(40)	110(20)
H(14B)	-1710(50)	6750(40)	1200(30)	52(12)
H(14A)	-1850(50)	7680(50)	370(30)	65(13)
H(15B)	1530(60)	8040(50)	-1300(40)	87(17)
H(15A)	2110(80)	7590(70)	-330(50)	110(20)
H(15C)	770(70)	8610(60)	-260(40)	100(20)
H(16B)	-320(70)	6910(60)	-760(40)	97(18)
H(16A)	1250(70)	5900(60)	-740(40)	93(19)
H(20)	4690(40)	4460(40)	-770(30)	41(11)
H(21)	6540(60)	3630(60)	-1780(40)	81(18)
H(22)	7900(60)	1390(50)	-1870(40)	82(17)
H(23)	7180(60)	0(60)	-760(30)	74(17)
H(24)	5360(50)	920(40)	310(30)	44(12)
H(25A)	5622	2539	1978	117
H(25B)	5583	1807	2927	117
H(26A)	7069	3080	2751	144
H(26B)	5634	3653	3465	144
H(26C)	5671	4387	2515	144

Crystallographic data for $[(L)_2ORe\text{-}O\text{-}ReO(L)_2]$ **(15)**.

Table A13: Atomic coordinates.

Table A14: Bond lengths and angles.

Table A15: Anisotropic parameters.

Table A16: Hydrogen coordinates.

Table A13. Atomic coordinates (x 10^4) and equivalent isotropic displacement parameters ($Å^2$ x 10^3) for $[(L)_2ORe\text{-}O\text{-}ReO(L)_2]$ **(15)**. U(eq) is defined as one third of the trace of the orthogonalized Uij tensor.

	x	y	z	U(eq)
Re(1)	826(1)	4606(1)	2178(1)	36(1)
O(1)	1465(3)	3940(3)	1953(3)	66(1)
S(1)	1498(1)	5818(1)	1999(1)	45(1)
N(1)	3005(3)	6428(4)	2612(3)	49(2)
C(1)	4457(5)	6030(6)	3293(4)	80(3)
S(1A)	586(1)	6626(1)	3563(1)	55(1)
N(1A)	1310(6)	8047(5)	3495(4)	99(3)
C(1A)	943(12)	9503(8)	3180(7)	177(8)
O(2)	108(3)	5232(3)	2530(2)	44(1)
S(2)	-166(1)	4684(1)	1104(1)	50(1)
N(2)	-1270(4)	3650(4)	364(3)	59(2)
C(2)	3758(5)	6651(5)	3179(3)	59(2)
Re(2)	-597(1)	5946(1)	2851(1)	42(1)
S(2A)	-552(1)	5023(1)	3713(1)	57(1)
N(2A)	-1376(4)	3685(4)	3839(3)	54(2)
C(2A)	1542(9)	8830(7)	3192(5)	118(5)
O(3)	1584(3)	4549(3)	3183(2)	50(1)
N(3)	2543(3)	5659(4)	3323(2)	44(1)
C(3)	2525(7)	7578(6)	1818(4)	96(3)
O(3A)	-556(3)	6661(3)	2021(2)	56(1)
N(3A)	500(4)	7665(4)	2482(3)	56(2)
C(3A)	2268(11)	7673(8)	4345(6)	143(6)
O(4)	194(3)	3602(3)	2432(2)	55(1)
C(4)	2972(5)	6772(5)	1955(4)	64(2)
N(4)	-884(4)	3244(4)	1445(3)	50(2)
O(4A)	-1559(3)	5257(3)	2152(2)	56(1)
N(4A)	-1869(4)	4169(3)	2776(3)	47(1)
C(4A)	1591(10)	8120(9)	4336(10)	181(9)
O(5)	-1337(3)	6594(3)	2961(3)	77(2)
C(5)	2398(4)	5942(4)	2701(3)	40(2)
C(5A)	772(5)	7485(5)	3130(4)	54(2)
C(6)	2131(4)	5064(4)	3527(3)	40(2)
C(6A)	-62(5)	7234(5)	1989(4)	54(2)
C(7)	2393(4)	4951(4)	4266(3)	45(2)
C(7A)	-103(5)	7501(5)	1303(4)	56(2)
C(8)	1858(5)	4528(5)	4535(4)	65(2)

C(8A)	-461(5)	6985(6)	776(4)	72(2)
C(9)	2095(7)	4418(6)	5235(4)	88(3)
C(9A)	-474(7)	7176(9)	125(5)	102(4)
C(10)	2839(8)	4730(6)	5648(4)	90(3)
C(10A)	-126(8)	7903(11)	30(6)	111(5)
C(11)	3351(7)	5169(6)	5374(4)	93(3)
C(11A)	239(8)	8440(8)	544(7)	113(4)
C(12)	3133(6)	5276(5)	4678(4)	69(2)
C(12A)	253(6)	8248(6)	1197(5)	81(3)
C(13)	-1823(6)	4906(6)	-337(4)	82(3)
C(13A)	-107(6)	3204(6)	4739(4)	82(3)
C(14)	-1257(5)	4156(5)	-210(3)	57(2)
C(14A)	-905(5)	3717(5)	4559(3)	59(2)
C(15)	-2555(11)	3023(9)	100(7)	173(7)
C(15A)	-2796(6)	3119(7)	3627(5)	104(4)
C(16)	-1766(6)	2750(10)	167(5)	120(5)
C(16A)	-1929(6)	2945(5)	3610(4)	75(3)
C(17)	-802(4)	3797(4)	994(3)	44(2)
C(17A)	-1319(4)	4248(4)	3400(4)	46(2)
C(18)	-430(4)	3178(4)	2079(3)	37(2)
C(18A)	-1962(4)	4627(4)	2249(3)	43(2)
C(19)	-648(4)	2450(4)	2448(3)	42(2)
C(19A)	-2703(4)	4399(4)	1653(3)	44(2)
C(20)	-1343(5)	1963(5)	2142(4)	56(2)
C(20A)	-3221(5)	3725(5)	1673(4)	62(2)
C(21)	-1472(7)	1252(6)	2477(5)	80(3)
C(21A)	-3922(5)	3555(6)	1146(4)	79(3)
C(22)	-920(7)	1039(5)	3094(5)	79(3)
C(22A)	-4149(5)	4066(7)	591(4)	80(3)
C(23)	-252(6)	1544(5)	3400(4)	67(2)
C(23A)	-3628(5)	4720(6)	546(4)	68(2)
C(24)	-116(5)	2265(4)	3087(3)	49(2)
C(24A)	-2915(5)	4888(5)	1076(3)	52(2)

Table A14. Bond lengths [Å] and angles/° for $[(L)_2ORe\text{-}O\text{-}ReO(L)_2]$ **(15)**.

Re(1)-O(1)	1.685(5)
Re(1)-O(2)	1.893(4)
Re(1)-O(4)	2.092(4)
Re(1)-O(3)	2.095(4)
Re(1)-S(1)	2.3378(17)
Re(1)-S(2)	2.3420(17)
S(1)-C(5)	1.753(7)
N(1)-C(5)	1.341(8)
N(1)-C(2)	1.476(8)
N(1)-C(4)	1.476(8)
C(1)-C(2)	1.496(11)
S(1A)-C(5A)	1.737(7)
S(1A)-Re(2)	2.3365(19)
N(1A)-C(5A)	1.332(9)
N(1A)-C(2A)	1.518(11)
N(1A)-C(4A)	1.69(2)
C(1A)-C(2A)	1.469(18)
O(2)-Re(2)	1.917(4)
S(2)-C(17)	1.748(7)
N(2)-C(17)	1.330(8)
N(2)-C(14)	1.463(8)
N(2)-C(16)	1.652(14)
Re(2)-O(5)	1.691(5)
Re(2)-O(4A)	2.113(5)
Re(2)-O(3A)	2.113(4)
Re(2)-S(2A)	2.3282(18)
S(2A)-C(17A)	1.757(7)
N(2A)-C(17A)	1.319(8)
N(2A)-C(14A)	1.471(9)
N(2A)-C(16A)	1.488(9)
O(3)-C(6)	1.274(8)
N(3)-C(6)	1.329(8)
N(3)-C(5)	1.336(7)
C(3)-C(4)	1.477(12)
O(3A)-C(6A)	1.254(8)
N(3A)-C(5A)	1.327(9)
N(3A)-C(6A)	1.348(9)
C(3A)-C(4A)	1.336(17)
O(4)-C(18)	1.269(7)
N(4)-C(18)	1.314(8)
N(4)-C(17)	1.341(8)

O(4A)-C(18A)	1.267(8)
N(4A)-C(18A)	1.301(8)
N(4A)-C(17A)	1.348(9)
C(6)-C(7)	1.488(8)
C(6A)-C(7A)	1.489(10)
C(7)-C(12)	1.369(10)
C(7)-C(8)	1.382(9)
C(7A)-C(8A)	1.362(11)
C(7A)-C(12A)	1.390(11)
C(8)-C(9)	1.411(10)
C(8A)-C(9A)	1.400(12)
C(9)-C(10)	1.365(14)
C(9A)-C(10A)	1.348(16)
C(10)-C(11)	1.373(13)
C(10A)-C(11A)	1.367(16)
C(11)-C(12)	1.405(10)
C(11A)-C(12A)	1.403(13)
C(13)-C(14)	1.503(11)
C(13A)-C(14A)	1.510(11)
C(15)-C(16)	1.355(15)
C(15A)-C(16A)	1.489(12)
C(18)-C(19)	1.511(8)
C(18A)-C(19A)	1.500(9)
C(19)-C(20)	1.379(9)
C(19)-C(24)	1.387(9)
C(19A)-C(24A)	1.395(9)
C(19A)-C(20A)	1.396(10)
C(20)-C(21)	1.395(10)
C(20A)-C(21A)	1.360(11)
C(21)-C(22)	1.376(13)
C(21A)-C(22A)	1.379(12)
C(22)-C(23)	1.363(12)
C(22A)-C(23A)	1.388(11)
C(23)-C(24)	1.389(9)
C(23A)-C(24A)	1.375(10)
O(1)-Re(1)-O(2)	171.2(2)
O(1)-Re(1)-O(4)	90.1(2)
O(2)-Re(1)-O(4)	82.61(18)
O(1)-Re(1)-O(3)	91.4(2)
O(2)-Re(1)-O(3)	83.13(18)
O(4)-Re(1)-O(3)	84.15(17)
O(1)-Re(1)-S(1)	95.88(18)
O(2)-Re(1)-S(1)	91.15(13)
O(4)-Re(1)-S(1)	172.97(14)

O(3)-Re(1)-S(1)	91.91(13)
O(1)-Re(1)-S(2)	94.51(19)
O(2)-Re(1)-S(2)	90.50(14)
O(4)-Re(1)-S(2)	91.66(14)
O(3)-Re(1)-S(2)	172.77(14)
S(1)-Re(1)-S(2)	91.63(6)
C(5)-S(1)-Re(1)	106.6(2)
C(5)-N(1)-C(2)	121.1(6)
C(5)-N(1)-C(4)	123.2(6)
C(2)-N(1)-C(4)	115.7(5)
C(5A)-S(1A)-Re(2)	106.9(3)
C(5A)-N(1A)-C(2A)	122.3(8)
C(5A)-N(1A)-C(4A)	124.3(7)
C(2A)-N(1A)-C(4A)	111.3(7)
Re(1)-O(2)-Re(2)	175.2(2)
C(17)-S(2)-Re(1)	107.3(2)
C(17)-N(2)-C(14)	124.5(6)
C(17)-N(2)-C(16)	119.6(6)
C(14)-N(2)-C(16)	114.7(6)
N(1)-C(2)-C(1)	112.9(6)
O(5)-Re(2)-O(2)	167.9(2)
O(5)-Re(2)-O(4A)	89.4(2)
O(2)-Re(2)-O(4A)	81.86(19)
O(5)-Re(2)-O(3A)	89.9(2)
O(2)-Re(2)-O(3A)	81.13(18)
O(4A)-Re(2)-O(3A)	85.82(18)
O(5)-Re(2)-S(2A)	97.2(2)
O(2)-Re(2)-S(2A)	91.47(13)
O(4A)-Re(2)-S(2A)	92.16(13)
O(3A)-Re(2)-S(2A)	172.53(15)
O(5)-Re(2)-S(1A)	97.5(2)
O(2)-Re(2)-S(1A)	90.92(14)
O(4A)-Re(2)-S(1A)	172.67(14)
O(3A)-Re(2)-S(1A)	91.84(14)
S(2A)-Re(2)-S(1A)	89.28(6)
C(17A)-S(2A)-Re(2)	108.7(3)
C(17A)-N(2A)-C(14A)	124.3(6)
C(17A)-N(2A)-C(16A)	119.9(6)
C(14A)-N(2A)-C(16A)	115.7(6)
C(1A)-C(2A)-N(1A)	110.5(11)
C(6)-O(3)-Re(1)	129.7(4)
C(6)-N(3)-C(5)	127.9(6)
C(6A)-O(3A)-Re(2)	129.9(5)
C(5A)-N(3A)-C(6A)	127.3(6)

C(18)-O(4)-Re(1)	130.8(4)
N(1)-C(4)-C(3)	112.0(7)
C(18)-N(4)-C(17)	128.2(6)
C(18A)-O(4A)-Re(2)	129.1(4)
C(18A)-N(4A)-C(17A)	129.6(6)
C(3A)-C(4A)-N(1A)	85.8(13)
N(3)-C(5)-N(1)	115.4(6)
N(3)-C(5)-S(1)	128.8(5)
N(1)-C(5)-S(1)	115.6(5)
N(3A)-C(5A)-N(1A)	113.1(7)
N(3A)-C(5A)-S(1A)	130.9(6)
N(1A)-C(5A)-S(1A)	115.9(6)
O(3)-C(6)-N(3)	129.5(6)
O(3)-C(6)-C(7)	115.7(6)
N(3)-C(6)-C(7)	114.7(6)
O(3A)-C(6A)-N(3A)	130.1(7)
O(3A)-C(6A)-C(7A)	116.0(7)
N(3A)-C(6A)-C(7A)	113.8(7)
C(12)-C(7)-C(8)	120.1(7)
C(12)-C(7)-C(6)	121.4(6)
C(8)-C(7)-C(6)	118.6(6)
C(8A)-C(7A)-C(12A)	119.5(8)
C(8A)-C(7A)-C(6A)	119.3(7)
C(12A)-C(7A)-C(6A)	121.1(8)
C(7)-C(8)-C(9)	119.3(8)
C(7A)-C(8A)-C(9A)	122.1(10)
C(10)-C(9)-C(8)	120.9(9)
C(10A)-C(9A)-C(8A)	117.6(12)
C(9)-C(10)-C(11)	119.0(8)
C(9A)-C(10A)-C(11A)	122.3(11)
C(10)-C(11)-C(12)	121.0(9)
C(10A)-C(11A)-C(12A)	120.1(11)
C(7)-C(12)-C(11)	119.6(8)
C(7A)-C(12A)-C(11A)	118.4(10)
N(2)-C(14)-C(13)	114.7(6)
N(2A)-C(14A)-C(13A)	112.2(6)
C(15)-C(16)-N(2)	97.9(13)
N(2A)-C(16A)-C(15A)	110.6(7)
N(2)-C(17)-N(4)	115.4(6)
N(2)-C(17)-S(2)	114.6(5)
N(4)-C(17)-S(2)	130.0(5)
N(2A)-C(17A)-N(4A)	116.0(6)
N(2A)-C(17A)-S(2A)	115.6(6)
N(4A)-C(17A)-S(2A)	128.4(5)

Appendix

O(4)-C(18)-N(4)	130.7(6)
O(4)-C(18)-C(19)	113.7(6)
N(4)-C(18)-C(19)	115.5(6)
O(4A)-C(18A)-N(4A)	131.7(7)
O(4A)-C(18A)-C(19A)	113.6(6)
N(4A)-C(18A)-C(19A)	114.6(6)
C(20)-C(19)-C(24)	120.9(6)
C(20)-C(19)-C(18)	120.3(6)
C(24)-C(19)-C(18)	118.7(6)
C(24A)-C(19A)-C(20A)	118.5(7)
C(24A)-C(19A)-C(18A)	120.2(6)
C(20A)-C(19A)-C(18A)	121.3(6)
C(19)-C(20)-C(21)	118.2(8)
C(21A)-C(20A)-C(19A)	120.8(8)
C(22)-C(21)-C(20)	121.1(8)
C(20A)-C(21A)-C(22A)	120.3(9)
C(23)-C(22)-C(21)	120.0(8)
C(21A)-C(22A)-C(23A)	120.0(8)
C(22)-C(23)-C(24)	120.3(8)
C(24A)-C(23A)-C(22A)	119.6(8)
C(19)-C(24)-C(23)	119.3(7)
C(23A)-C(24A)-C(19A)	120.6(7)

Symmetry transformations used to generate equivalent atoms:

Table A15. Anisotropic displacement parameters ($Å^2$ x 10^3) for $(L)_2ORe\text{-}O\text{-}ReO(L)_2$ **(15)**. The anisotropic displacement factor exponent akes the form: $-2\pi^2[h^2 a^{*2} U11 + ... + 2hk a^* b^* U12]$

	U11	U22	U33	U23	U13	U12
Re(1)	39(1)	33(1)	33(1)	1(1)	6(1)	-3(1)
O(1)	58(4)	61(3)	75(4)	-6(3)	17(3)	8(3)
S(1)	42(1)	51(1)	37(1)	6(1)	5(1)	-13(1)
N(1)	38(3)	63(4)	44(3)	1(3)	9(3)	-14(3)
C(1)	57(6)	115(8)	60(5)	-2(5)	7(4)	8(6)
S(1A)	64(1)	47(1)	47(1)	-3(1)	10(1)	-19(1)
N(1A)	147(8)	90(6)	58(5)	-11(4)	27(5)	-80(6)
C(1A)	280(20)	83(10)	142(13)	27(9)	26(14)	-16(12)
O(2)	46(3)	42(3)	46(3)	-1(2)	19(2)	-6(2)
S(2)	58(1)	51(1)	33(1)	4(1)	4(1)	-13(1)
N(2)	57(4)	68(4)	39(3)	2(3)	-1(3)	-25(4)
C(2)	54(5)	64(5)	44(4)	-4(4)	-2(4)	-24(4)
Re(2)	39(1)	40(1)	46(1)	-1(1)	13(1)	-5(1)
S(2A)	64(1)	67(1)	40(1)	-2(1)	16(1)	-28(1)
N(2A)	53(4)	58(4)	50(4)	8(3)	17(3)	-16(3)
C(2A)	175(13)	102(9)	74(7)	-11(7)	34(8)	-82(9)
O(3)	54(3)	47(3)	40(3)	6(2)	1(2)	-13(3)
N(3)	43(3)	54(3)	31(3)	3(3)	6(3)	-9(3)
C(3)	129(9)	63(6)	71(6)	16(5)	-2(6)	-26(6)
O(3A)	54(3)	46(3)	58(3)	18(3)	3(2)	-8(3)
N(3A)	68(4)	49(4)	51(4)	-4(3)	21(3)	-13(3)
C(3A)	225(19)	98(10)	103(9)	-24(8)	49(11)	-55(11)
O(4)	66(3)	47(3)	44(3)	6(2)	4(2)	-24(3)
C(4)	49(5)	87(6)	50(5)	6(5)	11(4)	-32(5)
N(4)	49(4)	58(4)	37(3)	3(3)	7(3)	-13(3)
O(4A)	42(3)	62(3)	55(3)	3(3)	4(2)	-15(3)
N(4A)	51(4)	40(3)	44(3)	1(3)	7(3)	-11(3)
C(4A)	145(14)	73(9)	350(30)	60(13)	110(17)	-7(9)
O(5)	58(4)	66(4)	116(5)	-15(3)	41(3)	-1(3)
C(5)	36(4)	39(4)	41(4)	1(3)	8(3)	-4(3)
C(5A)	54(5)	54(5)	57(5)	-12(4)	23(4)	-19(4)
C(6)	38(4)	41(4)	41(4)	4(3)	14(3)	4(3)
C(6A)	60(5)	45(4)	59(5)	9(4)	23(4)	10(4)
C(7)	45(4)	46(4)	39(4)	5(3)	7(3)	-4(3)
C(7A)	48(5)	60(5)	58(5)	25(4)	12(4)	16(4)
C(8)	66(6)	73(6)	50(5)	7(4)	10(4)	-8(5)
C(8A)	58(6)	92(7)	59(5)	22(5)	9(4)	22(5)

C(9)	134(10)	78(6)	57(6)	12(5)	39(6)	-19(7)
C(9A)	73(7)	157(12)	68(7)	34(7)	13(5)	35(8)
C(10)	147(10)	71(6)	37(5)	0(5)	9(6)	-20(7)
C(10A)	72(8)	188(15)	66(7)	53(9)	13(6)	41(9)
C(11)	125(9)	89(7)	40(5)	-4(5)	-8(5)	-28(7)
C(11A)	105(9)	117(10)	120(9)	76(9)	38(8)	16(8)
C(12)	77(6)	73(6)	48(5)	7(4)	9(4)	-16(5)
C(12A)	83(7)	72(6)	89(7)	41(5)	28(5)	11(5)
C(13)	83(7)	100(7)	54(5)	17(5)	10(5)	11(6)
C(13A)	84(7)	93(7)	68(6)	3(5)	25(5)	1(6)
C(14)	66(5)	65(5)	34(4)	2(4)	7(4)	-7(4)
C(14A)	74(6)	61(5)	46(4)	3(4)	23(4)	-19(5)
C(15)	250(20)	132(12)	186(15)	-4(11)	137(16)	50(14)
C(15A)	85(8)	123(9)	114(8)	-14(7)	47(7)	-39(7)
C(16)	59(7)	236(16)	54(6)	21(8)	1(5)	0(9)
C(16A)	89(7)	68(6)	67(5)	0(5)	25(5)	-27(5)
C(17)	42(4)	51(4)	37(4)	-4(3)	9(3)	-3(3)
C(17A)	46(4)	41(4)	58(5)	-4(4)	26(4)	0(3)
C(18)	41(4)	30(3)	41(4)	-1(3)	14(3)	-2(3)
C(18A)	34(4)	49(4)	49(4)	-6(4)	15(3)	-4(3)
C(19)	45(4)	41(4)	46(4)	-2(3)	24(3)	-7(3)
C(19A)	38(4)	47(4)	47(4)	-7(3)	12(3)	-3(3)
C(20)	59(5)	58(5)	52(4)	-4(4)	18(4)	-17(4)
C(20A)	58(5)	67(5)	57(5)	-5(4)	11(4)	-16(4)
C(21)	96(7)	70(6)	81(6)	-11(5)	39(6)	-46(6)
C(21A)	59(6)	98(7)	68(6)	-6(6)	5(5)	-30(5)
C(22)	105(8)	57(5)	93(7)	9(5)	57(7)	-20(6)
C(22A)	48(5)	112(8)	66(6)	-17(6)	-1(4)	-15(6)
C(23)	81(6)	67(5)	59(5)	16(4)	31(5)	-6(5)
C(23A)	67(6)	79(6)	46(4)	-3(4)	2(4)	1(5)
C(24)	53(5)	54(4)	46(4)	6(4)	23(4)	-6(4)
C(24A)	45(4)	63(5)	45(4)	-5(4)	8(4)	-8(4)

Table A16. Hydrogen coordinates (x 10^4) and isotropic displacement parameters ($Å^2$ x 10^3) for $[(L)_2ORe\text{-}O\text{-}ReO(L)_2]$ **(15)**.

	x	y	z	U(eq)
H(1A)	4930	6206	3663	120
H(1B)	4622	5989	2898	120
H(1C)	4266	5497	3391	120
H(1D)	1096	9991	2982	265
H(1E)	959	9626	3629	265
H(1F)	385	9331	2921	265
H(2A)	3601	6696	3582	70
H(2B)	3961	7192	3093	70
H(2C)	2108	9003	3452	142
H(2D)	1538	8714	2739	142
H(3A)	2519	7781	1389	143
H(3B)	2811	7972	2158	143
H(3C)	1957	7506	1820	143
H(3D)	2617	7587	4800	214
H(3E)	2582	7967	4107	214
H(3F)	2090	7145	4135	214
H(4A)	2687	6378	1607	76
H(4B)	3542	6845	1943	76
H(4C)	1717	8681	4508	217
H(4D)	1212	7840	4530	217
H(8)	1348	4318	4258	78
H(8A)	-704	6489	851	86
H(9)	1740	4129	5417	105
H(9A)	-714	6814	-230	122
H(10)	2996	4647	6108	108
H(10A)	-135	8044	-400	133
H(11)	3850	5398	5653	112
H(11A)	479	8934	462	136
H(12)	3490	5567	4498	82
H(12A)	495	8611	1549	97
H(13A)	-1776	5205	-718	123
H(13B)	-1659	5262	49	123
H(13C)	-2397	4731	-424	123
H(13D)	181	3244	5211	123
H(13E)	252	3408	4499	123
H(13F)	-248	2633	4621	123
H(14B)	-1421	3809	-607	69
H(14A)	-683	4341	-138	69
H(14E)	-1262	3514	4808	71
H(14D)	-761	4291	4689	71
H(15A)	-2942	2564	-16	259
H(15B)	-2718	3437	-246	259
H(15C)	-2563	3261	515	259
H(15F)	-3142	2634	3480	156
H(15E)	-3033	3577	3335	156
H(15D)	-2772	3256	4075	156
H(16A)	-1724	2524	-248	145
H(16B)	-1568	2342	522	145
H(16E)	-1694	2475	3898	90
H(16D)	-1953	2801	3157	90
H(20)	-1716	2105	1725	67
H(20A)	-3084	3387	2051	75
H(21)	-1938	916	2279	96
H(21A)	-4250	3092	1160	95
H(22)	-1002	551	3303	94
H(22A)	-4652	3973	247	96
H(23)	114	1404	3821	81
H(23A)	-3761	5042	160	81
H(24)	326	2620	3302	59
H(24A)	-2570	5331	1050	63

Appendix

Appendix B

Table B1. Shows the residual concentrations/M of the mononuclear and dinuclear complexes at 120 sec time intervals.

Time/sec	[Mononuclear Complex]			[Dinuclear Complex]		
	OMe	**OEt**	**O*i*Pr**	**OMe**	**OEt**	**O*i*Pr**
240	1.122 x 10-2	7.964 x 10-3	6.046 x 10-3	1.830 x 10-4	3.436 x 10-3	5.354 x 10-3
360	1.111 x 10-2	7.159 x 10-3	4.058 x 10-3	2.540 x 10-4	4.241 x 10-3	7.342 x 10-3
480	1.109 x 10-2	6.647 x 10-3	3.236 x 10-3	3.070 x 10-4	4.752 x 10-3	8.164 x 10-3
600	1.105 x 10-2	6.204 x 10-3	2.969 x 10-3	3.430 x 10-4	5.196 x 10-3	8.431 x 10-3
720	1.103 x 10-2	5.907 x 10-3	2.787 x 10-3	3.690 x 10-4	5.493 x 10-3	8.613 x 10-3
840	1.101 x 10-2	5.623 x 10-3	2.885 x 10-3	3.920 x 10-4	5.777 x 10-3	8.515 x 10-3
960	1.098 x 10-2	5.439 x 10-3	2.580 x 10-3	4.190 x 10-4	5.961 x 10-3	8.820 x 10-3
1080	1.097 x 10-2	5.285 x 10-3	2.656 x 10-3	4.330 x 10-4	6.115 x 10-3	8.744 x 10-3
1200	1.095 x 10-2	5.133 x 10-3	2.784 x 10-3	4.490 x 10-4	6.267 x 10-3	8.616 x 10-3
1320	1.094 x 10-2	4.992 x 10-3	2.677 x 10-3	4.590 x 10-4	6.408 x 10-3	8.723 x 10-3
1440	1.093 x 10-2	4.921 x 10-3	2.658 x 10-3	4.710 x 10-4	6.479 x 10-3	8.742 x 10-3
1560	1.092 x 10-2	4.847 x 10-3	2.562 x 10-3	4.840 x 10-4	6.553 x 10-3	8.838 x 10-3
1680	1.091 x 10-2	4.774 x 10-3	2.653 x 10-3	4.950 x 10-4	6.626 x 10-3	8.747 x 10-3
1800	1.090 x 10-2	4.679 x 10-3	2.777 x 10-3	5.030 x 10-4	6.721 x 10-3	8.623 x 10-3
1920	1.089 x 10-2	4.637 x 10-3	2.544 x 10-3	5.050 x 10-4	6.763 x 10-3	8.856 x 10-3
1980	1.088 x 10-2	4.602 x 10-3	2.724 x 10-3	5.100 x 10-4	6.798 x 10-3	8.676 x 10-3